Evolution of seasonal variations in motion of the Kaskawulsh Glacier, Yukon Territory

Émilie Herdes

Thesis submitted to the
Faculty of Graduate and Postdoctoral Studies
in partial fulfillment of the requirements
for the M.Sc. Degree in Physical Geography

Department of Geography
Faculty of Arts
University of Ottawa

Supervisor:

Dr. Luke Copland

Thesis Committee:

Dr. David Burgess

Dr. Michael Sawada

ABSTRACT

Differential GPS data from 2007-2014 are used to assess horizontal and vertical velocity variations of the Kaskawulsh Glacier at interannual and intra-annual timescales. These indicate that an upglacier propagating high velocity event occurs every spring at the onset of melt, and that a downglacier propagating high velocity event occurs every fall or winter after melt has finished. These events suggest that the subglacial drainage system alternates between a distributed system in the winter and channelized system in the summer and fall. In addition, there is a strong negative correlation between summer melt and velocity the following fall and winter, with strong melt years resulting in low velocities. For each additional metre of summer melt, an 8.6% average decrease in velocity is observed on the glacier the following fall-winter.

These results suggest that changes in the subglacial drainage system limit the sensitivity of glacier motion to increased meltwater inputs. Glacier motion will likely show a net decrease under a warming climate due to the negative correlation between surface melt rates and ice motion and a decrease in driving stresses as a result of reduced ice thicknesses. In addition, future fall-winter velocity patterns could be accurately predicted from only a month or two of summer melt data, with May-June melt providing the best indication of fall-winter motion. This study also suggests that the common assumption that glaciers are ‘stable’ in the late fall and winter is incorrect.

ACKNOWLEDGEMENTS

Funding and resources for this project were provided by:

- Natural Sciences and Engineering Research Council Canadian Graduate Scholarship
- Association of Canadian Universities for Northern Studies Garfield Weston Award
- Ontario Ministry of Training, Colleges and Universities Graduate Scholarship
- Fondation Baxter et Alma Ricard
- Yukon Territorial Government's Yukon Grant
- Yukon Research Centre and Northern Research Endowment Fund
- Yukon Foundation
- Parks Canada
- GLACIO-EX
- University of Ottawa
- Northern Scientific Training Program
- Polar Continental Shelf Program
- Canada Foundation for Innovation
- Natural Sciences and Engineering Research Council Discovery Grant
- Ontario Research Fund
- Kluane Lake Research Station

I would also like to thank all those who assisted with the field work and those who helped in any number of other ways. Thank you to Christian Zdanowicz and the Geological Survey of Canada for providing additional meteorological data, and to Camilo Rada and Dr. Christian Schoof for providing the KLRS base station dGPS data for comparison. Thank you to the members of the Laboratory of Cryospheric Research for their support throughout the project.

Thanks must also go to the staff at Trans North Helicopters in Haines Junction, especially Dion Parker, and to Sian Williams and Lance Goodwin at Kluane Lake Research Station for their assistance with the project since the beginning.

I would especially like to thank my supervisor, Dr. Luke Copland, for his guidance and support throughout this project, and for the many opportunities working with him has brought me.

I gratefully thank those who have offered invaluable support and encouragement throughout this project, especially my family. This project would not have been completed without them. Special thanks must go to Julien Revel for holding down the fort while I was off studying across the country and beyond, and for believing in me from the start.

TABLE OF CONTENTS

LIST OF FIGURES

LIST OF TABLES

Chapter 1 : Introduction

1.1 Study motivation and context

Mountain glaciers in Alaska-Yukon have lost substantial mass in the past 50+ years, and are currently providing the biggest contribution to global sea level rise outside of the major ice sheets (e.g., Dyurgerov and Meier, 2005; Larsen et al., 2007; Arendt et al., 2008; Lutchke et al., 2008; Barrand and Sharp, 2010; Berthier et al., 2010; Foy et al., 2011; Jacob et al., 2012). For example, this region experienced a reduction in mass of 46 ±77 Gt yr^{-1} over the period 2003-2011 (Figure 1.1) (Jacob et al., 2012). It has recently been suggested that an acceleration in ice motion due to increases in surface melt can cause substantial losses on the large ice sheets, particularly Greenland, in a process called dynamic thinning (Pritchard et al., 2009). However, it is unknown whether this acceleration is sustainable in the long-term (Murray et al., 2010; Sundal et al., 2011), and it is unknown whether mountain glaciers will respond to changes in meltwater input and mass balance in the same way. In particular, little work has previously been done on what negative mass balance means for the long-term evolution of glacier motion in large valley glaciers such as those found in the SW Yukon. The anticipated responses to a negative mass balance are either: (1) a speed up due to increased surface meltwater input to the glacier bed causing increased basal lubrication, or (2) a slow down due to reduced ice thicknesses and driving stresses, and/or to changes in the efficiency of the subglacial drainage system. This study builds on previous studies in the SW Yukon and Alaska to investigate variations in motion of the Kaskawulsh Glacier, Yukon, and what causes these variations.

1.2 Project objectives

The primary objective of this project is to determine the connections between surface melt and the velocity patterns of the Kaskawulsh Glacier, on both intra-annual (within year) and interannual (between years) timescales. Differential global positioning system (dGPS) data are used to provide a detailed assessment of velocity patterns over the past ~5 years and their relationship to water inputs to the glacier bed. These water inputs are derived from meteorological data that have been recorded on a nunatak adjacent to the glacier since 2007, and from air temperature and snow depth data that have been collected on the glacier surface since 2010. Variations in motion can provide insight about the structure of the subglacial drainage system and how it changes over time (Schoof, 2010; Sundal et al., 2011; Sole et al., 2013). The evolution of glacier motion patterns in response to changing melt and mass balance conditions can also provide information as to how large valley glaciers will respond to projected increases in air temperatures (IPCC, 2007).

1.3 Study site

The St. Elias Mountains, between southwestern Yukon and the Alaska border, are home to one of the largest non-polar icefields in the world with approximately 40,000 km^2 of glacierized area (Arendt et al., 2009). The Kaskawulsh Glacier is a large temperate valley glacier located in Kluane National Park, Yukon, within the St. Elias Icefields (138°51'W, 60°43'N; Figure 1.2). The glacier is approximately 70 km long, ranges in elevation between approximately 800 and 2500 m a.s.l., and is land-terminating. The equilibrium line altitude (ELA) marks the transition between the accumulation and ablation zone on

the glacier, and was at 1958 m a.s.l. in 2007 (Foy et al., 2011). The St. Elias Icefields also drain into a number of other lake- and land-terminating glaciers including the Donjek, Lowell and Tweedsmuir to the north and east. To the south and west, the icefields drain into larger Alaskan glaciers including some of the largest in North America, the Bering and Hubbard Glaciers (Arendt et al., 2009). The Kaskawulsh Glacier is divided into four main branches: the Central Arm, the South Arm, the North Arm and the Stairway Glacier, all fed by a number of small tributaries. The Kaskawulsh Glacier flows generally eastwards and drains into the Kaskawulsh and Alsek Rivers to the southeast (towards the Gulf of Alaska), and into the Slims River and then Kluane Lake to the north.

Since the 1960s, a number of glaciological studies have focused on the St. Elias Mountains. The Icefield Ranges Research Project, run from 1961 to the mid-1970s, provided meteorological and glaciological data on some of the glaciers within this area, including the Kaskawulsh Glacier (Wood, 1963; Marcus, 1974). Recent studies undertaken in the Alaska-Yukon region have mainly focused on mass balance. For example, Barrand and Sharp (2010) found that over the past 50 years the surface area of Yukon glaciers decreased by 22%, contributing 1.12 ±0.49 mm to global sea-level rise. They found the mean thinning rate of Yukon glaciers to be 0.78 ±0.34 m a^{-1} w.e. over the period 1957 to 2007, the highest regional thinning rate outside of Patagonia and Alaska. Berthier et al. (2010) tracked changes in ice extent and mass balance using satellite imagery and found that between 1968 and 2006, the St. Elias and Wrangell Mountains had an average negative mass balance of 0.47 ±0.09 m a^{-1} w.e. Arendt et al. (2013) used Gravity Recovery and Climate Experiment (GRACE) satellite data to estimate a regional

mass balance of -65 ±11 Gt a^{-1} for Gulf of Alaska glaciers for the period 2003-2010. These results are higher than previous estimates computed from GRACE data by Jacob et al. (2012) for the period 2003-2011 (i.e., 46 ±7 Gt a^{-1} for the Alaska-Yukon region), but lower than those computed by Luthcke et al. (2008) for the 2003-2007 period (i.e., -84 ±5 Gt a^{-1} for the Gulf of Alaska region).

Studies focusing specifically on the Kaskawulsh Glacier are limited. Brecher (1966) calculated velocities on the glacier's upper North Arm during summer 1964 using theodolites. He found mean annual surface velocities ranging between 120 and 150 m yr^{-1}, later confirmed by Clarke (1969) and Anderton (1973). In his study, Anderton (1973) derived annual and summer velocities for the North and Central arms of the Kaskawulsh Glacier. He found higher mean annual velocities on the Central Arm than on the North Arm (215 m yr^{-1} vs. 152 m yr^{-1}, respectively), and lower summer velocities on the Central Arm (150 m yr^{-1}) than on the North Arm (200 m yr^{-1}). More recently, Foy et al. (2011) studied volume and area changes of the glacier and found that between 1977 and 2007, there was a 1.53% decrease in glacier area and a 3.27-5.94 km^3 w.e. decrease in volume. The rate of volume loss was low until 1995, when it increased dramatically, and then remained relatively constant (at -0.50 km^3 yr^{-1}) until 2007. During the 1977-2007 period, the glacier thinned on average by 0.20-0.46 m yr^{-1}, with most of the thinning occurring in the ablation zone. Between 1956 and 2007, the terminus of the Kaskawulsh Glacier retreated by 655 m.

A recent University of Ottawa study (Darling, 2012) focused on seasonal velocity patterns of the Kaskawulsh Glacier from summer 2009 to summer 2011 based on dGPS measurements. In 2013, another University of Ottawa study determined velocities for the St. Elias region using remote sensing (Figure 1.3) (Waechter, 2013; Waechter et al., In review). This regional map shows that the Kaskawulsh Glacier velocity structure is similar to other land-terminating glaciers of similar size in the region, ranging between 50 and 400 m a^{-1}. This project builds upon these earlier studies by analyzing interannual and intra-annual variations in motion of the glacier, investigating the causes of these variations, and determining whether there is a relationship between summer melt and velocity the following winter.

1.4 Thesis structure

This is a traditional thesis presented in chapters. Chapter 2 provides a background review of glacier dynamics and summarizes current literature on variations in glacier motion. In Chapter 3, the methodology is described. The results of the study are presented in Chapter 4. In Chapter 5, controls on variations in motion observed at different timescales are discussed and compared to results from previous studies. Key findings and suggestions for future work are presented in Chapter 6. A list of cited references is presented in Chapter 7. Tables and figures are included at the end of each chapter.

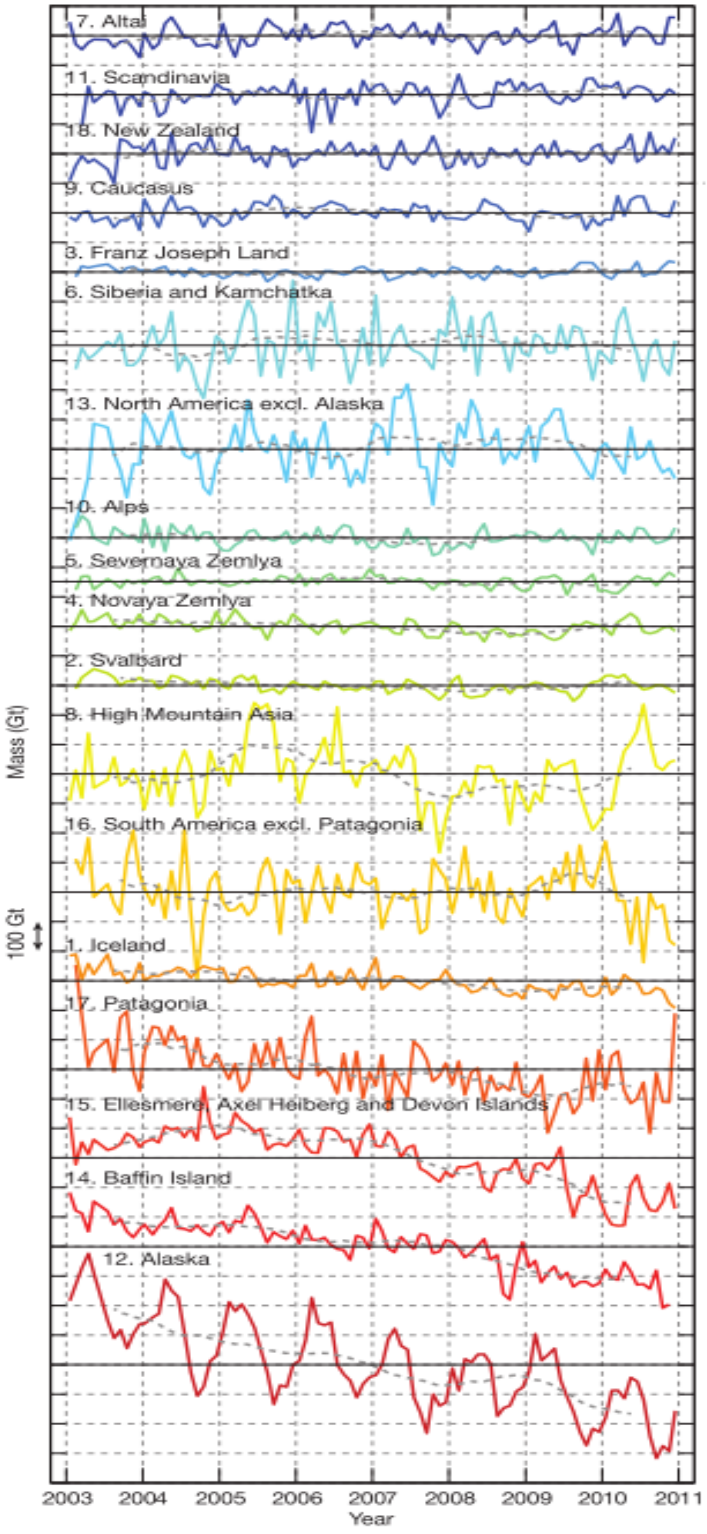

Figure 1.1 Mass change for glacier and ice cap regions, 2003-2010. The Kaskawulsh Glacier is included in region 12 – Alaska. Reproduced from Jacob et al. (2012).

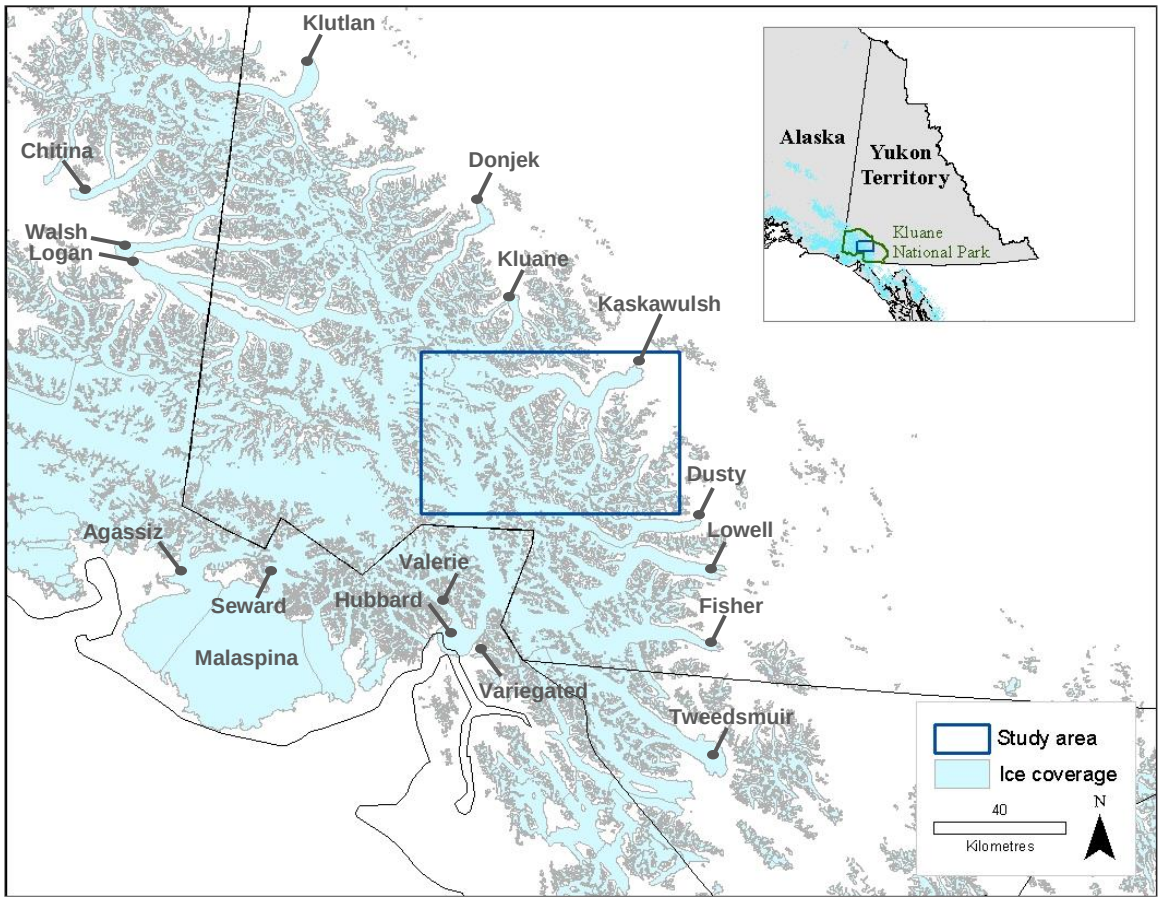

Figure 1.2 Location of study area: Kaskawulsh Glacier and surrounding glaciated regions in Yukon and Alaska. Source: GLIMS Randolph Glacier Inventory 3.2, 2013.

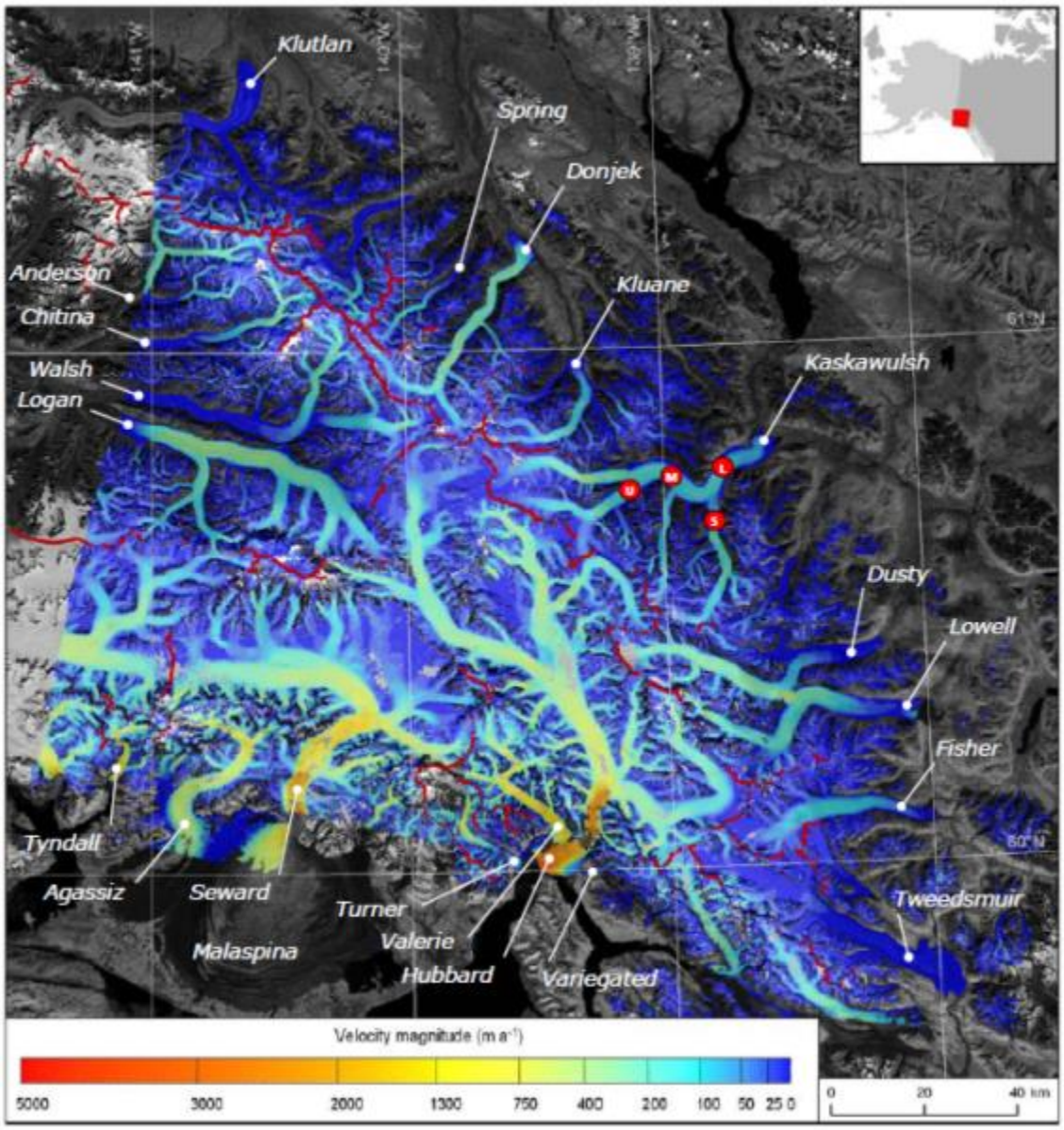

Figure 1.3 Velocity structure of glaciers in the St. Elias Mountains, derived from speckle tracking of ultrafine wide Radarsat-2 imagery from Feb. – Apr. 2012. Heavy red lines indicate primary ice divides; red circles indicate dGPS stations (L = Lower; M = Middle; U = Upper, S = South Arm). Note the non-linear colour scale. Base map: Landsat-8 band 5 mosaic, August 2013. Reproduced from Waechter et al. (In review).

Chapter 2 : Background

2.1 Basics of glacier dynamics

Large valley glaciers, such as those present in the St. Elias Mountains, are typically formed when ice is discharged from an icefield into a bedrock valley. Constrained by surrounding topography, valley glaciers typically have steep slopes and cover large altitudinal ranges (Benn and Evans, 2010). The mass balance of a glacier is described as the annual balance between the mass of snow and ice accumulated on the glacier surface and the mass lost (ablation), primarily through surface melt for glaciers in the St. Elias Mountains. Glacier motion is driven by mass balance, as glacier flow transfers ice from the accumulation zone to the ablation zone. Glacier flow occurs as a result of ice deformation, bed deformation and basal sliding processes that are influenced by driving and resisting forces, gravity and friction (Figure 2.1) (Paterson, 1994; Benn and Evans, 2010).

Ice deformation within a glacier mainly occurs through creep, described as movement within or between individual ice crystals (Weertman, 1983), or sometimes through fracturing. Creep rates are affected by temperature, ice crystal structure, the presence of natural impurities and water content. The main controls on creep rates are ice thickness and surface slope (Benn and Evans, 2010). Bed deformation occurs when unconsolidated sediment present at the glacier bed is deformed by the weight of overlying ice, with this process particularly effective when the basal sediments are water saturated (Boulton and Jones, 1979). Basal sliding occurs when a glacier slides along its bed, primarily due to the

presence of subglacial water that can act as a lubricant and reduce basal friction (Paterson, 1994; Schoof, 2010).

For the above processes it is clear that the temperature of the ice provides a major control on ice motion, since warm ice allows for higher ice deformation rates, and basal sliding and basal sediment deformation can only occur where the ice is at the melting point. There are three main types of glacier thermal regime: cold, polythermal and temperate. Temperate glaciers are most common in areas with both high winter accumulation rates and high summer melt rates (Benn and Evans, 2010), such as in the SW Yukon. The Kaskawulsh Glacier is likely a primarily temperate glacier, characterized by warm ice (i.e., ice at the pressure melting point) throughout. The exception is a relatively thin layer (up to ~10 m) of cold near-surface ice in the ablation area that forms during the winter, although it is likely that this layer becomes entirely warm by the end of the summer. During the summer, the entire annual snowpack in the accumulation area reaches 0°C (Darling, 2012). In contrast, a cold glacier is almost entirely composed of ice below the melting point and is frozen to its bed, while a polythermal glacier is made up of a mixture of warm and cold ice (Paterson, 1994).

Glacier hydrological processes play an important role in glacier motion. Water from precipitation, surface ablation and basal melting is evacuated from temperate glaciers through supraglacial, englacial and subglacial drainage systems (Benn and Evans, 2010). The majority of rain and meltwater accumulated on the surface of temperate glaciers flows along supraglacial channels and is then redistributed vertically into the glacier via

moulins and crevasses (Figure 2.2) (Fountain and Walder, 1998), while on polythermal glaciers this supraglacial water frequently flows off the margins. Water flowing into crevasses and moulins is redistributed downglacier and towards the glacier bed via englacial conduits, after which it enters the subglacial drainage system. Englacial and subglacial conduits are important in glacier motion as they route meltwater to the glacier bed, lubricating it and reducing friction, leading to glacier motion via basal sliding or bed deformation.

Studies have shown that the subglacial drainage system evolves through the melt season, from a distributed system with many small, poorly connected "threads", to a more efficient channelized system with fewer larger channels (Hock and Hooke, 1993; Willis, 1995; Nienow et al., 1998; Mair et al., 2002; Bartholomew et al., 2010). At the beginning of the melt season, the high water pressure in the distributed system typically forces the drainage system to expand. Then, as the subglacial drainage system evolves through the summer and the channels increase in size, the water pressure decreases. Subglacial water pressure plays a key role in glacier motion. In fact, it is the pressure of the water at the bed, and not the volume of water, which is the determining factor in short-term basal motion changes (Paterson, 1994; Benn and Evans, 2010; Schoof, 2010).

2.2 Variations in glacier motion

A number of studies have considered the effect of changes in subglacial water input and pressure on variations in glacier motion (e.g., Iken and Truffer, 1997; Mair et al., 2002; Zwally et al., 2002; Bartholomew et al., 2010; Schoof, 2010; Andersen et al.; 2011;

Sundal et al., 2011). Short-term variations in velocity, including daily and sub-daily variations, are attributable to water input from precipitation and surface melt events enhanced by warm periods in the summer. Studies in locations such as Greenland and the European Alps have shown that short-term variations in meltwater input to a glacier bed can cause short-term increases in motion through increased basal sliding (e.g., Zwally et al., 2002; Mair et al., 2003; Bingham et al., 2008; Quincey et al., 2009; Shepherd et al., 2009; Bartholomew et al., 2010; Andersen et al., 2011; Podrasky et al., 2012; Shannon et al., 2013). Short-term glacier speed-up events have been linked to rapid increases in subglacial water pressure (Iken et al., 1983; Hubbard et al., 1995; Willis, 1995; Iken and Truffer, 1997; Vieli et al., 2004). The exact nature of the surface meltwater input and glacier motion relationship appears to be complex, however, as the magnitude and timing of velocity events varies through the summer melt season.

Willis (1995) provided a review of intra-annual variations in glacier motion and demonstrated that on seasonal intervals, spring and summer velocities normally exceed fall and winter velocities on most glaciers, and, in general, kinematic waves of high velocity move downglacier. This is not always the case, however, as was demonstrated by a study on the Kaskawulsh Glacier, where spring events propagated upglacier, but winter events propagated downglacier (Darling, 2012). Similar results have been found on a Greenland outlet glacier and on other glaciers (Willis, 1995; Bartholomew et al., 2010). In addition to seasonal motion patterns, medium- and short-term surface velocity variations associated with meltwater input have been observed on a number of glaciers. For example, Willis (1995) found that medium-interval (daily to weekly) variations in

motion are correlated with patterns of water input from surface melt and rainfall, but that the importance of this relationship generally decreases throughout the melt season (i.e., increases in water input have little effect on glacier motion after the first medium-interval velocity increase of the season). Short-interval (sub-daily) velocity variations include diurnal cycles, linked to daily air temperature variations, and dramatic acceleration events linked with glacier surface uplift. Willis (1995) found that, during these large magnitude events, surface velocity can be much greater than background velocities (e.g., up to 900% of background speeds on Mitdalsbreen, Norway). The events mainly occur early in the melt season when the subglacial drainage system is poorly developed, and are associated with periods of high surface melt or heavy rainfall, resulting in high subglacial water pressure.

Due to its influence on subglacial water pressure, the structure of the subglacial drainage system plays a key role in the effect of meltwater inputs on glacier motion. Studies have shown that high meltwater inputs can cause high basal water pressures if they occur early in a melt season due to overpressurization of a distributed subglacial drainage system, resulting in rapid velocity increases (Mair et al., 2002; Bartholomew et al., 2010; Schoof, 2010; Sundal et al., 2011; Fitzpatrick et al., 2013). However, similarly high meltwater inputs later in a melt season can cause negligible changes in velocity since the channelized system that develops during the summer can now accommodate this water flow. After the original distributed subglacial drainage system has developed into a channelized one shortly after the start of a melt season, it is frequently found that basal water pressure decreases and surface velocities drop to a background summer level.

Velocities then tend to remain fairly constant throughout the melt season unless there is a large short-term increase in meltwater supply (e.g., from a large rainfall event or period of major surface melt), which would once again overpressurize the drainage system and cause the glacier to speed-up (van de Wal et al., 2008; Schoof, 2010). Therefore, variations in surface water input, rather than mean water supply, are crucial factors in driving basal glacier motion. For example, Schoof (2010) outlines a process by which a long-term deceleration in glacier motion could occur as a response to increases in surface meltwater input, due to a negative feedback mechanism by which enlarged subglacial channels can accommodate increased basal water flow. A study by Sundal et al. (2011) on the Greenland Ice Sheet found that in years of high melting, average summer velocity was lower than in years of low melting (Figure 2.3). In years of high melting, fast channelization early in the melt season (after an initial large speed-up event) caused water pressure within the drainage system to remain low, meaning that the input of meltwater later in the season had little or no effect on glacier velocity. In years of low melting, the water pressure in the relatively undeveloped drainage system remained high and caused a number of smaller velocity events which added up to a greater total seasonal velocity.

On an interannual timescale, Heid and Kääb (2012) found that a long-term negative mass balance over the past few decades (from 1953-2009, depending on study region) has led to reduced glacier surface velocities in five of the six regions they studied. For example, 8 of 9 glaciers in the Alaska Range with an estimated regional mass balance of -0.3 m w.e. yr^{-1} (Berthier et al., 2010), have seen reductions in velocity or kept a constant speed

between 1986-2010, adding up to a 26% decrease in speed for the area over the study period. Heid and Kääb (2012) attributed this decrease to the thinning of the glaciers, which has reduced driving stresses. However, other studies of ice motion variations in regions with negative glacier mass balance have observed both increases and decreases in speed. For example, studies in the French and Austrian Alps have found strong glacier deceleration since the 1980s linked with negative mass balance (Span and Kuhn, 2003; Vincent et al., 2009), while Vincent et al. (2000) found increased velocities between 1957 and 1997 on the Glacier de Saint-Sorlin, France, in response to long-term negative mass balance.

On the Greenland Ice Sheet, measurements have indicated a number of large outlet glaciers with pronounced, accelerating mass loss (e.g., Rignot et al., 2011; Jacob et al., 2012; Shepherd et al., 2012), with a large increase in speed between the mid-1990s and 2005 (Joughin et al., 2004; Rignot and Kanagaratnam, 2006). A later study found that some of these glaciers returned to their prior lower velocities in the following years (Howat et al., 2007), while others found that Greenland ice velocities have undergone a long-term decrease between 1990 and 2007 (van de Wal et al., 2008). A recent study on Gulf of Alaska glaciers found an 11% decrease in overwinter velocity per additional metre of summertime melt (Burgess et al., 2013), consistent with previous studies suggesting that sensitivity to interannual surface melt variations is limited due to the evolution of the subglacial drainage system (Schoof, 2010; Sundal et al, 2011; Sole et al., 2013).

In summary, there are many factors that control ice motion over both intra-annual and interannual timescales, but we have little idea as to whether (and how) they are influencing the motion of large valley glaciers in the Yukon such as the Kaskawulsh. This motivates the current study.

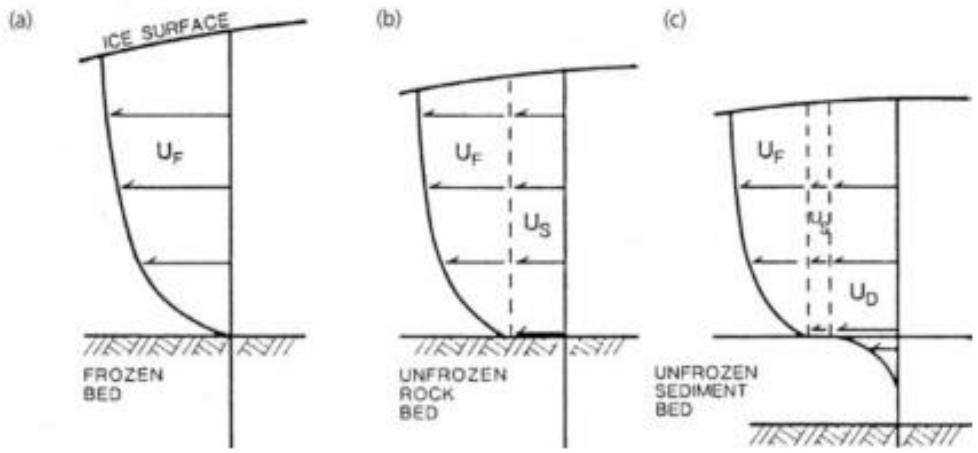

Figure 2.1 Vertical distribution of velocity for different types of glacier motion: a) ice deformation, b) ice deformation and basal sliding, and c) ice deformation, basal sliding and deformation of subglacial sediments. Reproduced from Benn and Evans (2010).

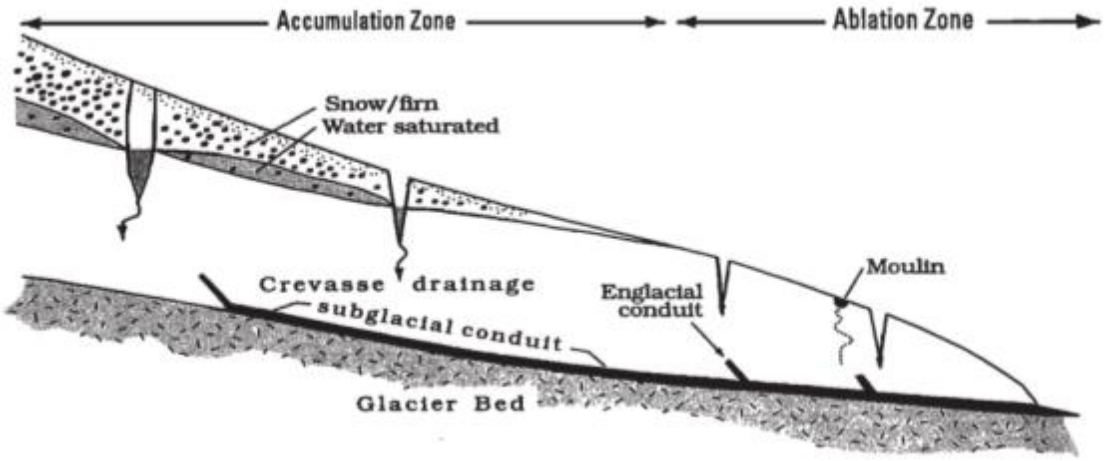

Figure 2.2 Cross-section of a temperate glacier showing surface water migration routes to the glacier bed. Reproduced from Fountain and Walder (1998).

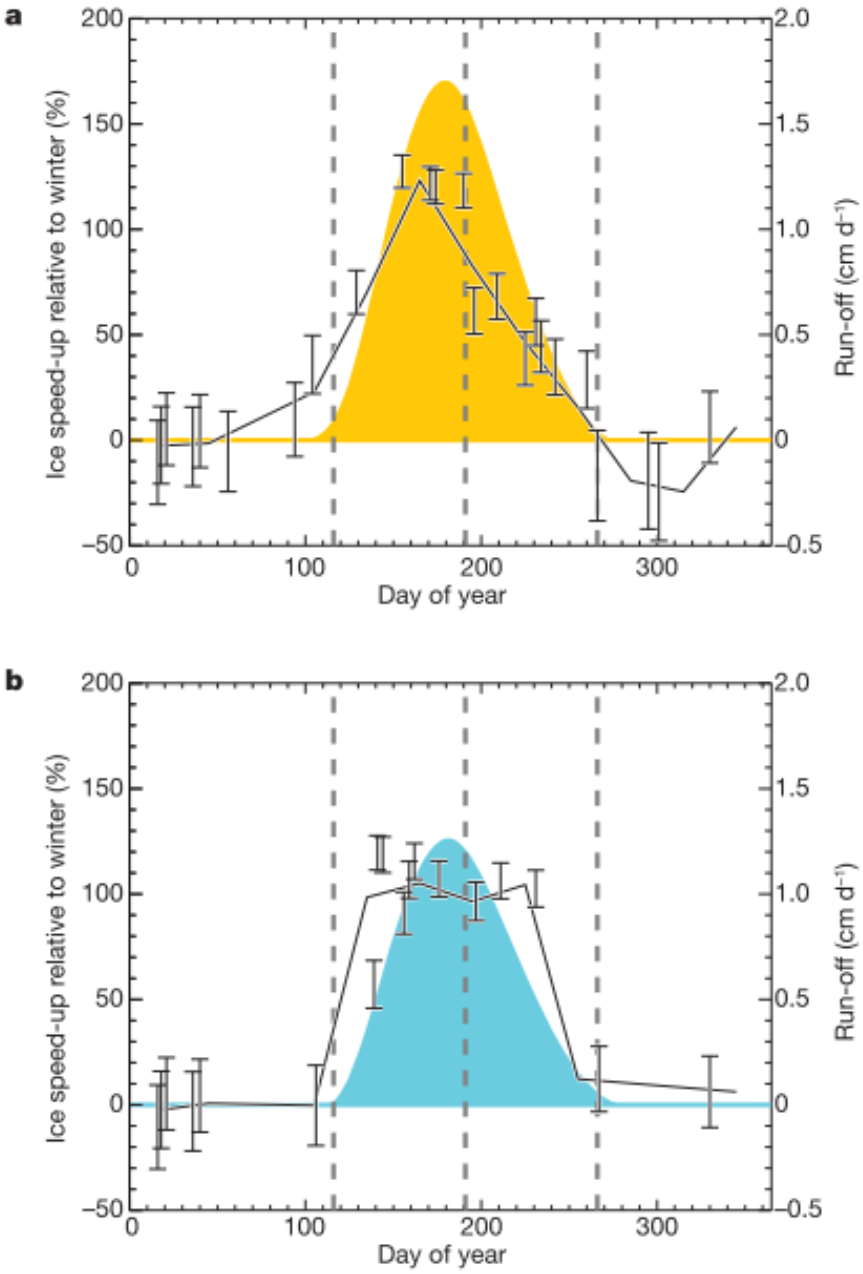

Figure 2.3 Monthly averaged ice speed-up relative to winter during years of: a) high surface melting, and b) low surface melting, on a land-terminating sector of southwest Greenland. Error bars show the one-sigma uncertainty of speed-up measurements. Model estimates of daily surface run-off rates within the study area are shown in orange (high melt years) and blue (low melt years). Vertical dashed lines indicate the beginning, midway-point and end of the run-off period used to define the summer period. Reproduced from Sundal et al. (2011).

Chapter 3 : Methodology

The evolution of seasonal variations in motion of the Kaskawulsh Glacier are assessed using field dGPS measurements. Meteorological data are used to quantify meltwater inputs and their temporal and spatial variability. These data are used to assess the relationship between short- and long-term velocity patterns, and water inputs to the glacier bed.

3.1 dGPS measurements

This study focuses on ice motion derived from high-resolution dGPS data recorded by a network of four stations across the Kaskawulsh Glacier. These stations have been running since as long ago as summer 2007. Three stations are located in a transect along the centreline of the Central Arm, from the glacier terminus to near the equilibrium line, and the fourth station is located midway up the South Arm (Figure 3.1). On Julian Day (JD) 1, 2013, the Lower Station (60°46'N, 138°45'W) elevation was 1167 m, the Middle Station (60°45'N, 138°57'W) was at 1541 m, the Upper Station (60°43'N, 139°07'W) was at 1720 m, and the South Arm Station (60°40'N, 138°47'W) was at 1493 m.

Each station consists of a Trimble R7 dual frequency GPS receiver and Trimble Zephyr Geodetic antenna, with power provided by a 20 W solar panel, solar regulator, and two 12-volt, 100 Ah sealed gel cell batteries. The antenna is mounted on a 6 m pole initially drilled 5 m into the ice, and the GPS receiver and 12-volt batteries are enclosed in a waterproof Underwater Kinetics case (Figure 3.2). The dGPS stations record their

position at 15 second intervals for 24 hours per day during the summer (typically May to August). Between September and April, the stations are switched to a winter program to preserve battery power, and typically take measurements every 15 seconds for 3 hours per day. The dGPS' were programmed with Trimble GPS Configurator (USB interface) and Trimble GPS Configuration Toolbox (serial interface). The data were downloaded directly from the 2 GB CompactFlash memory card installed in each unit.

The Lower, Middle and Upper stations were installed by Dr. Luke Copland of the University of Ottawa on July 4 (JD 185), 2007, followed by the South Arm station on May 6 (JD126), 2010. The Lower and Middle dGPS' only recorded a few weeks of data in 2007, while the Upper Station recorded data into September 2008. All three stations were reset on July 24 (JD 205), 2009. The Lower Station recorded data between July 2009 and November 2013, while the Middle Station recorded data until June 2011, and again from May 2012 until October 2013. The Middle Station recorded intermittently between July and November 2011. The Upper Station recorded data between July 2009 and October 2013. The South Arm Station recorded data between May 2010 and July 2013, after which the station was removed from the glacier.

In August 2013, an attempt to switch the Lower, Middle and Upper dGPS' to their winter program was unsuccessful due to a software bug, so they continued to record data at 15 second intervals for 24 hours per day into the fall. For this reason, the batteries were drained at all stations throughout winter 2013, and data were only recorded for part of the

season. On March 17, 2014, the stations were reset and recorded data continuously up to July 4, 2014, the end date of the data collection for this study. Table 3.1 provides a summary of dGPS data collected between 2007 and 2014 on the Kaskawulsh Glacier.

3.2 dGPS data post-processing

The Precise Point Positioning (PPP) method used in this study provides positions to within ~2-5 cm horizontal accuracy and ~3-10 cm vertical accuracy without the need for a base station. This method is based on the use of precise orbital and clock information for the GPS satellites, which is made available in its most accurate 'Final' form 13 days after data acquisition (NRCan, 2014). The PPP method produces results consistent with those obtained through other processing methods (e.g., use of base stations), especially when a longer data collection period is processed (Orgiazzi et al., 2005). For example, a study in the central Karakoram by Copland et al. (2009) found that when dGPS data post-processed with NRCan's PPP method was compared with velocities derived from optical feature-tracking, the velocity magnitudes were typically within the estimated error limit for feature-tracking, and variation in motion direction between the two methods was <5%. Zhang and Andersen (2006) and Bartholomew et al. (2010) similarly found this method to be effective to determine surface velocities on the Amery Ice Shelf, Antarctica and on the western margin of the Greenland Ice Sheet, respectively. The high accuracy positions obtained by dGPS along the Kaskawulsh are used to analyze the glacier's horizontal and vertical velocity patterns, and to assess the controls on them.

For this study, raw daily data files in Trimble t01 file format from the Trimble R7 dGPS' were converted to RINEX format in Trimble 'Convert to Rinex' software (version 2.1.7.0), and then post-processed using NRCan's PPP Direct service (online: http://www.nrcan.gc.ca/node/9078) in kinematic mode. The kinematic processing mode produces a corrected track of the dGPS position for every 15-sec sample interval (coordinates in NAD 1983 and ellipsoidal height; NRCan, 2014). These positions were converted to Universal Transverse Mercator (UTM) Zone 7N coordinates using ENVI's 'ASCII Coordinate Conversion' tool. Data acquisition times associated with the 15-sec positions were converted from coordinated universal time (UTC) to local time (UTC -7 hours).

Mean daily positions for each station were calculated by averaging the 15-sec data points available for the day. den Ouden et al. (2010) and Dunse et al. (2012) found that daily averaging significantly reduced the standard deviation in positions derived from dGPS measurements. Mean daily easting and northing displacements on the Kaskawulsh Glacier were calculated by subtracting the positions on one day from the positions the previous day. Seasonal, annual and interannual displacements were calculated by subtracting the mean daily easting and northing coordinates at the end of the measurement period (i.e., season) from the coordinates at the beginning of the period, and dividing by the time interval. Total horizontal displacement (c) was then calculated from the easting (a) and northing (b) coordinates of the displacements using the Pythagorean Theorem:

$$c = \sqrt{(a^2 + b^2)} \quad (1)$$

All horizontal displacement values are quoted in annual velocities (m a^{-1}) for standardization. Trigonometry was used to derive the direction of displacement (in degrees) from the easting and northing values. Short-term variations in horizontal and vertical motion are presented for 2010-2014, when dGPS data are nearly continuous. Seasonal to interannual variations are presented for 2007-2014.

3.3 dGPS base station (data validation)

Data from a semi-permanent, fixed dGPS base station at Kluane Lake Research Station (KLRS; ~25 km NE of the terminus of the Kaskawulsh Glacier) were processed and used to validate the results derived from PPP processing. This base station is comprised of a Trimble R7 receiver attached to the side of a building, and is powered continuously by a battery bank and solar power system. The station has been operated since at least 2009 by Dr. Christian Schoof of the University of British Columbia, and the data are available via a collaborative agreement. These data provide an assessment of the accuracy of the PPP method. Any apparent motion detected using data collected at the fixed dGPS base station provides information on the noise level in the PPP processed data, and can help assess whether changes measured on the glacier are beyond error limits.

The dGPS base station data were post-processed with PPP following the same procedure as for the Kaskawulsh dGPS station data. Two weeks per season in 2011 were chosen at random for processing. Each daily file (with 2 second data intervals) was post-processed and the coordinates converted to UTM. The northing, easting and elevation values were

then averaged for each day. All accuracy estimates are presented at the 95% confidence interval.

3.4 Meteorological data

In addition to the dGPS data, air temperature and snow depth data are used to model and measure surface melt and accumulation rates from 2010 to 2014. Air temperature and relative humidity (RH) loggers were mounted on the four dGPS stations when they were initially installed in July 2007 (Lower, Middle, Upper stations), and May 2010 (South Arm Station). The U23-001 HOBO automatic temperature/RH loggers are mounted inside radiation shields and record measurements every 30 minutes with an accuracy of ±0.2°C and a resolution of 0.02°C for temperature, and an accuracy of ±2.5% and a resolution of 0.03% for relative humidity.

Automated snow depth sounders were installed on the Upper Kaskawulsh and South Arm stations in 2010 (Figure 3.2). In 2013, the snow depth sounder from the South Arm Station was removed in July and reinstalled at the Lower Kaskawulsh Station in August. The Judd Communications LLC snow depth sounders take a measurement every 30 minutes, recording the distance from the instrument to the snow or ice surface with an ultrasonic sensor. These data are recorded on a H22 Hobo Energy Logger Pro via an analog module. An increase in distance between the instrument and surface indicates melt, and a reduction in distance indicates snow accumulation. The accuracy of the snow depth sounder is 1 cm or 0.4% of the distance to the surface with a resolution of 3 mm. In

addition to the snow depth sounder data, snow accumulation at all stations was measured in-situ each spring during the site visit.

An automatic weather station (AWS) located at an elevation of 1845 m on a rock nunatak ~2.5 km northwest of the Upper Kaskawulsh dGPS Station provides additional meteorological data for this study (Figure 3.3). This station is operated by the Geological Survey of Canada (GSC), and the data are available through a collaborative agreement with them. The AWS has been recording air temperature, incoming shortwave solar radiation, and wind speed and direction on an hourly basis since summer 2006. The station is powered by a solar panel connected to two rechargeable 12V batteries. A Campbell Scientific CR10X logger stores the data collected by the different sensors. Air temperature is measured by a Campbell Scientific 107F temperature probe with an accuracy of ±0.2ºC. Wind speed and direction are measured by a R. M. Young 01503 anemometer with an accuracy of ±0.3 m s^{-1} (speed) and ±3º (direction), and incoming radiation is measured by a Kipp and Zonen CM21 pyranometer with an accuracy of ±10% of daily sums.

Given the strong relationship between positive air temperatures and melt (e.g., Hock, 2005), the air temperature record is used to derive surface melt rates back to 2007, and infer spatial and temporal variations in water input to the glacier bed. Surface melt rates were derived as follows:

1) Monthly cumulative positive degree days (PDDs) were calculated for the Upper dGPS Station and compared to those from the AWS for periods when both stations operated simultaneously. This comparison showed a strong relationship between these variables ($R^2 = 0.99$; Figure 3.4), so data from the AWS were used to complete the summer temperature record for the Upper dGPS Station for the entire study period.

2) Using the reconstructed PDD record for the Upper dGPS Station, a relationship between monthly cumulative PDDs and melt measured at the station was established for each summer month. These monthly ratios were then applied to months when melt wasn't measured at the station (Table 3.2, method a). Overall, 60% of monthly melt values were measured directly at the Upper Station, while 40% were derived based on this method.

3) Using the monthly ratios between melt measured at the Upper Station and South Arm Station (or Lower Station, in 2014), melt rates on the lower glacier were calculated for months when no melt rates were measured there (Table 3.2, method b). Melt measured at the South Arm Station is assumed to represent melt on the lower glacier (i.e., the Lower Station). Overall, 38% of melt rates were measured directly at the South Arm or Lower stations, while 62% were derived based on the extrapolation of monthly melt ratios from the Upper Station. Finally, melt rates at the Middle Station were calculated as the average between melt rates on the lower and upper glacier (Table 3.2, method c).

All melt rates were standardized to cm snow water equivalent (SWE), with May melt assumed to be snow with a density of 0.51 g cm^{3}, and June-September melt assumed to be ice with a density of 0.90 g cm^{-3} (insignificant melt occurred between October and April). Monthly melt rates for May to September each year were summed to obtain total annual melt values.

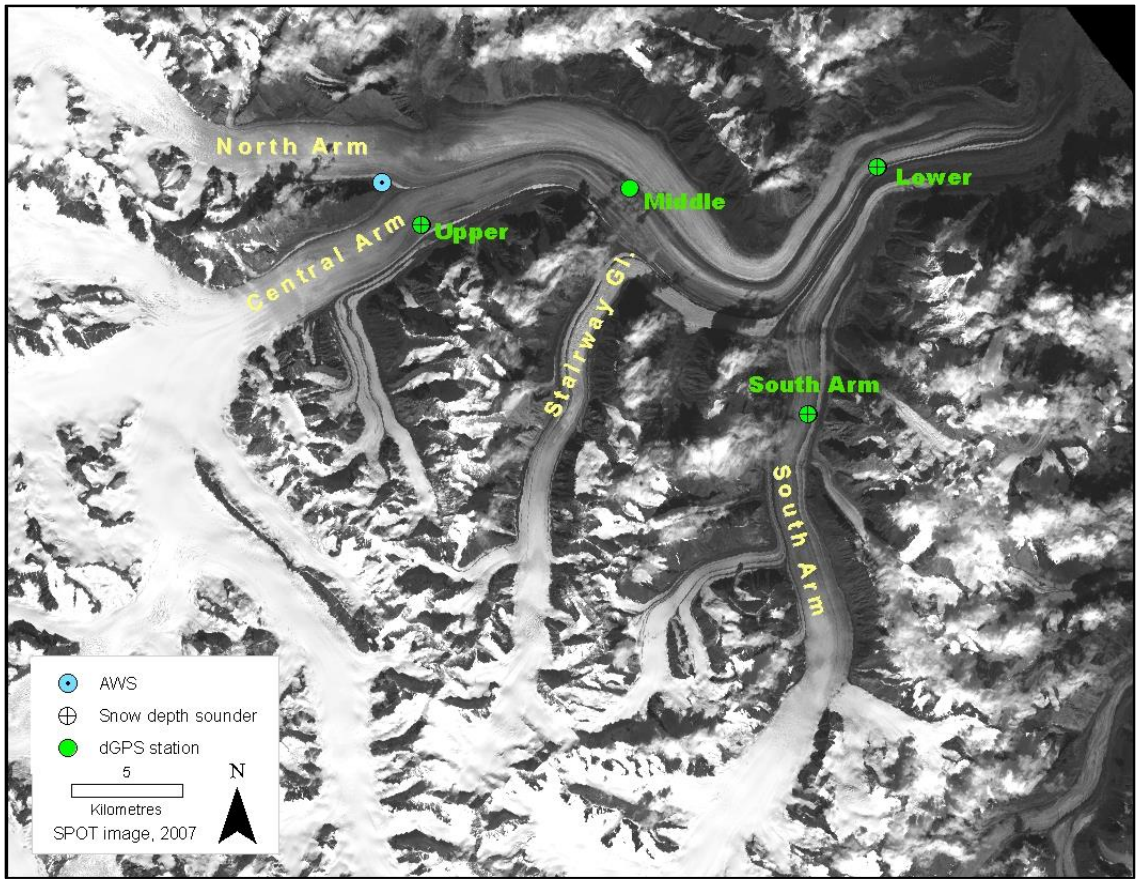

Figure 3.1 Map of Kaskawulsh Glacier showing location of dGPS stations, the automatic weather station (AWS), and snow depth sounders.

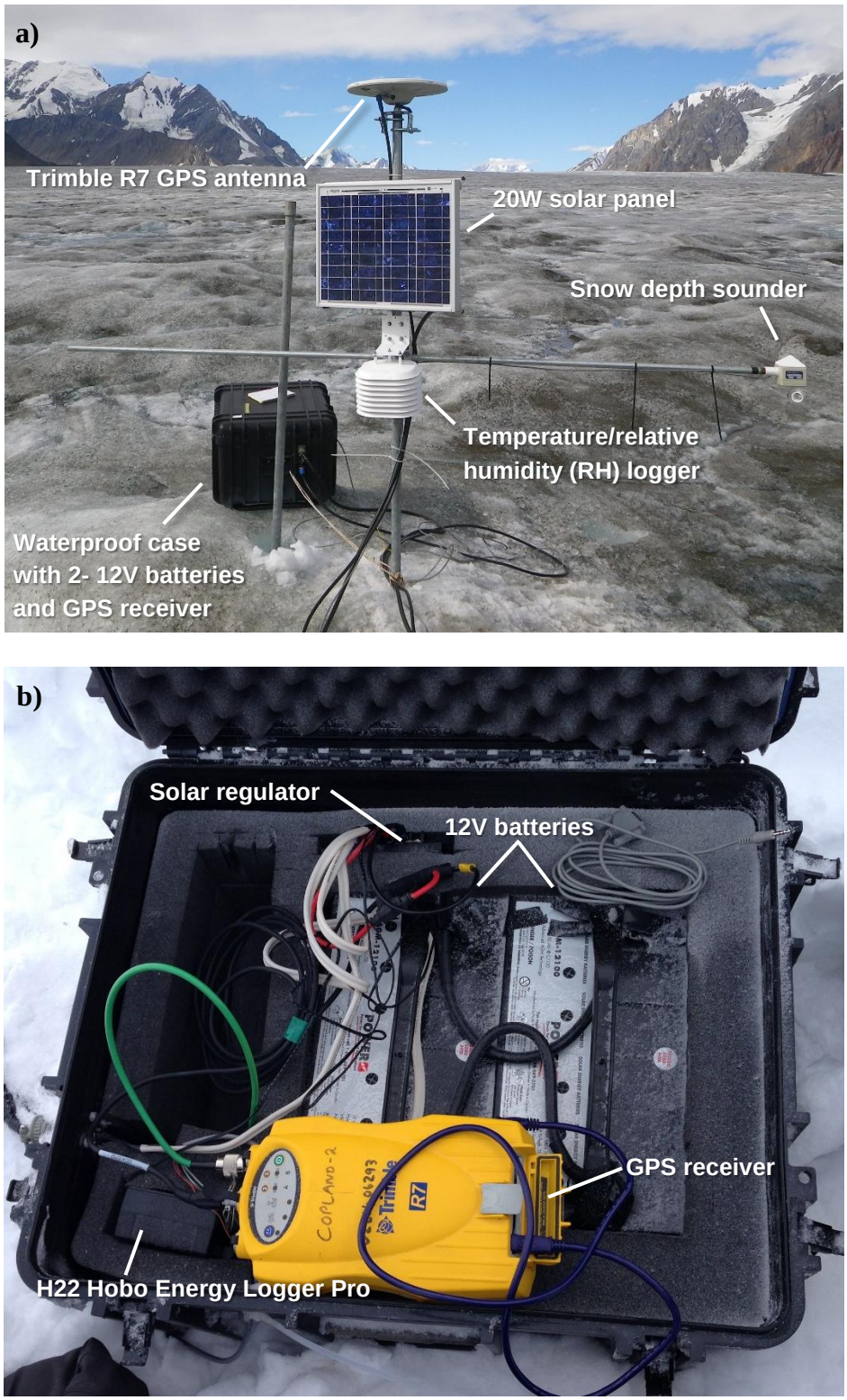

Figure 3.2 Upper Kaskawulsh Glacier a) dGPS station set up with temperature logger and snow depth sounder in July 2013, and b) view inside the waterproof case.

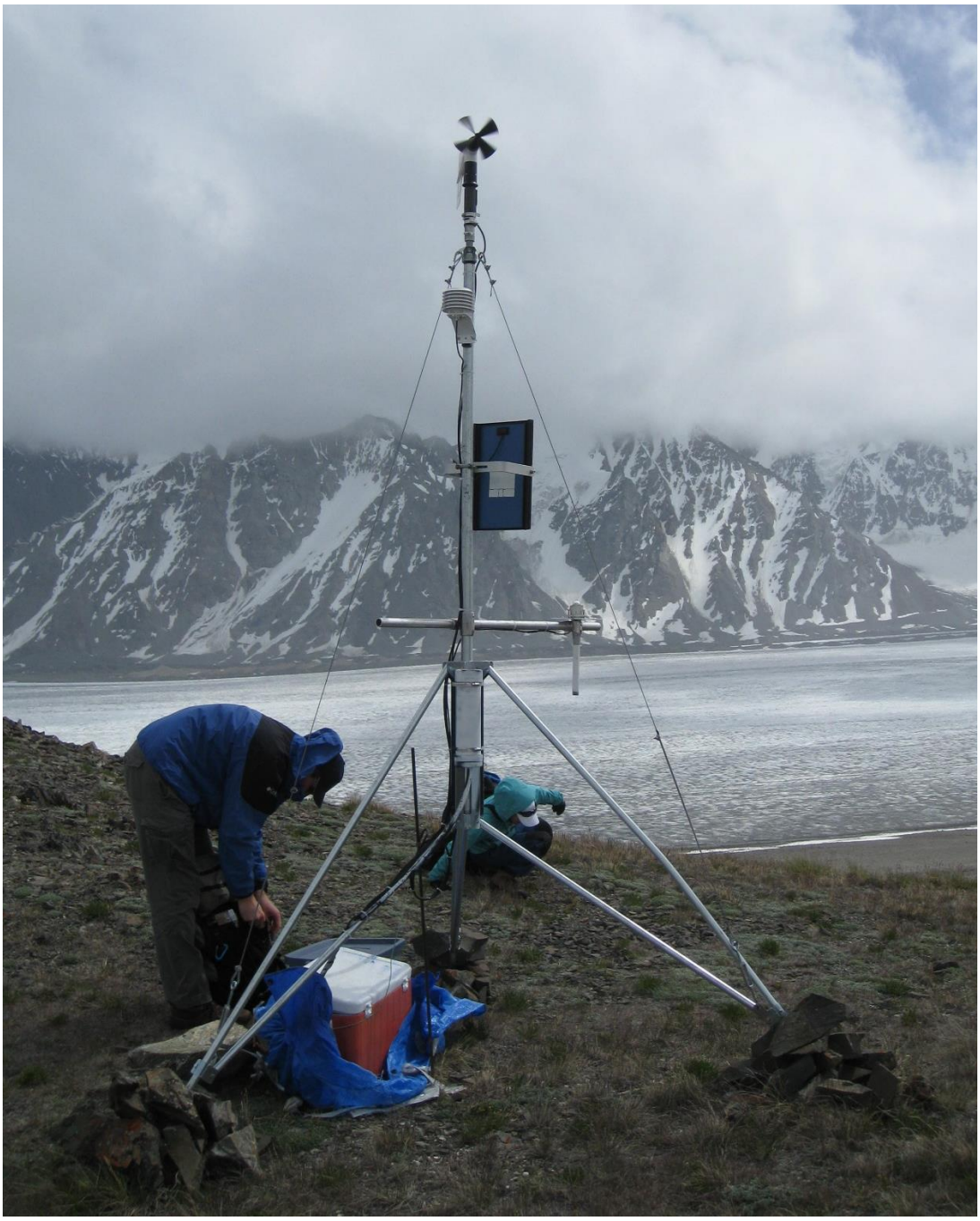

Figure 3.3 Geological Survey of Canada automatic weather station, July 2010.

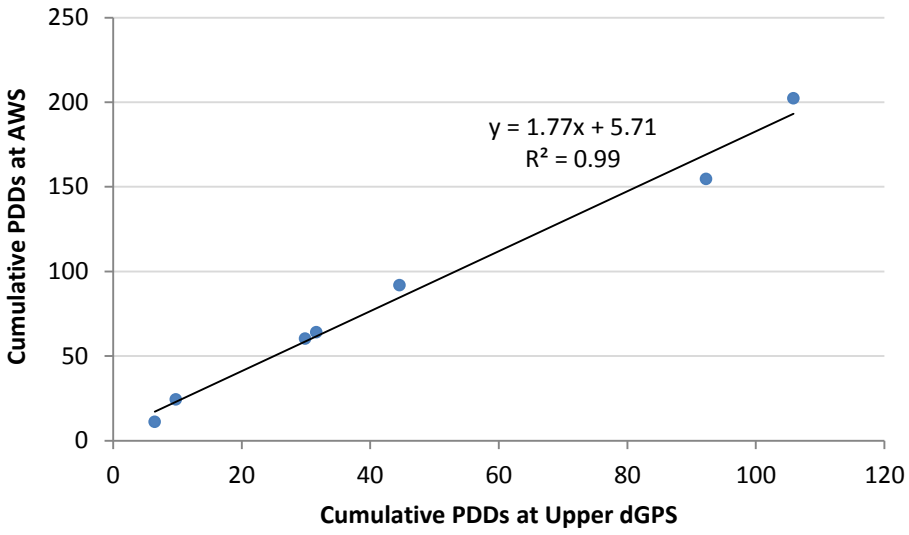

Figure 3.4 Relationship between monthly cumulative PDDs at the AWS and at the Upper dGPS Station, 2007-2014.

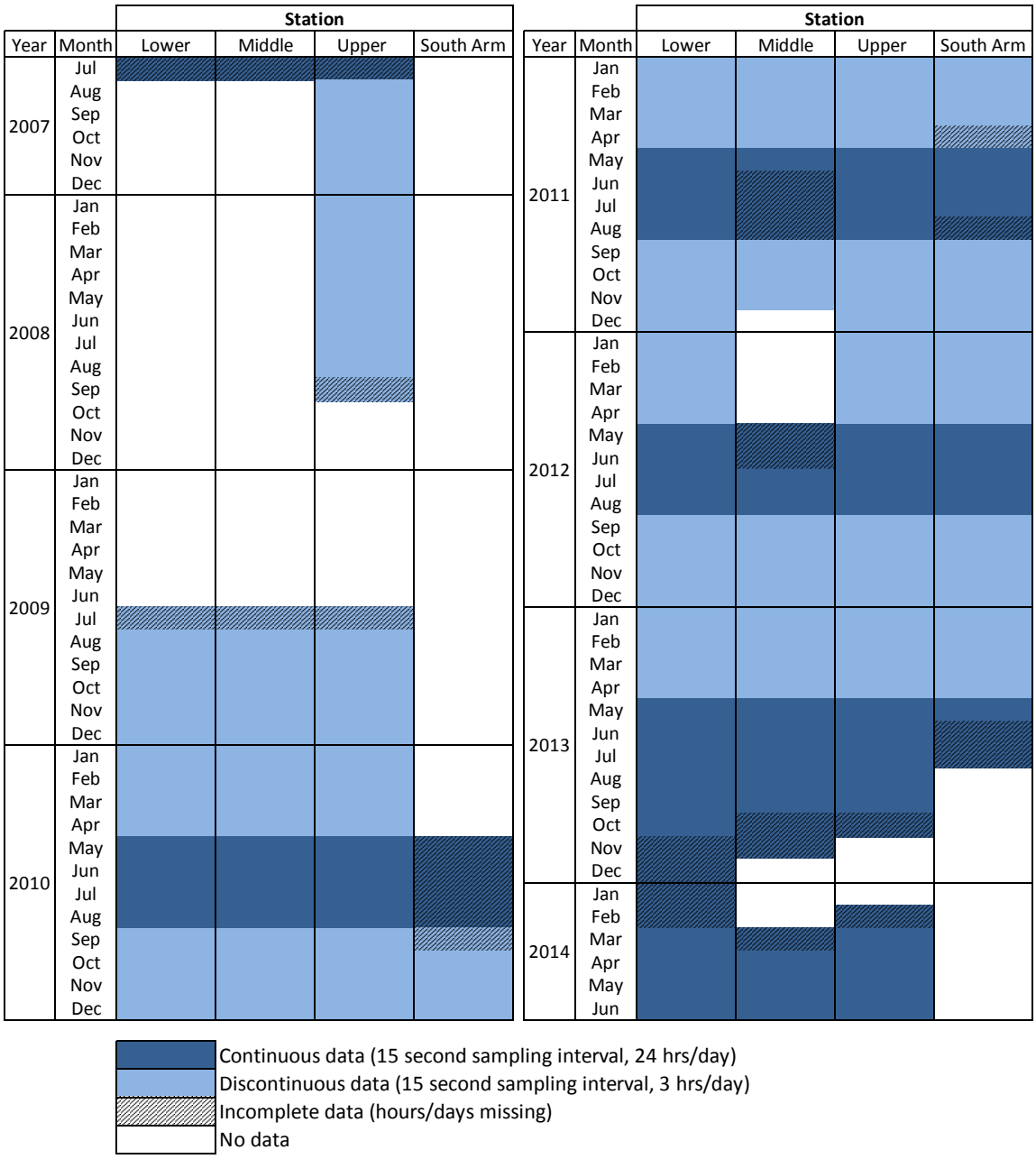

Table 3.1 Availability of dGPS data collected at Kaskawulsh Glacier stations between 2007 and 2014.

Surface melt (cm SWE)				
Year	Month	Lower	Middle	Upper
2007	May	*20.6* [b]	*17.8* [c]	*14.9* [a]
	Jun	*129.1* [b]	*132.8* [c]	*136.5* [a]
	Jul	*109.4* [b]	*117.0* [c]	124.6
	Aug	*152.1* [b]	*139.8* [c]	127.4
	Sep	*8.4* [b]	*8.3* [c]	8.1
	Annual	**419.6**	**415.6**	**411.5**
2008	May	*41.4* [b]	*35.7* [c]	*30.0* [a]
	Jun	*73.2* [b]	*75.3* [c]	*77.4* [a]
	Jul	*99.3* [b]	*106.2* [c]	*113.0* [a]
	Aug	*98.5* [b]	*90.5* [c]	*82.5* [a]
	Sep	*15.8* [b]	*15.5* [c]	*15.2* [a]
	Annual	**328.1**	**323.1**	**318.2**
2009	May	*35.1* [b]	*30.3* [c]	*25.5* [a]
	Jun	*129.7* [b]	*133.4* [c]	*137.1* [a]
	Jul	*204.7* [b]	*218.9* [c]	*233.1* [a]
	Aug	*131.4* [b]	*120.8* [c]	*110.1* [a]
	Sep	*18.2* [b]	*17.9* [c]	*17.5* [a]
	Annual	**519.1**	**521.2**	**523.3**
2010	May	44.7	*28.8* [c]	*13.0* [a]
	Jun	135.8	*139.7* [c]	*143.6* [a]
	Jul	156.9	*161.0* [c]	165.0
	Aug	*135.9* [b]	*124.9* [c]	113.8
	Sep	27.4	*28.7* [c]	29.9
	Annual	**500.7**	**483.0**	**465.3**
2011	May	53.8	*46.5* [c]	*39.1* [a]
	Jun	126.9	*112.4* [c]	98.0
	Jul	136.1	*157.7* [c]	179.3
	Aug	79.4	*73.0* [c]	66.6
	Sep	*5.1* [b]	*5.0* [c]	5.0
	Annual	**401.4**	**394.6**	**387.8**
2012	May	*9.6* [b]	*8.3* [c]	6.9
	Jun	*77.8* [b]	*80.1* [c]	82.3
	Jul	*123.3* [b]	*131.8* [c]	140.4
	Aug	*142.1* [b]	*130.6* [c]	119.1
	Sep	*14.3* [b]	*14.0* [c]	13.8
	Annual	**367.1**	**364.7**	**362.4**
2013	May	37.9	*32.2* [c]	26.4
	Jun	105.0	*122.9* [c]	140.9
	Jul	164.1	*167.9* [c]	171.8
	Aug	*184.1* [b]	*169.2* [c]	154.2
	Sep	55.8	*51.2* [c]	46.6
	Annual	**546.9**	**543.4**	**539.9**
2014	May	47.4	42.7	38.0
	Jun	112.2	83.1	53.9
2007-2014 average		**440.4**	**435.1**	**429.8**

Table 3.2 Monthly and annual surface melt at the Kaskawulsh dGPS stations. Values in black were measured, while values in blue italics were calculated from air temperature data. Superscript refers to methods described in Section 3.4.

Chapter 4 : Results

In this chapter, the velocity regime of the Kaskawulsh Glacier is described. First, a brief validation of the dGPS results is presented. Next, detailed velocity patterns at the interannual, annual and seasonal timescales derived from dGPS measurements are presented, followed by a summary of meteorological conditions. As outlined in Table 3.1, dGPS data were collected at four stations across the glacier between 2007 and 2014. Interannual velocity patterns are presented for 2007-2014, while intra-annual patterns are presented for 2010-2014 when the dGPS data record is nearly continuous.

4.1 dGPS results validation

The dGPS measurements at the fixed KLRS base station provide an estimate of error limits associated with processing data with PPP. For daily averaging of positions at 2-second intervals, the 95% confidence interval (1.96 x standard distance) for the horizontal position is 0.050 m, and the 95% confidence interval (1.96 x standard deviation) for elevation is 0.097 m (Figure 4.1). The 95% confidence interval for averaged daily positions over a weekly or monthly period is 0.024 m for horizontal position and 0.035 m for elevation (Figure 4.2). These standard distance and standard deviation values confirm that dGPS measurements post-processed with PPP are accurate to within ~2-5 cm in horizontal position and ~3-10 cm in vertical location.

To further demonstrate the effectiveness of the dGPS measurements to determine daily variations in ice motion, it is useful to plot the daily change in northing and easting coordinates of each station (Figure 4.3). These plots demonstrate that ice motion is

clearly detectable over this timescale, with the typical daily motion of ~0.3 m day^{-1} much higher than the horizontal or vertical errors in the PPP processing mentioned above. There is generally little variability in ice motion direction over the period of either a month (Figure 4.3), or the multi-annual period 2010-2013 (Figure 4.4). The close alignment between the long-term ice motion direction and medial moraines also provides evidence that the methods outlined in Chapter 3 produce accurate results (Figure 4.4; Van Wychen et al., 2012). In addition, a comparison of ice velocities and direction of motion derived from speckle tracking of pairs of Radarsat-2 satellite scenes with overlapping periods of dGPS measurements on the Kaskawulsh Glacier provides further verification of the accuracy of on-ice measurements (Table 4.1 and Table 4.2). Velocities derived from dGPS measurements are, on average, within 8% of those derived by speckle tracking, while direction of motion derived from the two methods are within 1-5° (Darling, 2012; Waechter, 2013).

4.2 Interannual velocity patterns

The long-term (~5-year) average horizontal displacement for the Kaskawulsh Glacier ranges between 141.3 and 164.3 m a^{-1}, while the long-term average vertical displacement ranges between 0.6 and 4.5 m a^{-1} (Table 4.3, Figure 4.5). The long-term displacement direction is 54.8° at the Lower Station, 124.3° at the Middle Station, 45.2° at the Upper Station, and 9.8° at the South Arm Station (Table 4.3). The largest difference in annual direction of motion was observed at the Lower Station, with direction varying up to 8.6° from the long-term direction. The annual displacement direction at all other stations was within 4.8° of the long-term direction.

The average horizontal and vertical displacement values and the direction of motion are based on annual displacements between JD 101 and JD 100 the following year. For years where no data were available on these dates, the position of the station(s) was interpolated based on the measured positions closest to the dates, which were no more than 25 days apart. Since glacier horizontal and vertical motion in the winter months is relatively stable (Figure 4.6 and Figure 4.7), a linear interpolation was used. Only the positions of the South Arm Station 2010 and of the Middle Station in 2012 were interpolated. For the Upper Station, the long-term averages are based on 6 years of data (2007-2008 and 2009-2014), while for the Middle and Lower stations the averages are based on 5 years of data (2009-2014). For the South Arm Station, the long-term averages are based on 3 years of data (2010-2013). The highest overall average horizontal displacement is at the Lower Station, at 164.3 m a^{-1}, followed by the South Arm Station at 159.9 m a^{-1}. The highest average vertical displacement, 4.5 m a^{-1}, is at the South Arm Station, and is nearly double the vertical displacement at the Lower Station (2.4 m a^{-1}). The minimum average displacements are at the Middle Station, with 141.3 m a^{-1} of horizontal displacement and 0.6 m a^{-1} of vertical displacement.

Between 2007 and 2014, annual velocities were typically within ±10% of the long-term average at all stations, with the exception of the Middle Station where 2011-12 and 2012-13 annual velocities were within ±18% of the long-term average (Table 4.3). Maximum annual velocities were observed in 2007-08 (at the Upper Station only, up to 8.6% higher than the long-term average) and in 2012-13 (at all other stations). The 2012-13 difference from the long-term average velocity was highest at the Middle Station

(18.3%), followed by the Lower, Upper and South Arm stations with differences of 10.1%, 7.3% and 5.9%, respectively. Minimum annual velocities were observed in 2011-12 at the Lower, Middle and South Arm stations with differences from the long-term average velocity of -7.0%, -16.3% and -4.2%, respectively. The minimum annual velocity at the Upper Station was observed in 2013-14 with a -5.7% difference from the long-term average velocity. Annual velocities do not appear to follow an increasing or decreasing trend over the period of study (Figure 4.5).

4.3 Intra-annual velocity patterns

The Kaskawulsh Glacier undergoes marked variations in intra-annual motion that are typically consistent between stations and from one year to the next (Figure 4.6 to Figure 4.8). These patterns can be broken down into four main seasonal regimes, with unique horizontal motion and vertical uplift patterns for each. The periods used to define the seasons are therefore based on these velocity variations, rather than following traditional climatological definitions. The direction of motion remains nearly constant between seasons (Figure 4.4), so only the horizontal and vertical motion patterns are described in detail in the following sections.

4.3.1 Winter regime

The winter regime is defined as JD 1 to JD 110, and is characterized by low velocities and relatively low variability in daily average velocities (Figure 4.6). Average winter velocity (calculated for years 2010-2013, when data were available for all stations) at the Central Arm (Lower, Middle, Upper) stations ranged between 115.8 and 143.7 m a^{-1}

(Figure 4.9, Table 4.4). At the South Arm Station, average winter velocity was 154.2 m a^{-1}. The highest winter velocities for the 2008-2014 period were observed in 2008 and 2013, while the lowest velocities were observed in 2014. In 2008, average winter velocity at the Upper Station was 153.2 m a^{-1}, and in 2013, average velocities on the Central Arm ranged between 123.3 and 147.4 m a^{-1}, and were 161.9 m a^{-1} at the South Arm Station. Winter velocities typically ranged between ~100 and 170 m a^{-1}, although velocities as high as 232 m a^{-1} occurred during short-term motion events.

The timing and number of high velocity events was variable from one winter to another, although they all shared the same characteristics of initiating at the top of the Central Arm and propagating downglacier (these events are described further in Section 4.4.1). One to two events were observed at these stations each winter from 2010 to 2014, with the exception of 2013 when no short-term motion event was clearly discernable (although there was a marked event in fall 2012). In winter 2013, velocities at the Central Arm stations were much more variable than in other years. Following winter motion events, horizontal velocities at the Central Arm stations typically increase by 5 to 15%. In late winter (JD 90 to 110), velocities were typically ~5% higher than the average winter velocities for that year. Late winter velocities continued to have low variability into early spring.

During the winter regime, the Lower and Middle stations undergo constant vertical uplift with peaks in uplift associated with peaks in horizontal velocity during the winter motion events (Figure 4.7). The vertical position of the Upper Station decreased slightly

throughout the winter in 2010 and 2011, and stayed relatively stable in 2012 and 2013. In 2014, the vertical position of the Upper Station increased throughout the season. The vertical position of the South Arm Station also typically decreased throughout the winter (i.e., surface lowering), except for in 2011 when the station underwent vertical uplift. The Upper Station only underwent minor surface uplift during horizontal velocity events, while there was no vertical change at the South Arm Station during these events.

4.3.2 Spring regime

The spring regime, defined as JD 110 to JD 165, is dominated by a large peak in horizontal motion and vertical uplift observed across both the Central and South Arms of the glacier (Figure 4.6 and Figure 4.7). For the period 2010-2014, the increase in horizontal velocity began at the Lower Station between JD 121 and JD 135, and propagated upglacier (these events are described in detail in Section 4.4.2.). The earliest spring event initiation was in 2014 (on JD 121), and the latest was in 2011 (JD 135). In most years, the maximum annual velocity at the lower stations (i.e., Lower and South Arm stations) was reached during the spring speed-up event. Average 2010-2013 spring velocities at the Central Arm stations ranged between 159.3 m a^{-1} at the Upper Station and 217.4 m a^{-1} at the Lower Station (Figure 4.9, Table 4.4). At the South Arm station, average spring velocity was 200.0 m a^{-1}. Maximum spring velocities for the 2008-2014 period were observed in 2013 and ranged between 173.6 m a^{-1} at the Upper Station and 245.3 m a^{-1} at the Lower Station. Minimum spring velocities were observed in 2014 and ranged between 137.6 m a^{-1} at the Upper Station and 188.4 m a^{-1} at the Lower Station.

The spring motion events were accompanied by a period of rapid vertical uplift observed at the Lower and South Arm stations (Figure 4.7). Vertical uplift peaked simultaneously with, or shortly after, the peak in horizontal motion. Vertical height increases of up to 1 m occurred over a period of 1-4 weeks, followed by a period of pronounced downward motion (up to 1.5 m over a 2-week period). At the Middle and Upper stations, vertical uplift during the spring speed-up event was relatively small, ranging from 0.1 to 0.2 m.

4.3.3 Summer regime

The summer regime is defined as JD 165 to JD 270. It is characterized by high velocities, high variability in velocities, and a long-term reduction in average velocity throughout this season (Figure 4.6). During the summer, velocities typically range between 150 and 350 m a^{-1}, and can reach up to 520 m a^{-1}. Average summer velocities for 2010-2013 ranged between 173.7 and 184.5 m a^{-1} at all stations (Figure 4.9, Table 4.4). Frequent short speed-up events were observed each summer, during which velocities increased by up 220% over the period of a few days before returning to previous velocities over a similar period. These events occur simultaneously or nearly simultaneously at all stations, and typically occurred in the first half of the summer regime. In the second half of summer, the variability and magnitude of horizontal velocities decreased steadily into the fall regime. Two unique late season speed-up events occurred in 2012, between JD 261 and JD 274, and JD 278 and 290, when velocities were up to 300% higher than background velocities. These were the only such late summer events in the 5-year record, and are described in detail in Section 4.4.3. Vertical position decreased throughout the

summer, at approximately the same rate as after the spring peak, until late summer when the vertical position plateaued (Figure 4.7).

4.3.4 Fall regime

The fall regime, from JD 270 to JD 365, is characterized by minimum annual velocities and low variability in daily velocities (Figure 4.6). Daily velocities typically reach an annual minimum in fall and remain fairly constant throughout the fall and into the start of winter. Daily horizontal velocities were between 90 and 165 m a^{-1}. Long-term average seasonal velocities were between 133.3 and 142.7 m a^{-1} at all stations (Figure 4.9, Table 4.4). Similar to horizontal velocity, vertical uplift reaches a minimum in fall and typically remains stable at all stations throughout this season (Figure 4.7).

4.4 Short-term velocity events

As briefly described above, three types of speed-up events were observed on the glacier: an upglacier propagating velocity event in spring, a number of simultaneous speed-up events during the melt season, and up to two downglacier propagating events in the late fall and winter (Figure 4.10). The timing, duration and magnitude of velocity events were variable. All three types of events were accompanied by some change in vertical motion.

4.4.1 Downglacier propagating motion events

Up to two downglacier propagating events occurred after the end of the melt season every year; in most years they occurred in the following winter, but in 2012 a downglacier propagating event occurred in the fall (Figure 4.6). These events were observed at all the

Central Arm stations, but not at the South Arm Station. In 2010 and 2011, two winter speed-up events were observed, while in all other years only one event was observed. The events always initiate at the Upper Station and propagate downglacier (Figure 4.10a). The timing varies from year to year, with events peaking as early as JD 320 (e.g., in 2012), and as late as JD 81 (e.g., in 2014). The peak velocity during winter motion events was reached 3-5 days after event initiation, propagating downglacier over 8-10 days at speeds of 1.8 to 2.5 km day^{-1}. The peak was most pronounced at the Lower Station, followed by the Middle and Upper stations, respectively. Peak velocities at all stations were typically 110-170% higher than background winter velocity. Peak velocities during the fall 2012 event were in a similar range, between 115-180% higher than the background fall velocity. The peaks in horizontal velocity were accompanied by a short period of increased vertical uplift (which was most pronounced at the Lower Station), followed by a return to the previous rate of uplift (Figure 4.7, Figure 4.10a).

4.4.2 Upglacier propagating motion events

A major speed-up event was observed each spring across the Kaskawulsh Glacier (Figure 4.6). The events begin at the Lower Station and propagate upglacier (Figure 4.10b). At the Middle, Upper and South Arm stations, the spring event was typically initiated ~10 days after the acceleration was observed at the Lower Station. The peak in horizontal velocity was reached 2-4 weeks after the event initiation and propagated upglacier over 1-3 days at speeds of 3-10 km day^{-1}, and sometimes as fast as 20 km day^{-1} (e.g., in 2012). Peak horizontal velocities during the events were 160-350% higher than background velocities and ranged from 381 to 521 m a^{-1} at the Lower Station, from 271 to 322 m a^{-1}

at the Middle Station, from 220 to 257 m a^{-1} at the Upper Station, and from 363 to 448 m a^{-1} at the South Arm Station. The peaks in horizontal velocity were accompanied by an equivalent period of increased vertical uplift most pronounced at the Lower and South Arm stations, followed by significant surface lowering at all stations (Figure 4.7).

4.4.3 Simultaneous motion events

A number of simultaneous or nearly-simultaneous motion events occurred each year throughout the summer and sometimes into early fall (Figure 4.6). Simultaneous motion events are typically observed in the first half of the summer regime, with horizontal velocities reaching up to 300% higher than the seasonal background over the period of a few days (Figure 4.10c). Late summer and fall 2012 stand out as two periods when large motion events were observed across the glacier. These events occurred within a few weeks of each other between JD 262 and JD 285, and the peak velocity for each event was reached 3 to 6 days after its initiation. Peak velocities were 160-300% higher than background velocities during the first event, and 110-240% higher during the second event. The peak was most pronounced at the Middle Station, followed by the Lower Station and then the Upper Station. The peak at the South Arm Station during the second event was negligible. During these events, vertical uplift peaked at all stations simultaneously with horizontal motion, followed by a return to the previous rate of motion (Figure 4.7).

4.5 Meteorological conditions

Air temperature, together with melt and accumulation rates, showed marked temporal and spatial variability across the study area. For 2007-2014, average daily air temperature ranged between -35.6 and 12.4°C across the glacier. At the AWS, average daily air temperatures were typically 2.5 to 4°C warmer than on the glacier and ranged between -29.9 and 17.4°C over the period 2007-2014. The 2007-2013 average annual temperature was -4.8°C at the Lower Station, -7.0°C at the Middle Station, -6.9°C at the Upper Station, and -6.3°C at the South Arm Station (Table 4.5). This compares to an average annual temperature of -2.9°C at the AWS. The lapse rate between the Lower and Middle stations is -0.58°C per 100 m elevation, while the lapse rate between the Middle and Upper stations is negligible. 2012 stands out as the coldest year on record, with average annual temperatures 0.5 to 1.1°C below the long-term average. 2009, 2010 and 2013 were 0.5 to 0.8°C warmer than average across the glacier, with the exception of the Lower Station in 2010 which had an average annual temperature equal to the long-term average.

The long-term average (2007-2014) melt season dates were JD 128 to JD 277 at the Lower Station, and JD 137 to JD 274 at the Middle and Upper stations, with an average duration of 148 days (Lower Station) and 135 days (Middle and Upper stations) (Table 4.6). These were defined from days above 0°C. Melt at the Middle and Upper stations typically begins a few days to a few weeks after melt begins at the Lower Station. The end date of the melt season is often similar across the glacier, but can be up to 13 days later at the Lower Station than at the Middle and Upper stations. Total annual melt varies

slightly across the glacier, with melt at the Lower Station typically 10-35 cm SWE greater than melt at the Upper Station (Table 3.2). The highest monthly melt typically occurs in July, followed by either June or August, depending on the year. The long-term (2007-2014) average melt is 440.4 cm SWE at the Lower Station, 435.1 cm SWE at the Middle Station, and 429.8 cm SWE at the Upper Station (Table 3.2). Minimum annual melt rates were observed in 2008, when they ranged between 318.2 cm SWE at the Upper Station and 328.1 cm SWE at the Lower Station. The highest melt rates on record were observed in 2013, and ranged between 539.9 and 546.9 cm SWE across the glacier (Figure 4.11, Table 3.2). Snow accumulation is highest at the Upper Station, with a long-term average annual accumulation of 66.3 cm SWE (Table 4.7). At the South Arm Station, the long-term average snow accumulation is just over half of that at the Upper Station, at 38.6 cm SWE. The snowpack was greatest in winter 2011-12 with 85.9 cm SWE of accumulation at the Upper Station. In winter 2012-13, the snowpack was much lower than average, with only 36.2 cm SWE of accumulation at the Upper Station.

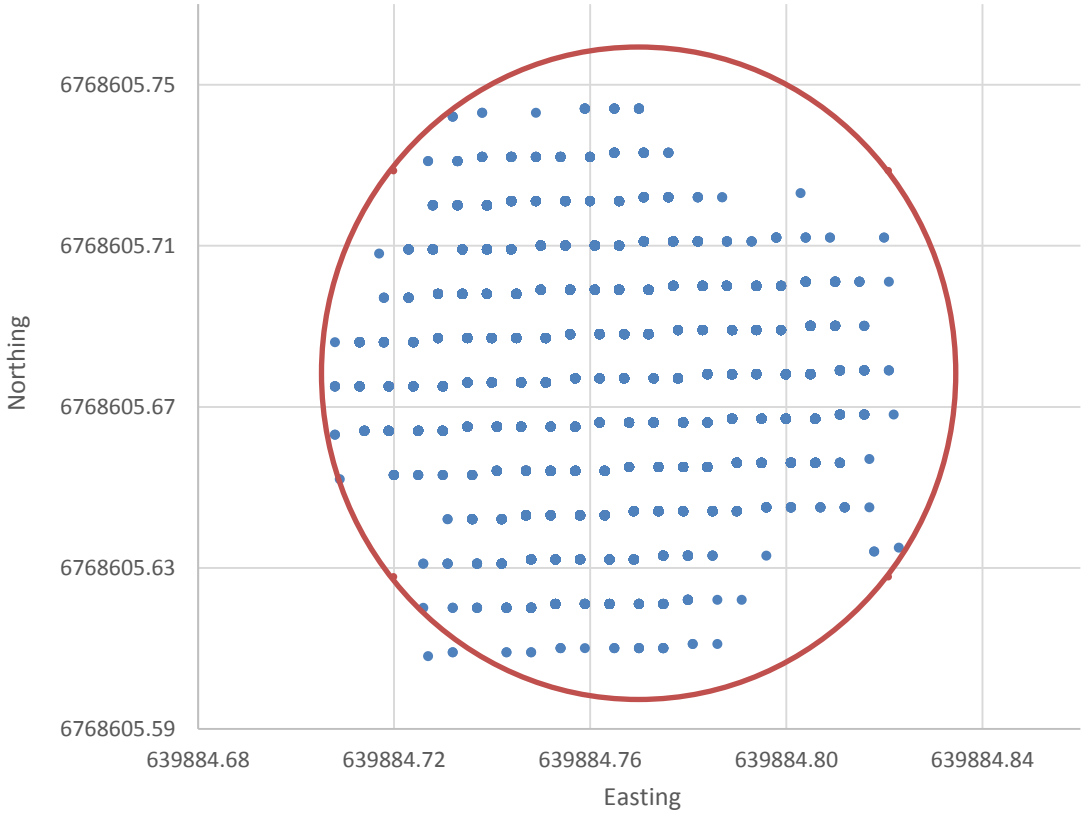

Figure 4.1 Computed horizontal position of KLRS dGPS base station at 2-second intervals over a 24-hour period (JD 191, 2011). The red circle shows the 95% confidence interval (1.96 x standard distance). Coordinates are in UTM Zone 7N. The gridded pattern of the positions is due to the limited precision of the latitude and longitude information produced by the PPP processing, prior to conversion to UTM coordinates.

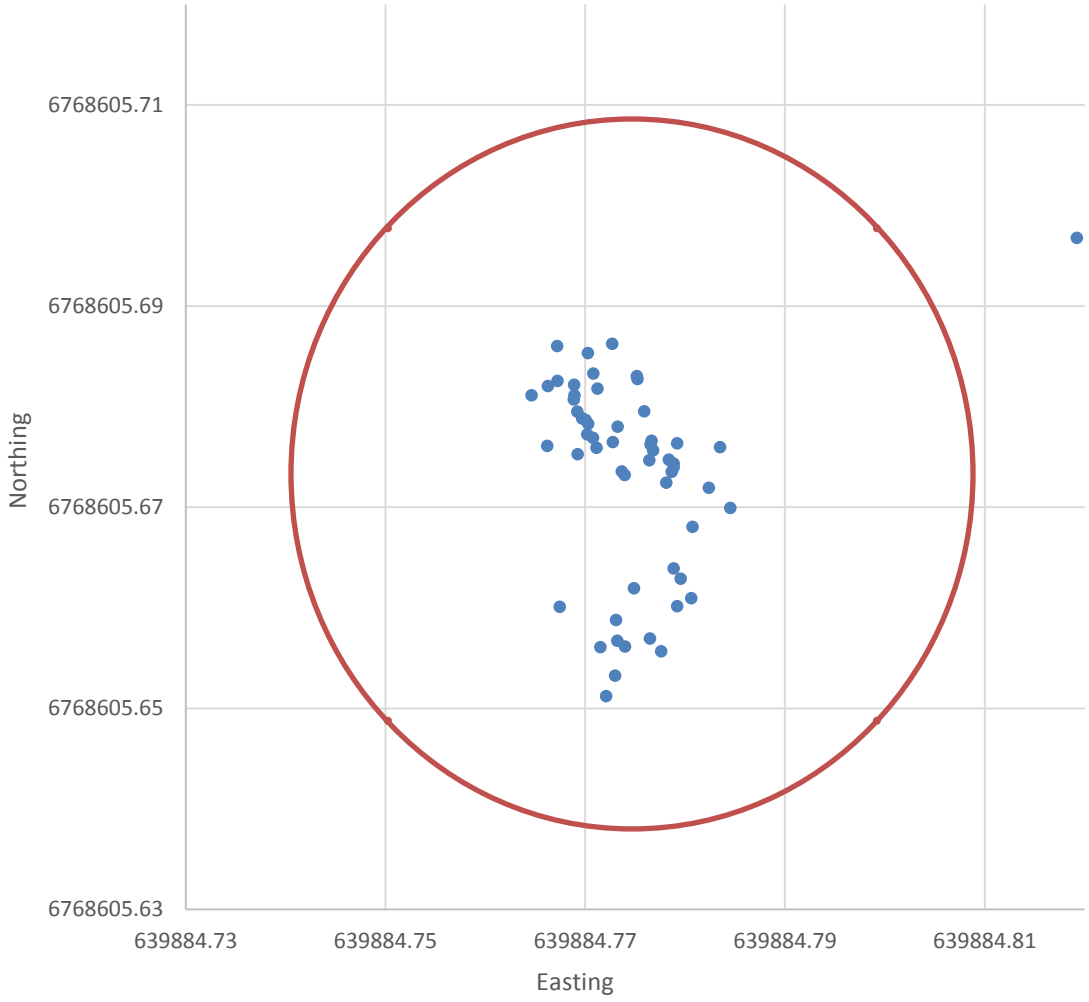

Figure 4.2 Computed average daily horizontal position of KLRS dGPS base station for 2 weeks per season in 2011. The red circle shows the 95% confidence interval (1.96 x standard distance). Coordinates are in UTM Zone 7N.

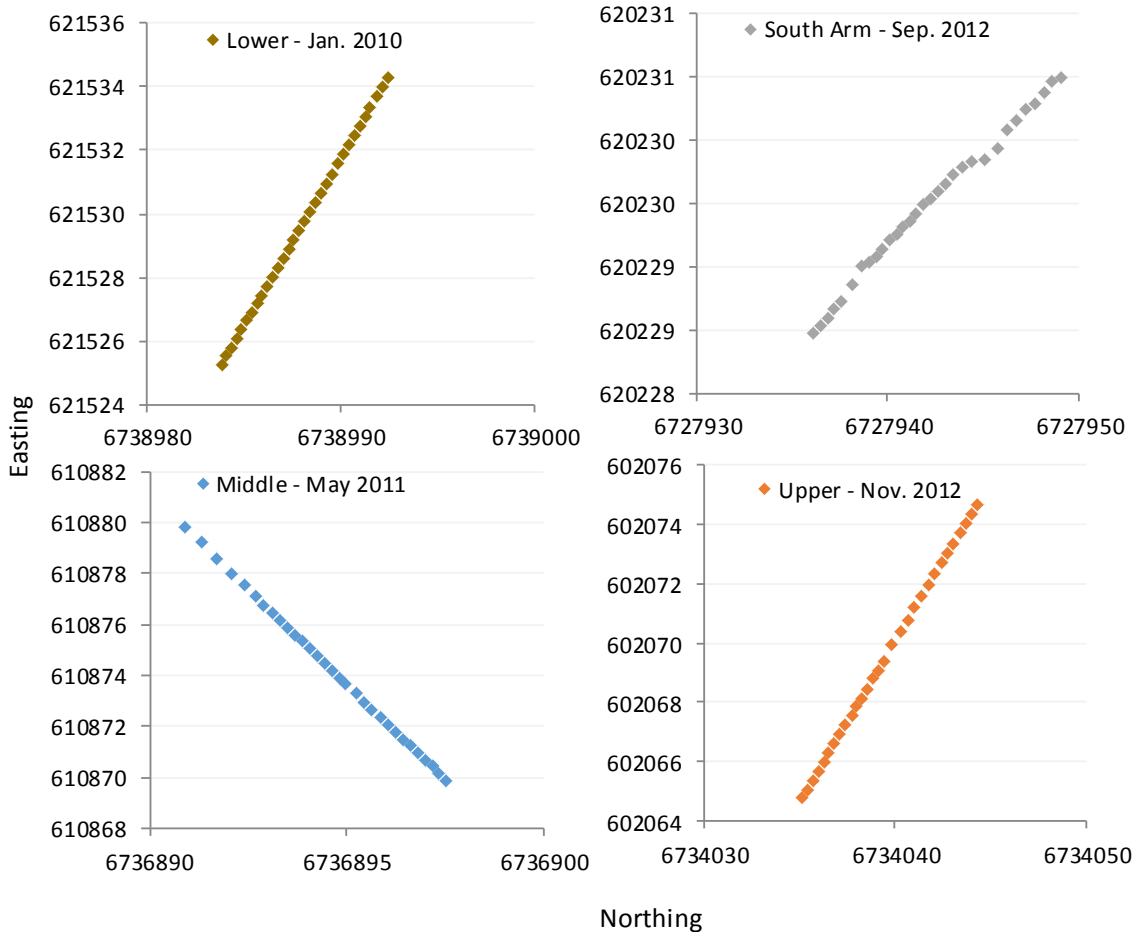

Figure 4.3 Daily position in UTM Zone 7N of Kaskawulsh dGPS stations during one month per season in 2010-2012.

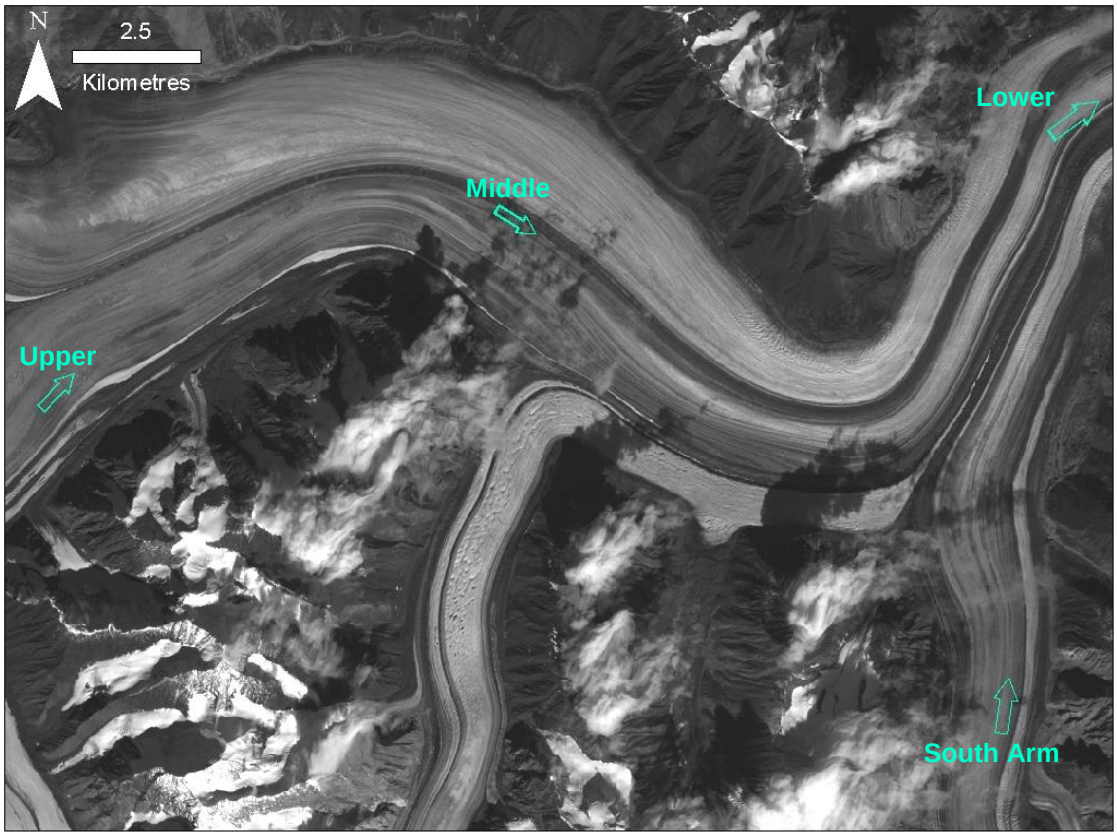

Figure 4.4 Long-term direction of motion of Kaskawulsh dGPS stations (JD 1, 2010 – JD 1, 2013).

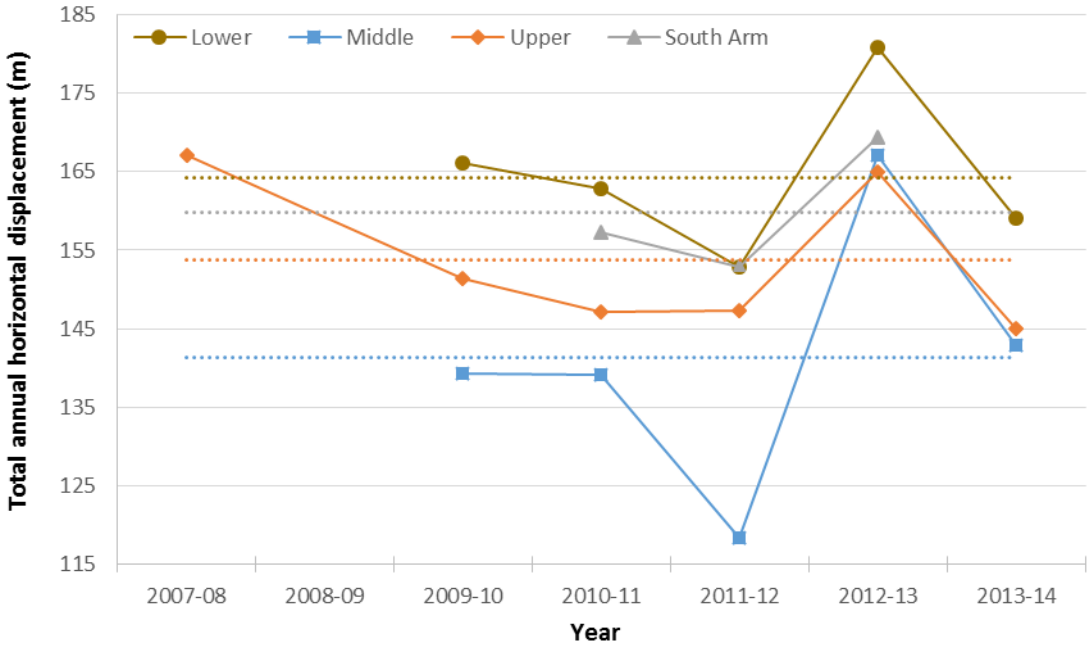

Figure 4.5 Total annual horizontal displacement of Kaskawulsh stations derived from dGPS measurements between JD 101 and JD 100 the following year, for 2007-08 to 2013-14. Dotted lines show the long-term average annual displacement for each station.

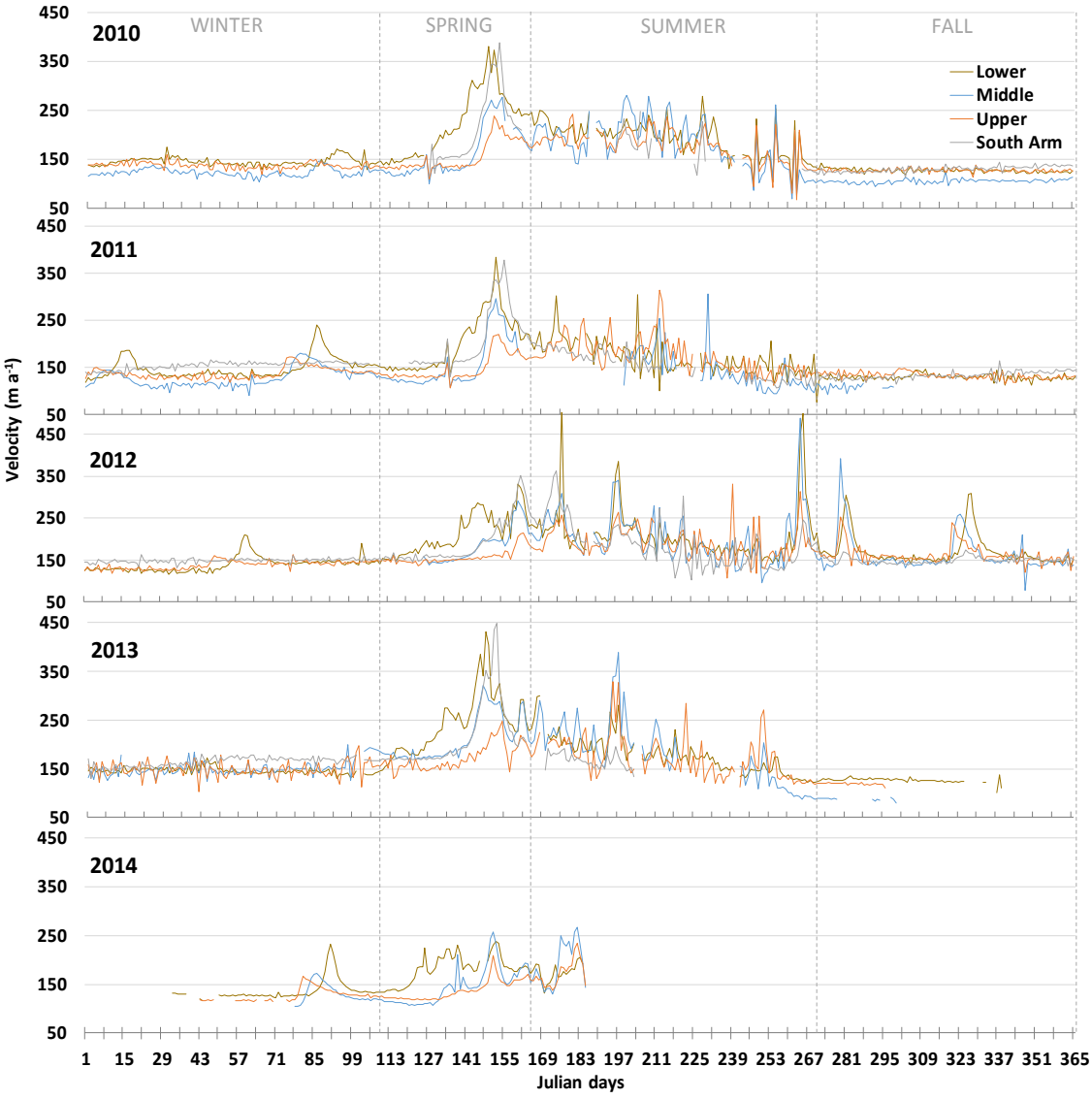

Figure 4.6 Horizontal velocity derived from mean daily dGPS position of Lower, Middle and Upper Kaskawulsh and South Arm stations for 2010-2014.

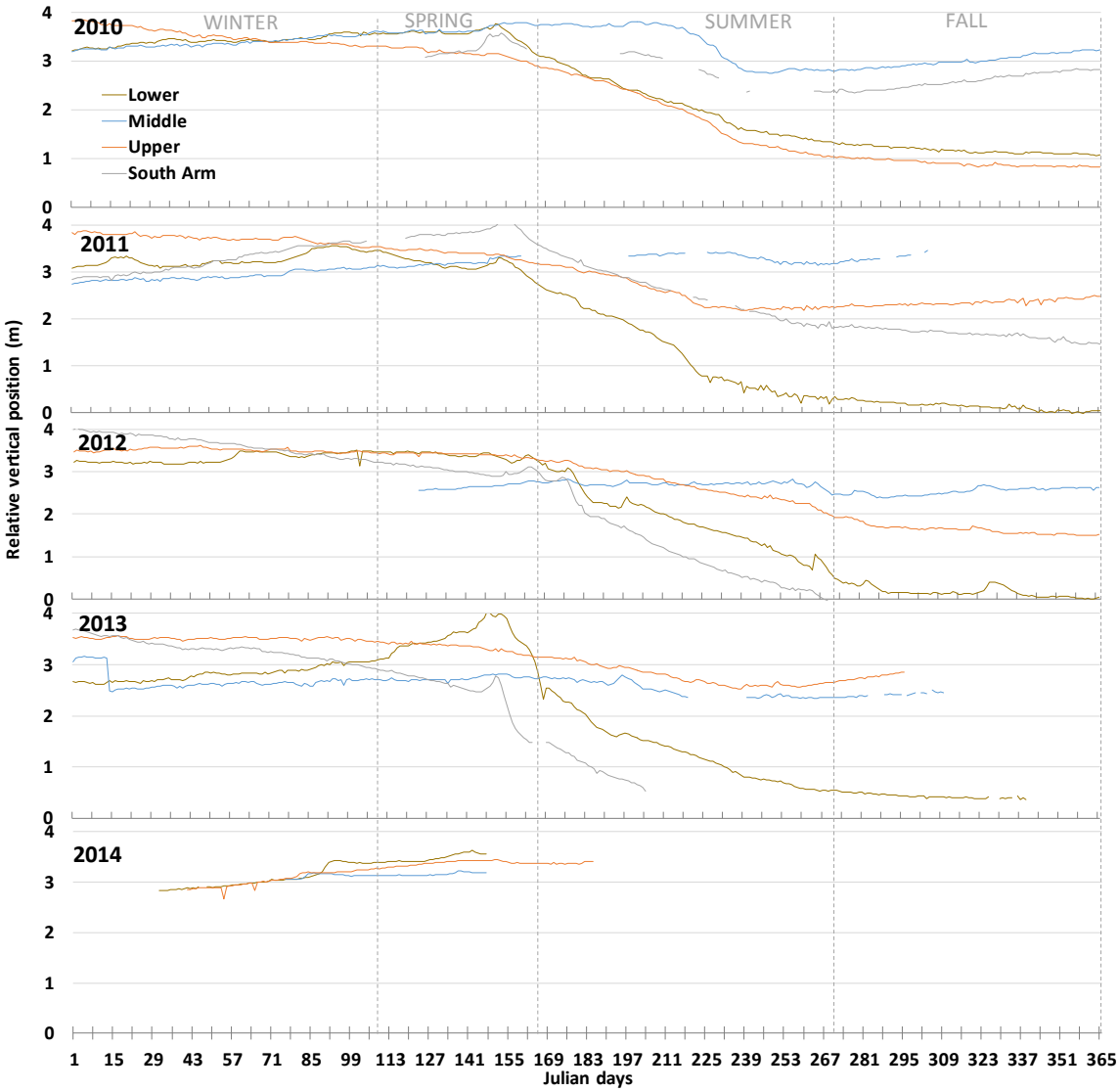

Figure 4.7 Relative vertical position derived from mean daily dGPS position of Lower, Middle and Upper Kaskawulsh and South Arm stations for 2010-2014.

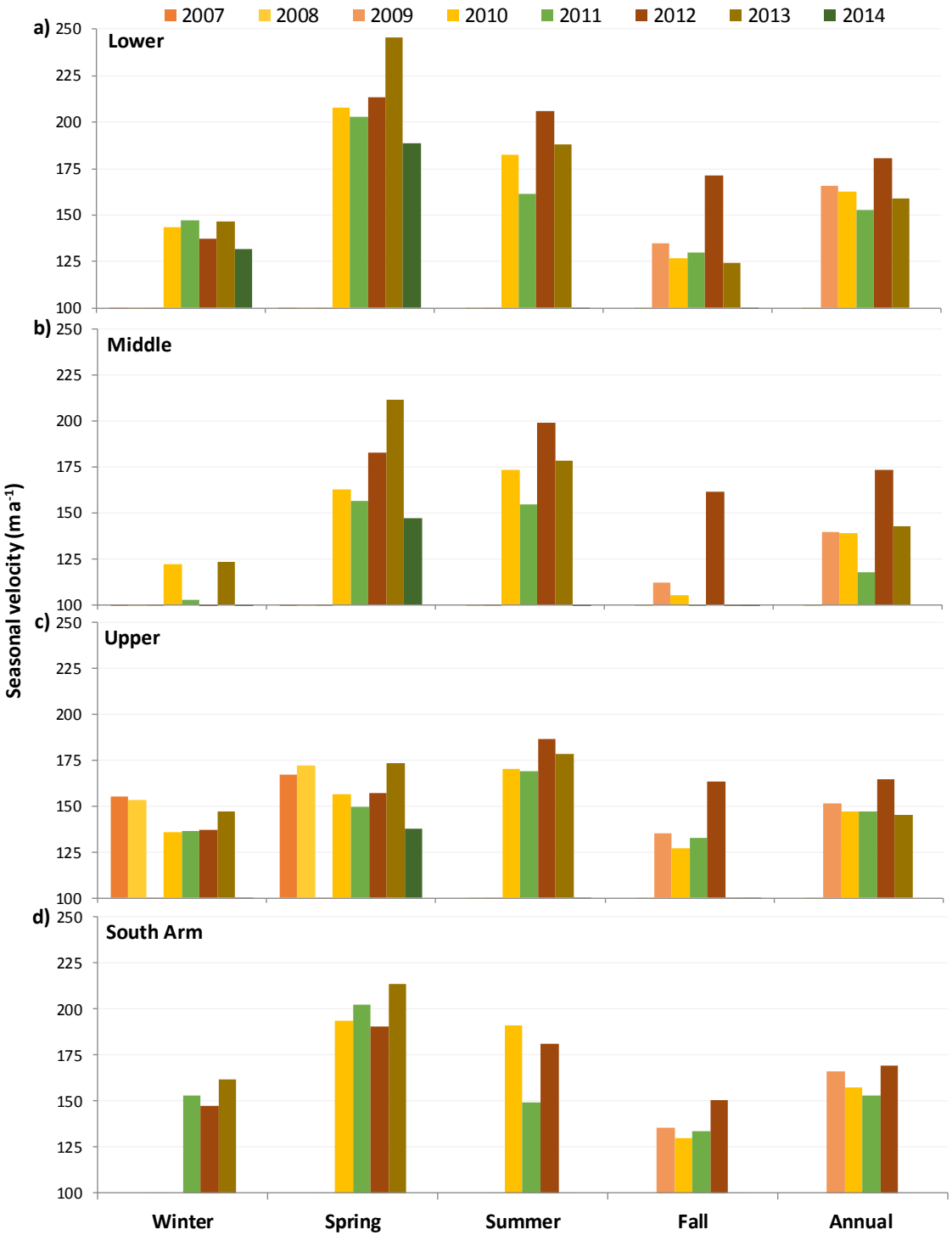

Figure 4.8 Seasonal and annual horizontal velocities for 2007-2014 at Kaskawulsh stations: a) Lower, b) Middle, c) Upper, and d) South Arm.

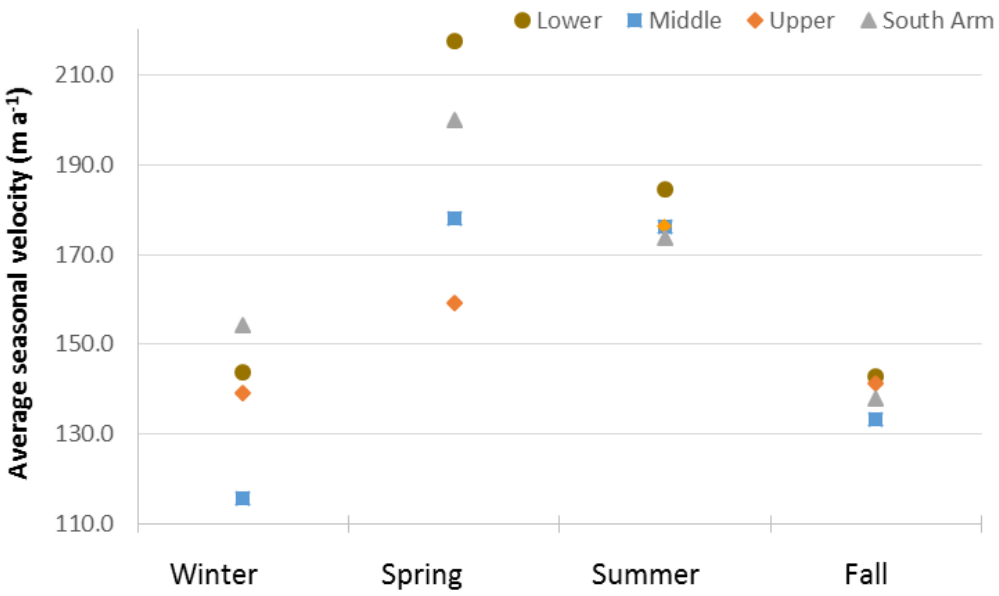

Figure 4.9 Average seasonal horizontal velocity derived from 2010-2013 dGPS measurements at the Kaskawulsh Glacier stations. Fall average velocities are derived from 2010-2012 dGPS measurements.

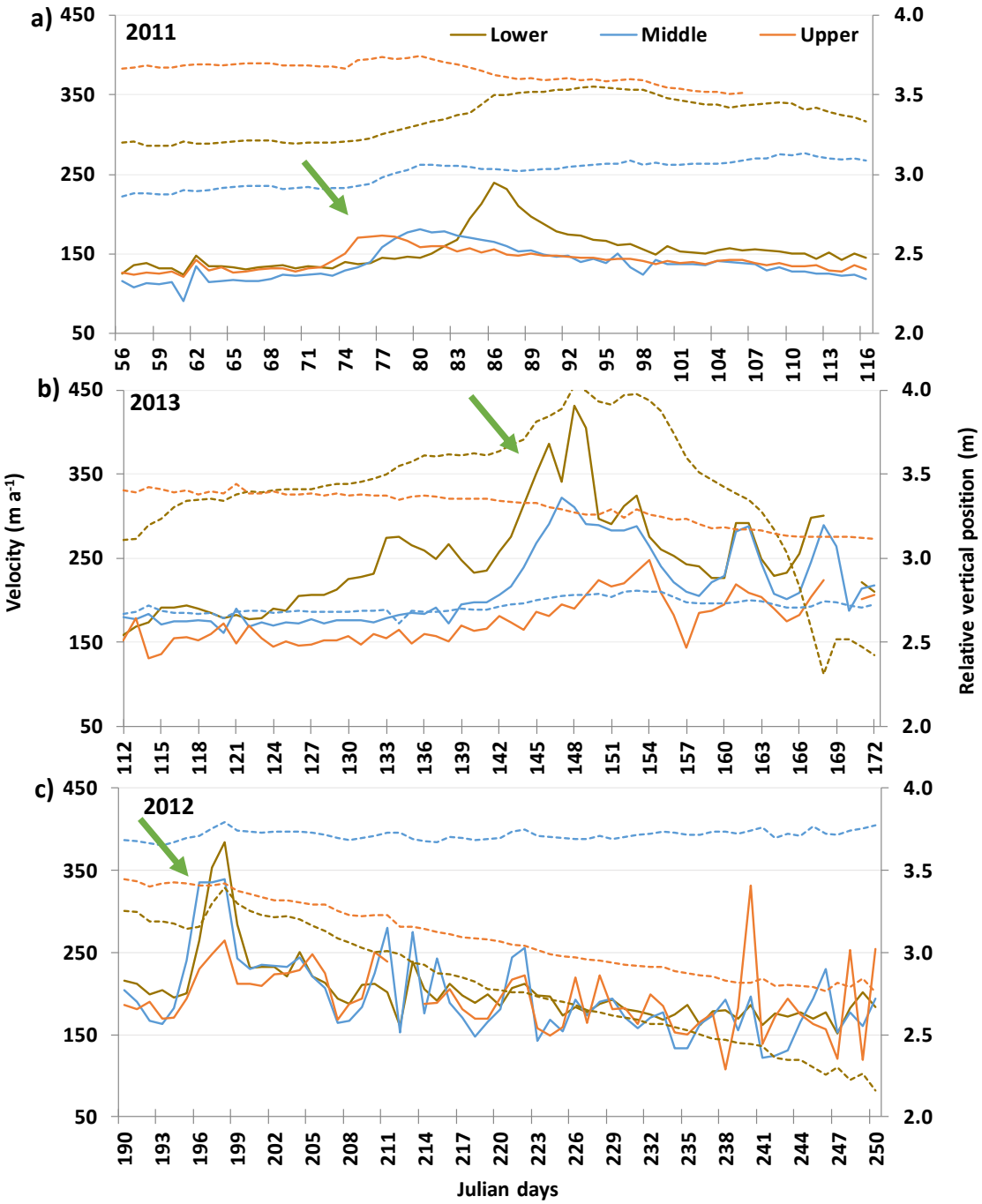

Figure 4.10 Horizontal velocity (solid lines) and relative vertical position (dotted lines) during different types of short-term motion events on the Kaskawulsh Glacier: a) Downglacier propagating event between JD 72-99, 2011; b) Upglacier propagating event between JD 123-160, 2013; c) Simultaneous event between JD 194-201, 2012. Green arrows indicate the events.

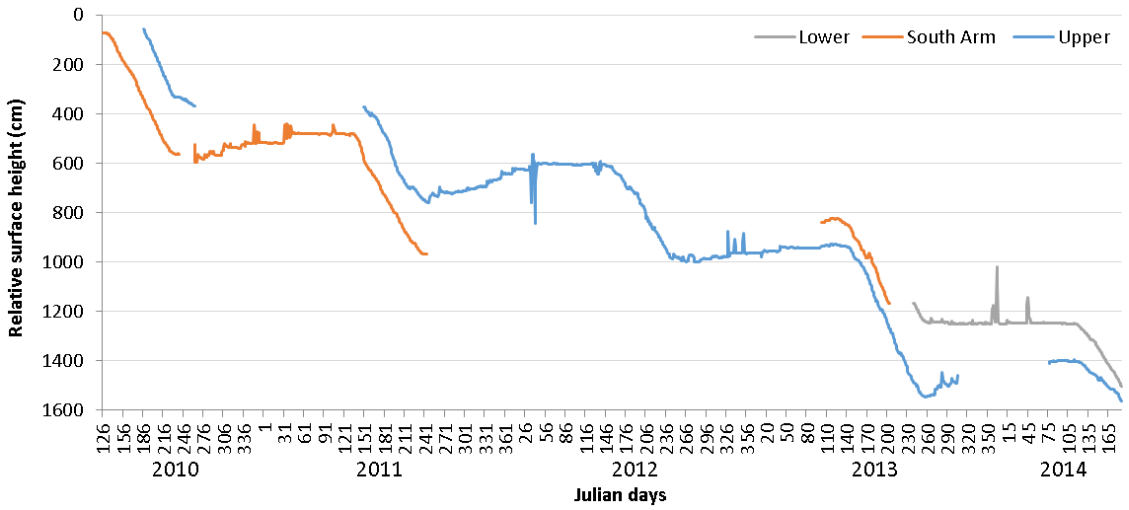

Figure 4.11 Relative surface height at Kaskawulsh dGPS stations measured by snow depth sounder between 2010 and 2014.

	Lower Station			Middle Station		
Date interval	**ST *v* (m a^{-1})**	**dGPS *v* (m a^{-1})**	**% difference**	**ST *v* (m a^{-1})**	**dGPS *v* (m a^{-1})**	**% difference**
Jan. 18 - Feb. 11, 2010 [1]	167.8	150.2	-11.7	136.4	127.1	-7.3
Oct. 20 - Nov. 13, 2010 [1]	150.1	127.0	-18.2	119.2	103.9	-14.7
Nov. 2 - Nov. 26, 2010 [1]	110.1	126.9	13.2	85.6	105.2	18.6
Nov. 13 - Dec. 7, 2010 [1]	163.8	126.2	-29.8	150.3	106.9	-40.6
Nov. 26 - Dec. 20, 2010 [1]	192.0	125.2	-53.4	135.7	105.8	-28.2
Dec. 7 - Dec. 31, 2010 [1]	124.9	124.2	-0.6	107.1	106.5	-0.5
Dec. 20 - Jan. 13, 2010-11 [1]	130.5	129.9	-0.4	150.5	120.9	-24.5
Dec. 31 - Jan. 24, 2010-11 [1]	161.1	148.6	-8.4	121.6	126.6	3.9
Jan. 13 - Feb. 6, 2011 [1]	92.3	147.6	37.5	107.1	114.9	6.8
Jan. 24 - Feb. 17, 2011 [1]	123.2	134.9	8.7	100.8	112.6	10.5
Feb. 6 - Mar. 2, 2011 [1]	177.7	135.6	-31.1	131.0	112.6	-16.3
Jan. 3 - Jan. 27, 2011 [2]	154.3	150.1	-2.8	126.1	125.7	-0.3
Feb. 14 - Mar. 10, 2011 [2]	141.8	135.5	-4.7	-	-	-
Feb. 21 - Mar. 16, 2012 [2]	172.2	158.7	-8.5	-	-	-
Average velocity	**147.3**	**137.2**	**-7.4**	**122.6**	**114.1**	**-7.5**
	Upper Station			**South Arm Station**		
Date interval	**ST *v* (m a^{-1})**	**dGPS *v* (m a^{-1})**	**% difference**	**ST *v* (m a^{-1})**	**dGPS *v* (m a^{-1})**	**% difference**
Jan. 18 - Feb. 11, 2010 [1]	132.2	140.2	5.7	-	-	-
Oct. 20 - Nov. 13, 2010 [1]	200.4	128.0	-56.6	246.7	127.8	-93.0
Nov. 2 - Nov. 26, 2010 [1]	109.5	128.0	14.4	-	-	-
Nov. 13 - Dec. 7, 2010 [1]	151.4	127.3	-19.0	349.7	132.1	-164.7
Nov. 26 - Dec. 20, 2010 [1]	166.4	126.2	-31.8	222.1	133.3	-66.6
Dec. 7 - Dec. 31, 2010 [1]	125.2	126.0	0.6	134.4	135.5	0.8
Dec. 20 - Jan. 13, 2010-11 [1]	127.6	134.1	4.9	118.4	138.4	14.4
Dec. 31 - Jan. 24, 2010-11 [1]	125.9	137.4	8.4	126.8	142.6	11.1
Jan. 13 - Feb. 6, 2011 [1]	155.4	131.0	-18.6	189.6	148.5	-27.7
Jan. 24 - Feb. 17, 2011 [1]	147.3	129.0	-14.2	151.5	153.6	1.4
Feb. 6 - Mar. 2, 2011 [1]	147.2	127.7	-15.3	187.2	158.4	-18.2
Jan. 3 - Jan. 27, 2011 [2]	131.8	136.4	3.4	138.3	143.8	3.8
Feb. 14 - Mar. 10, 2011 [2]	-	-	-	151.4	159.1	4.8
Feb. 18 - Mar. 13, 2012 [2]	139.9	145.3	3.7	-	-	-
Mar. 13 - Apr. 6, 2012 [2]	142.7	143.7	0.7	-	-	-
Feb. 21 - Mar. 16, 2012 [2]	-	-	-	147.7	150.8	2.0
Average velocity	**143.1**	**132.9**	**-7.7**	**180.3**	**143.7**	**-25.5**

Table 4.1 Comparison of velocities derived from dGPS measurements and from speckle tracking (ST) results for the corresponding time intervals. ST results were derived from fine beam imagery (8 m resolution) except for 2012 results which were derived from ultrafine imagery (3 m resolution). ST results are from Darling, 2012 ([1]) and Waechter, 2013 ([2]).

	Lower Station			Middle Station		
Date interval	**ST dir (°)**	**dGPS dir (°)**	**Difference (°)**	**ST dir (°)**	**dGPS dir (°)**	**Difference (°)**
Jan. 18 - Feb. 11, 2010 [1]	43.6	46.7	3.1	149.6	122.2	-27.4
Oct. 20 - Nov. 13, 2010 [1]	42.8	50.8	8.0	125.7	123.1	-2.6
Nov. 2 - Nov. 26, 2010 [1]	47.9	50.7	2.8	140.4	123.0	-17.4
Nov. 13 - Dec. 7, 2010 [1]	49.1	50.8	1.7	123.2	123.2	0.0
Nov. 26 - Dec. 20, 2010 [1]	45.1	51.1	6.0	131.9	123.3	-8.6
Dec. 7 - Dec. 31, 2010 [1]	40.0	51.2	11.2	124.6	123.4	-1.2
Dec. 20 - Jan. 13, 2010-11 [1]	52.9	50.8	-2.1	130.6	123.4	-7.2
Dec. 31 - Jan. 24, 2010-11 [1]	42.4	51.2	8.8	125.3	123.1	-2.2
Jan. 13 - Feb. 6, 2011 [1]	45.6	51.6	6.0	113.4	123.2	9.8
Jan. 24 - Feb. 17, 2011 [1]	45.8	51.4	5.6	124.5	123.2	-1.3
Feb. 6 - Mar. 2, 2011 [1]	42.2	51.2	9.0	114.7	123.4	8.7
Jan. 3 - Jan. 27, 2011 [2]	51.5	51.4	-0.1	126.8	123.3	-3.6
Feb. 21 - Mar. 16, 2012 [2]	57.4	55.2	-2.2	-	-	-
Average direction	**46.6**	**51.1**	**4.5**	**127.6**	**123.2**	**-4.4**
	Upper Station			**South Arm Station**		
Date interval	**ST dir (°)**	**dGPS dir (°)**	**Difference (°)**	**ST dir (°)**	**dGPS dir (°)**	**Difference (°)**
Jan. 18 - Feb. 11, 2010 [1]	46.6	43.5	-3.1	-	-	-
Oct. 20 - Nov. 13, 2010 [1]	42.2	44.8	2.6	24.3	11.0	-13.3
Nov. 2 - Nov. 26, 2010 [1]	51.2	44.9	-6.3	-	-	-
Nov. 13 - Dec. 7, 2010 [1]	57.6	45.0	-12.6	-	-	-
Nov. 26 - Dec. 20, 2010 [1]	51.2	45.0	-6.2	-	-	-
Dec. 7 - Dec. 31, 2010 [1]	49.6	45.1	-4.5	12.2	11.5	-0.7
Dec. 20 - Jan. 13, 2010-11 [1]	51.5	44.9	-6.6	12.0	11.1	-0.9
Dec. 31 - Jan. 24, 2010-11 [1]	45.0	44.8	-0.2	11.4	10.9	-0.5
Jan. 13 - Feb. 6, 2011 [1]	39.4	44.9	5.5	6.8	11.1	4.3
Jan. 24 - Feb. 17, 2011 [1]	47.5	45.1	-2.4	10.3	11.3	1.0
Feb. 6 - Mar. 2, 2011 [1]	44.3	44.6	0.3	18.8	10.8	-8.0
Jan. 3 - Jan. 27, 2011 [2]	46.3	44.8	-1.5	2.2	11.0	8.8
Feb. 18 - Mar. 13, 2012 [2]	49.5	45.7	-3.8	-	-	-
Mar. 13 - Apr. 6, 2012 [2]	48.2	46.0	-2.2	-	-	-
Feb. 21 - Mar. 16, 2012 [2]	-	-	-	11.0	9.9	-1.2
Average direction	**47.9**	**44.9**	**-2.9**	**12.1**	**11.0**	**-1.2**

Table 4.2 Comparison of direction of motion from dGPS measurements and from speckle tracking (ST) results for the corresponding time intervals. ST results were derived from fine beam imagery (8 m resolution) except for 2012 results which were derived from ultrafine imagery (3 m resolution). ST results are from Darling, 2012 ([1]) and Waechter, 2013 ([2]).

Year	Lower	Middle	Upper	S. Arm	Lower	Middle	Upper	S. Arm
Total annual horizontal displacement (m)					Difference from long-term average (m) *(Percent difference)*			
2007-08	-	-	167.1	-	-	-	13.2 *(+8.6%)*	-
2008-09	-	-	-	-	-	-	-	-
2009-10	166.0	139.3	151.4	-	1.7 *(+1.1%)*	-2.1 *(-1.5%)*	-2.5 *(-1.6%)*	-
2010-11	162.8	139.1	147.2	157.4	-1.5 *(-0.9%)*	-2.2 *(-1.6%)*	-6.7 *(-4.3%)*	-2.5 *(-1.6%)*
2011-12	152.8	118.3	147.4	152.9	-11.5 *(-7.0%)*	-23.0 *(-16.3%)*	-6.5 *(-4.2%)*	-7.0 *(-4.4%)*
2012-13	180.8	167.2	165.0	169.3	16.5 *(+10.1%)*	25.8 *(+18.3%)*	11.2 *(+7.3%)*	9.5 *(+5.9%)*
2013-14	159.0	142.8	145.0	-	-5.3 *(-3.2%)*	1.5 *(+1.1%)*	-8.8 *(-5.7%)*	-
2007-2014 average	**164.3**	**141.3**	**153.8**	**159.9**				
Total annual vertical displacement (m)					Difference from long-term average (m)			
2007-08	-	-	3.0	-	-	-	1.1	-
2008-09	-	-	-	-	-	-	-	-
2009-10	1.8	-0.8	3.4	-	-0.6	-1.4	1.5	-
2010-11	2.1	1.6	2.8	5.3	-0.3	1.0	0.9	0.8
2011-12	3.2	-0.9	1.0	2.9	0.7	-1.5	-0.9	-1.6
2012-13	3.0	0.1	1.9	5.3	0.6	-0.5	0.0	0.8
2013-14	2.1	3.0	-0.6	-	-0.4	2.4	-2.6	-
2007-2014 average	**2.4**	**0.6**	**1.9**	**4.5**				
Annual displacement direction (°)					Difference from long-term direction (°)			
2007-08	-	-	40.4	-	-	-	4.8	-
2008-09	-	-	-	-	-	-	-	-
2009-10	47.3	122.6	43.8	-	7.4	1.7	1.4	-
2010-11	50.5	123.6	44.6	10.4	4.3	0.7	0.6	0.6
2011-12	54.4	124.0	45.9	10.3	0.4	0.3	0.7	0.5
2012-13	58.2	125.1	46.9	8.7	3.5	0.8	1.8	1.1
2013-14	63.4	126.3	49.5	-	8.6	1.9	4.3	-
2007-2014 direction	**54.8**	**124.3**	**45.2**	**9.8**				

Table 4.3 Total annual horizontal and vertical displacement, annual direction of displacement, and differences from long-term average displacements and long-term direction, derived from dGPS measurements between JD 101 and JD 100 the following year.

	Seasonal velocity per station (m a^{-1})				
	Year	**Upper**	**Middle**	**Lower**	**South Arm**
Winter: JD 1-110	2008	153.2	-	-	-
	2009	-	-	-	-
	2010	135.8	121.8	143.7	-
	2011	136.6	102.3	147.1	153.1
	2012	137.4	-	137.2	147.5
	2013	147.4	123.3	146.7	161.9
	2014	-	-	131.8	-
	2010-2013 average	**139.3**	**115.8**	**143.7**	**154.2**
Spring: JD 110-165	2008	172.3	-	-	-
	2009	-	-	-	-
	2010	156.8	162.4	207.9	193.7
	2011	149.7	156.3	203.1	202.1
	2012	157.4	182.4	213.3	190.3
	2013	173.6	211.5	245.3	213.9
	2014	137.6	146.9	188.4	-
	2010-2013 average	**159.3**	**178.1**	**217.4**	**200.0**
Summer: JD 165-270	2007	-	-	-	-
	2008	-	-	-	-
	2009	-	-	-	-
	2010	170.6	173.2	182.3	190.8
	2011	169.2	154.8	161.7	149.4
	2012	186.7	198.9	205.7	181.0
	2013	178.2	178.0	188.1	-
	2010-2013 average	**176.2**	**176.2**	**184.5**	**173.7**
Fall: JD 270-365	2007	155.2	-	-	-
	2008	-	-	-	-
	2009	135.6	112.3	135.1	-
	2010	127.0	105.0	126.9	129.9
	2011	133.0	-	129.7	133.5
	2012	163.6	161.6	171.6	150.7
	2013	-	-	124.4	-
	2010-2012 average	**141.2**	**133.3**	**142.7**	**138.0**

Table 4.4 Annual and average seasonal horizontal velocity derived from dGPS measurements across the Kaskawulsh Glacier.

	Monthly and annual average temperatures (2007-2013)				
Month	Lower	Middle	Upper	South Arm	GSC AWS
Jan	-15.7	-16.2	-15.6	-15.4	-13.3
Feb	-8.9	-11.4	-11.7	-10.9	-11.7
Mar	-12.1	-15.7	-15.9	-14.1	-12.2
Apr	-5.4	-9.3	-10.0	-8.1	-4.4
May	1.4	-2.0	-3.0	-1.1	3.1
Jun	3.9	2.4	1.7	3.1	9.4
Jul	5.2	3.6	3.5	4.1	10.6
Aug	5.2	3.5	2.7	3.9	8.9
Sep	2.7	0.3	-1.0	0.3	3.0
Oct	-3.9	-6.4	-5.5	-7.3	-4.7
Nov	-15.5	-17.2	-16.3	-16.5	-10.4
Dec	-14.4	-15.4	-12.4	-14.0	-12.9
Annual	**-4.8**	**-7.0**	**-6.9**	**-6.3**	**-2.9**

Table 4.5 Long-term average monthly and annual temperature at Kaskawulsh Glacier dGPS stations and at Geological Survey of Canada automatic weather station. Average temperatures are based on data from 2007-2013.

Melt season duration (Julian days)						
Year	Start date		End date		Total length	
	Lower	Upper	Lower	Upper	Lower	Upper
2007	118	141	265	265	147	124
2008	137	139	267	255	130	116
2009	137	142	285	285	148	143
2010	118	141	268	268	150	127
2011	136	138	268	255	132	117
2012	136	142	285	285	149	143
2013	121	130	303	303	182	173
2014	118	122	-	-	-	-
2007-2014 Average	**128**	**137**	**277**	**274**	**148**	**135**

Table 4.6 Melt season start and end dates, total length of melt season per year, and. Long-term average start and end dates, for the Lower and Upper dGPS stations. Start and end dates are derived from air temperature (days above 0°C) at each dGPS stations.

Total snow accumulation (cm SWE)			
Year	Lower	Upper	South Arm
2009-10	*0*	*65.8*	*38.3*
2010-11	*0*	*73.5*	42.7
2011-12	*0*	85.9	*50.0*
2012-13	*0*	36.2	*21.1*
2013-14	0	70.2	*40.9*
2009-2014 average	0	66.3	38.6

Table 4.7 Annual and average snow accumulation at Kaskawulsh dGPS stations for 2009-10 to 2013-14. Values in black represent snow depth sounder measurements, values in blue are derived from manual snow depth measurements in spring. Values in red are derived from snow depth sounder measurements at the Upper station, corrected for elevation at the South Arm station.

Chapter 5 : Discussion

The results presented in Chapter 4 indicate that short-term and seasonal variations in motion occur on the Kaskawulsh Glacier each year. These variations are reflected in changes in both horizontal and vertical motion. In this chapter, controls on variations in motion observed at different timescales are discussed and compared to results from previous studies. First, residual vertical velocity and basal cavity opening and closing estimates are presented. Then, controls on intra-annual and interannual motion variations are discussed. Finally, a theoretical model of the annual development of the subglacial drainage system of the Kaskawulsh Glacier is presented.

5.1 Residual vertical velocity

It is clear from the dGPS records that substantial variations in vertical motion occur in relation to horizontal velocity events across the Kaskawulsh Glacier. To evaluate the cause of these vertical variations, it is first necessary to understand the different factors that can cause vertical motion on a glacier. Previous studies (e.g., Iken et al., 1983; Hooke et al., 1989; Copland et al., 2003) have indicated that vertical motion at the glacier surface can be caused by:

(a) vertical strain from compression and extension of the ice, primarily due to ice deceleration and acceleration, respectively;

(b) horizontal motion along a sloped bed (i.e., downhill movement); and

(c) opening and closing of basal cavities.

Processes (a) and (b) reflect vertical changes due to horizontal motion of the ice, while process (c) reflects physical changes at the glacier bed, and is typically referred to as 'residual vertical motion' since it comprises motion that cannot be accounted for by regular horizontal movement of the ice. To understand how much of the Kaskawulsh Glacier's vertical motion can be attributed to changes in the subglacial drainage system, residual vertical motion was calculated for each dGPS station, and cavity opening and closing rates were estimated. The terms cavity opening and cavity closing do not infer a physical process, but are used in this study to describe changes at the glacier bed that aren't otherwise accounted for by downslope motion or vertical strain. In some other studies this has been referred to as 'hydraulic jacking' (e.g., Iken and Truffer, 1997). These estimates of cavity opening and closing are based on a modified equation for calculating residual vertical velocity (W_c) from Hooke et al. (1989) and Copland et al. (2003). The original equation is:

$$W_c = W_s - U_s tan ß - E_{zz} h \quad (2)$$

where W_s is measured surface vertical velocity (positive when cavity opening is occurring, negative when there is cavity closing), U_s is horizontal surface velocity, ß is bed slope, E_{zz} is the vertical strain rate, and h is ice thickness. Bed slope is assumed to be the same as surface slope, with the long-term surface slope (ß) calculated for each station from:

$$ß = \tan \delta_{hz} / \delta_v \quad (3)$$

where δ_{hz} is the total horizontal displacement between JD 1, 2010 and JD 1, 2013, and δ_v is the total vertical displacement over the same period.

For this study, the vertical strain rates could not be calculated due to lack of data. However, in the absence of subglacial cavity opening and closing, we know that glacier acceleration would lead to reduced strain and ice thinning, while deceleration would cause increased strain and surface thickening. Therefore, if thickening occurs when the ice is accelerating, or thinning occurs when the ice is decelerating, then it can't be explained by surface strain. If we isolate the periods when these situations are occurring, then we can define a minimum estimate of times when cavity opening and closing could occur. During these periods, we can ignore the $E_{zz}h$ component in Equation (2) and simplify it to:

$$W_c = W_s - U_s tan ß \quad (4)$$

If we define the vertical motion arising from downhill movement (i.e., $U_s tan ß$) during these periods, then we can assume that the remaining, unexplained vertical motion, must be due to basal cavity opening and closing. Using this approach, basal cavity opening and closing estimates during short-term motion events are presented in Section 5.2.

Seasonal residual vertical motion patterns are typically similar between stations and between years (Figure 5.1). The winter and spring regimes see a slow and steady increase in surface elevation until the peak in vertical position associated with the annual spring motion event. Following the spring event, surface elevation decreases steadily into the summer. By mid- to late summer, vertical position plateaus before beginning to increase slowly throughout fall and into winter. In 2012 and 2013, the residual vertical motion patterns at the South Arm Station are substantially different from those at other stations and at the same station in other years, with a constant and pronounced decrease in surface

elevation and only a few short-term periods of uplift associated with horizontal velocity events (Figure 5.1). Field observations and comparisons with 1 m resolution GeoEye satellite imagery indicate that the South Arm Station moved through a small crevasse field and associated steeper terrain during this period, which likely explains these differing patterns.

5.2 Intra-annual motion variations

The intra-annual motion of the Kaskawulsh Glacier is characterized by four seasonal regimes with distinct patterns of horizontal velocity and vertical position, as presented in Chapter 4. Within each seasonal regime, short-term velocity events occur. The propagation of these events along the length of the glacier varies significantly between seasons, responding to different triggers. A clear distinction exists between upglacier propagating events in the spring at the start of the melt season, simultaneous motion events throughout the melt season, and downglacier propagating events in the winter when there is no surface melt. Previous studies have documented similar upglacier propagating motion events in the spring, including studies of the Haut Glacier d'Arolla, Switzerland (Mair et al., 2001; Mair et al., 2003), of Bench Glacier, Alaska (Anderson et al., 2004) and of the western margin of the Greenland Ice Sheet (Bartholomew et al., 2010). Simultaneous or nearly simultaneous short-term motion events in the summer were observed at a number of glaciers including Storglaciären, Sweden (Hooke at al., 1989), the Haut Glacier d'Arolla (Mair et al., 2002) and John Evans Glacier, Nunavut (Bingham et al., 2003; Copland et al., 2003), while downglacier propagating events were observed on Findelengletscher, Switzerland (Iken and Bindschadler, 1986; Iken and

Truffer, 1997) and Variegated Glacier, Alaska (Kamb et al., 1985; Kamb and Engelhardt, 1987). These studies have made clear the link between variations in horizontal velocities, vertical position, and variations in subglacial water pressure, and provide insight as to how the intra-annual dGPS measurements can be used to infer the annual evolution of the subglacial drainage system of the Kaskawulsh Glacier.

5.2.1 Upglacier propagating motion events

An upglacier propagating motion event dominates the spring regime across the Kaskawulsh Glacier in every year of the study (Figure 4.6). The timing of the spring event is closely related to the onset of melt each year, suggesting that the speed-up is attributable to the subglacial water pressure increase resulting from a sudden large input of meltwater to the glacier bed (Figure 5.2 to Figure 5.4). Previous theoretical studies have described the connections between water pressure, the form of the subglacial drainage system, and enhanced motion. The key points are summarized as follows:

(a) There is a direct relationship between water discharge (i.e., water input to the glacier bed) and subglacial water pressure in a distributed subglacial drainage system (Willis, 1995);

(b) A distributed subglacial drainage system is stable under low discharge conditions because the deformation of ice can keep pace with melting of the roofs of cavities (Kamb, 1987). However, under high discharge conditions the ice deformation is unable to keep pace with the melting, which favours the formation of a channelized subglacial system; and

(c) There is an inverse relationship between water discharge and water pressure in a channelized system. The largest channels have the lowest water pressures, so therefore grow at the expense of the smaller ones (since water always moves from areas of higher to lower pressure) (Willis, 1995).

The speed-up observed each spring across the Kaskawulsh Glacier appears to be caused by the switch from a distributed to channelized subglacial drainage system. As air temperatures increase to above freezing at the Lower Station, large amounts of meltwater enter the poorly developed distributed subglacial drainage system and cause a rapid increase in basal water pressure, causing basal motion to peak. The channelized drainage then likely expands upglacier as air temperatures at higher elevations increase to above freezing over the next few days. Subglacial water pressure would then decrease as the distributed drainage system opens up and the channelized system develops, causing velocities to drop back down to pre-speed-up levels. Basal cavity opening and closing estimates provide further evidence of large meltwater inputs to the glacier bed during spring events, with cavity opening consistently occurring on the rising limb of the horizontal motion graph and cavity closing occurring on the falling limb (Figure 5.2 to Figure 5.4). This suggests that the glacier is being uplifted at its bed during periods of rapid horizontal motion as basal water pressures increase, and that it falls back onto the glacier bed as the horizontal motion decreases and basal water pressures decrease.

The timing of spring motion events is closely related to the snowpack and temperature conditions on the glacier surface (Table 5.1). In particular, in years with a large

snowpack, it takes longer for meltwater to reach meltwater input points to the glacier interior such as moulins and crevasses. A deeper snowpack therefore results in a later spring motion event start date (R^2 = 0.52) and a smaller horizontal velocity magnitude during the event (R^2 = 043). The magnitude of horizontal velocity during spring events is strongly influenced by the sum of PDDs prior to the event, with larger magnitude events associated with warmer spring temperatures (R^2 = 0.36). Spring events with high horizontal velocity are of longer duration (R^2 = 0.54). Melt in the previous summer and overwinter velocity do not seem to control the characteristics of spring events, suggesting that the subglacial drainage system essentially 'resets' itself by spring. This relationship is discussed in more detail in the following sections.

5.2.2 Downglacier propagating motion events

Downglacier propagating motion events occur across the Central Arm of the Kaskawulsh Glacier every year, typically partway into the winter regime (between January and March), but sometimes much earlier, late in the fall regime (i.e., November 2012) (Figure 4.6). In contrast with the melt-driven events in spring, fall/winter events occurred after prolonged periods of well below freezing air temperatures with no apparent relation to snowfall or other changes in surface weather (Figure 5.5 to Figure 5.7), suggesting that the control on these events is internal. The increase in horizontal velocity (up to 15%) immediately following downglacier propagating events suggests that they likely result from the collapse of the channelized subglacial drainage system formed during the spring/summer, and the subsequent pressurization of the glacier bed as a distributed subglacial drainage system forms. In his theoretical study, Kamb (1987) suggests that

under low discharge conditions, the walls of the subglacial channels will collapse and deform under the weight of overlying ice, and that this makes them unstable. In this situation the formation of a distributed subglacial drainage system is favoured. On the Kaskawulsh Glacier it appears that when the switch from channelized to distributed subglacial drainage occurs, there is enough water left in the system to cause water pressures at the bed to rise and, therefore, velocities to briefly peak beginning at the Upper Station where the channelized system is the least developed because of the shorter melt season.

The interannual variability in timing of events supports this hypothesis. After high melt summers the downglacier propagating events occur later in the following winter; for example, the winter event in 2014 occurred relatively late in the season (peaking on JD 91), following a high melt summer in 2013, whereas in 2011 the first winter event peaked much earlier (peaking on JD 19), following average melt in summer 2010. After the lowest melt year on record in 2012, the downglacier propagating motion event actually occurred in late fall (peaking on JD 328), much earlier than the event(s) in any other year. This suggests that the subglacial drainage system is more developed in high melt summers, with larger channels that take longer to close up the following fall and winter. The short-term increase in vertical uplift (and associated basal cavity opening) during the winter events further suggests an increase in water pressurization at the bed as the channelized subglacial drainage system collapses, beginning at the Upper Station and propagating downglacier (Figure 5.5 to Figure 5.7). Downglacier propagating motion events with similar propagation speeds have been observed on Variegated Glacier,

Alaska (Kamb and Engelhardt, 1987) and on Findelengletscher, Switzerland (Iken and Truffer, 1997). In contrast with the downglacier propagating events observed on the Kaskawulsh Glacier, the "mini-surge" events of Variegated Glacier and Findelengletscher occurred during the melt season and were attributed to increases in basal water pressure from the sudden release of meltwater accumulated in subglacial reservoirs into the subglacial drainage system.

5.2.3 Simultaneous motion events

Throughout the summer and early fall regimes, a number of short-term motion events occur across the glacier (Figure 4.6). The events occur nearly simultaneously at all stations and appear closely linked to meteorological conditions; for example, similar events occurred in July 2012 and July 2013 following a period of pronounced surface melt (i.e., in the 10 days leading up to each event, there was ~45 – 50 cm of surface melt) (Figure 5.8). The surface melt in the days preceding the July events was not unusually high (i.e., the average melt for 10 days in July is ~35 – 75 cm SWE), but followed lower than average June melt inputs. In the days leading up to the September and October 2012 events, temperatures increased from well below freezing to up to 8°C and surface melt of ~20 cm occurred (Figure 5.9). The simultaneous events likely represent the response to a sudden large water input across the glacier (e.g., high melt, rain) that overpressurizes the subglacial drainage system. Willis (1995) describes dramatic acceleration events linked with glacier surface uplift occurring early in the melt season when the subglacial drainage system is poorly developed. He associates the events with periods of high surface melt or heavy rainfall, resulting in high subglacial water pressure. Such mid-summer high

velocity events following rapid meltwater inputs were observed on John Evans Glacier, Nunavut (Copland et al., 2003) and the Haut Glacier d'Arolla, Switzerland (Mair et al., 2002). On the Kaskawulsh Glacier, the motion events occur after the annual snowpack has melted, when there is a good hydrological connection between the glacier surface and bed (i.e., there is no snow to retard water flow, and typically a short travel distance between any surface melt and an input location to the glacier bed) (Figure 5.10). Like the other types of motion events, simultaneous motion events are accompanied by vertical uplift at the surface, and basal cavity opening (Figure 5.8 and Figure 5.9).

5.3 Interannual motion variations

Moving beyond the intra-annual timescale, it is evident that the influence of surface melt also extends to the interannual timescale. The dGPS data from 2007 to 2014 presented in Chapter 4 show that while there is little interannual variability in direction of motion, there is significant variability in horizontal and vertical velocities across the Kaskawulsh Glacier (Table 4.3). This interannual variability suggests that, at this timescale too, surface motion is closely linked to changes in the subglacial drainage system structure which is controlled, in large part, by surface melt.

Surface melt rates across the Kaskawulsh Glacier are assumed to represent the amount of water flowing to the glacier bed, given the large number of moulins on the glacier (Figure 5.10), and that little water flows along marginal streams. Monthly and annual melt rates for May through September 2007-2013 at the Upper Station are presented in Figure 5.11. Melt rates at the Upper Station are used to represent melt patterns across the entire

ablation area of the glacier, as melt rates at the Middle and Lower stations were on average within 1.2 and 2.4% of those at the Upper Station, respectively (Table 3.2). The 2007-2013 average annual surface melt at the Upper Station was 429.8 cm SWE, and ranged between a minimum of 318.2 cm SWE in 2008, and a maximum of 539.9 cm SWE in 2013.

A comparison of annual melt rates and seasonal velocities at each station revealed a strongly negative correlation between summer melt and velocities the following fall-winter (i.e., JD 270 to JD 90) (Figure 5.12). For example, the melt rate in summer 2013 was the highest on record at the Upper Station (539.9 cm SWE, compared to a 2007-2014 average of 429.8 cm SWE), with velocities in fall-winter 2013-14 approximately 25% below those in fall-winter 2012-2013 and 10% lower than any previously recorded fall-winter velocity at this location (Table 5.2). Furthermore, the highest fall-winter velocities on record in 2012/2013 followed the lowest melt rates on record in summer 2012 (362.4 cm SWE at the Upper Station). Fall-winter velocities at the Central Arm stations were up to 23% higher in these seasons than the 2007-2014 average.

A comparison of summer melt rates with monthly horizontal velocities during the following year provides further insights into the drivers of velocity variations (Figure 5.13). The correlation between summer melt and the following months' velocities is always negative, with the exception of August, which is positively correlated. Pearson correlation coefficients for September through May are statistically significant at the 95%

level or greater. However, this relationship breaks down by the time the following summer is reached, with the correlation between June and July velocities and the previous summers melt being not statistically significant. November provides the strongest inverse relationship to previous summer melt, with an R^2 value of 0.58, followed by October, December and February, with R^2 values of 0.41 to 0.48.

Given the connection between melt and fall-winter velocities, an important question is whether it is the total summer melt that has the biggest influence on horizontal motion, or whether the melt in particular months has a stronger influence than other months. To evaluate this, monthly melt values were individually correlated with both total and monthly motion in the following year. Monthly velocities are more highly correlated to early season melt (i.e., in May and June) than to late season melt (i.e., July to September) (Table 5.3). For example, May melt seems to have the biggest influence on velocities the following fall and early winter, followed by June melt and then July melt. The relationship between melt and monthly velocity decreases after January, and February to April velocities seem more closely related to late summer melt than early summer melt.

5.4 A theoretical model of the annual development of the subglacial drainage system of the Kaskawulsh Glacier

The variability in surface velocities on the Kaskawulsh Glacier at the intra-annual and interannual timescales is strongly linked to surface meltwater inputs and their influence on the development of the subglacial drainage system. The patterns of vertical position (Figure 5.1) support the hypothesis of horizontal motion as an indicator of the condition

of the subglacial drainage system, with vertical uplift and cavity opening occurring simultaneously with the peak in horizontal velocity for all three types of velocity events. Each year, spring melt causes high subglacial water pressures as large water volumes reach a distributed subglacial drainage system that is too small to accommodate them. This results in high velocities, which propagate upglacier as the melt of the snowpack moves upglacier (Figure 5.2 to Figure 5.4). However, the distributed system is unstable during high water discharges, and so develops into a channelized subglacial drainage system (Kamb, 1987). This channelized system is much better able to accommodate typical summer meltwater flows, resulting in basal water pressures that fall during the summer. However, rapid melt or rain events can still overwhelm the channelized system, resulting in simultaneous high velocity events (Figure 5.8 and Figure 5.9).

The amount of summer melt, particularly early in the summer, defines the size of subglacial channels, with very large channels forming in high melt years (Schoof, 2010). Their size defines how long it takes for them to collapse and become re-pressurized after the end of the summer, causing the negative relationship between summer melt and motion the following fall and winter (Figure 5.12). As subglacial drainage channels collapse throughout fall and winter, the relationship between previous summer melt and velocity breaks down (Figure 5.13).

Velocities typically reach their annual minimum in the fall as any water at the glacier bed can be easily transported by the remnant subglacial channels from the previous summer, resulting in very low basal water pressures. However, as these subglacial channels

collapse due to the weight of overlying ice, the glacier bed becomes pressurized again, resulting in a downglacier propagating velocity event. This event propagates downglacier as the highest elevation regions of the glacier had the smallest subglacial channels (due to lower melt input), and because the ice thins towards the glacier terminus (slowing down the closure rate of subglacial channels there). After the end of the downglacier propagating events, horizontal velocities become higher as the subglacial drainage system reverts to a distributed system with relatively high subglacial water pressures. This system is most stable under low subglacial water flow conditions (Kamb, 1987), so persists throughout the winter until rapid melt occurs again the following spring (Figure 5.5 to Figure 5.7). Because the channelized system was relatively undeveloped in summer 2012 due to low melt, the transition to distributed drainage occurred much earlier than in other years, with the 'winter' event which marks the transition in drainage occurring in late fall.

These annual patterns suggest that the glacier has a 'memory' of past summer conditions from the reorganization of subglacial drainage that can last long into the following winter, consistent with recently observed patterns in Alaska by Burgess et al. (2013) and in SW Greenland by Sundal et al. (2011), and with theoretical studies by Schoof (2010). Burgess et al. (2013) observed an average 11% decrease in January motion for each additional metre of summer melt. This relationship is based on velocities derived by offset tracking and modelled melt rates derived from cumulative summer PDDs at 160 glaciers in Alaska for the period 2006 to 2011. Sundal et al. (2011) found that summers with high melt led to suppressed annual velocities in a land-terminating sector of SW

Greenland between 1993 and 1998, based on velocities derived from intensity tracking and locally measured melt rates. Similarly, a theoretical study by Schoof (2010) suggests that large meltwater inputs, such as those expected in years of high melting, would lead to lower annual velocities as the increased efficiency of the subglacial drainage system keeps basal water pressures low. On the Kaskawulsh Glacier, for each additional metre of melt, fall-winter velocity (JD 270 – JD 90) decreases by 5.1 – 14.5%, representing an average decrease of 8.6% across the glacier. This represents a velocity decrease of 13.8 m a^{-1} per additional metre of melt at the Upper Station, 22.7 m a^{-1} at the Middle Station, 10.3 m a^{-1} at the Lower Station, and 8.3 m a^{-1} at the South Arm Station. The subglacial drainage system seems to 'reset' itself by spring, however, as there is no correlation between spring event characteristics and past summer melt or overwinter velocity.

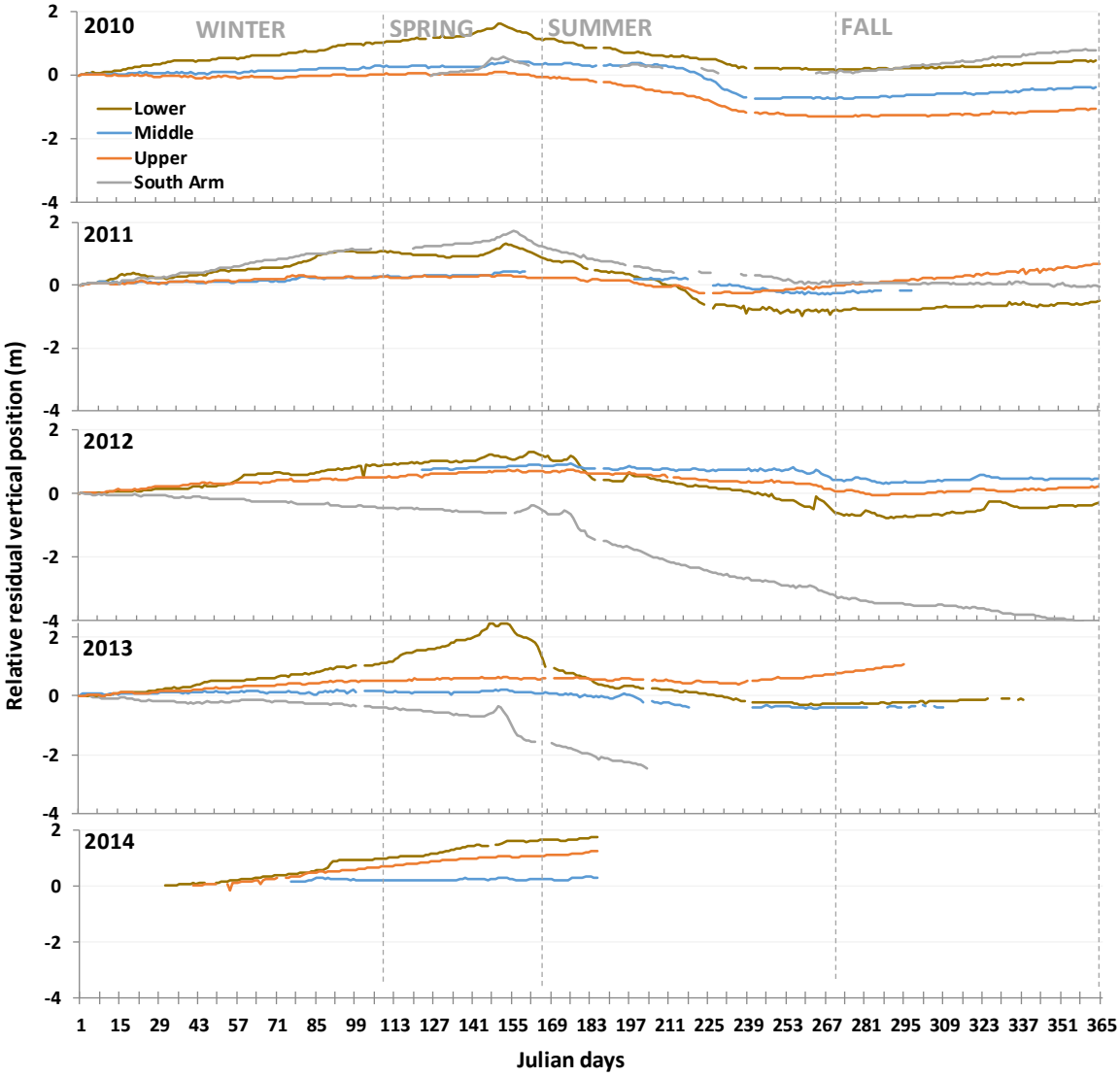

Figure 5.1 Relative residual vertical position (with vertical component due to downslope movement removed) derived from mean daily dGPS elevation of Lower, Middle, Upper and South Arm stations for 2010-2014.

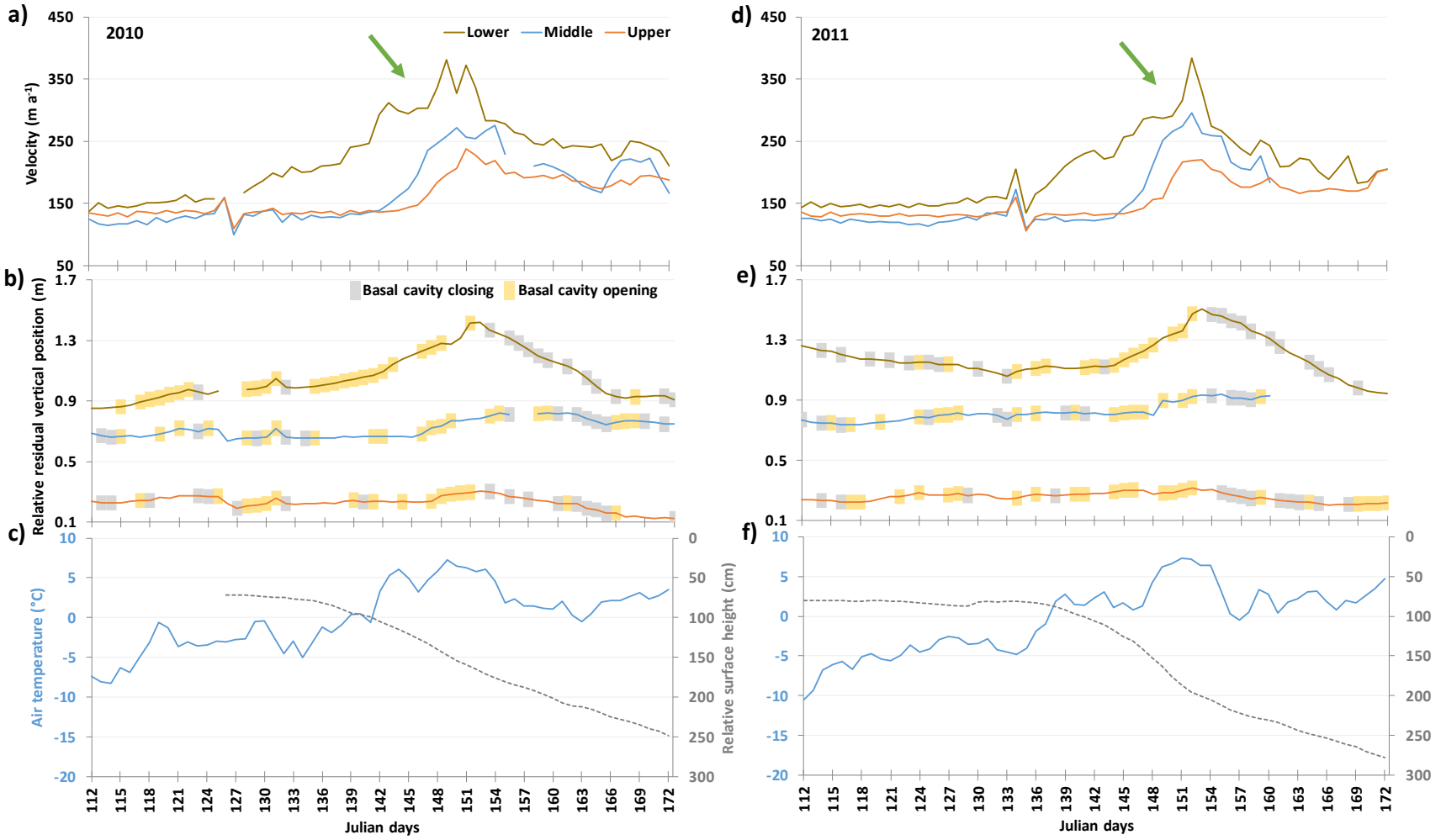

Figure 5.2 (a,d) Horizontal velocity; (b,e) Relative residual vertical position (yellow shading = cavity opening; grey shading = cavity closing); (c,f) Air temperature and relative surface height at Kaskawulsh dGPS stations during the upglacier propagating events in spring 2010 and 2011. Relative surface height was measured at the South Arm Station.

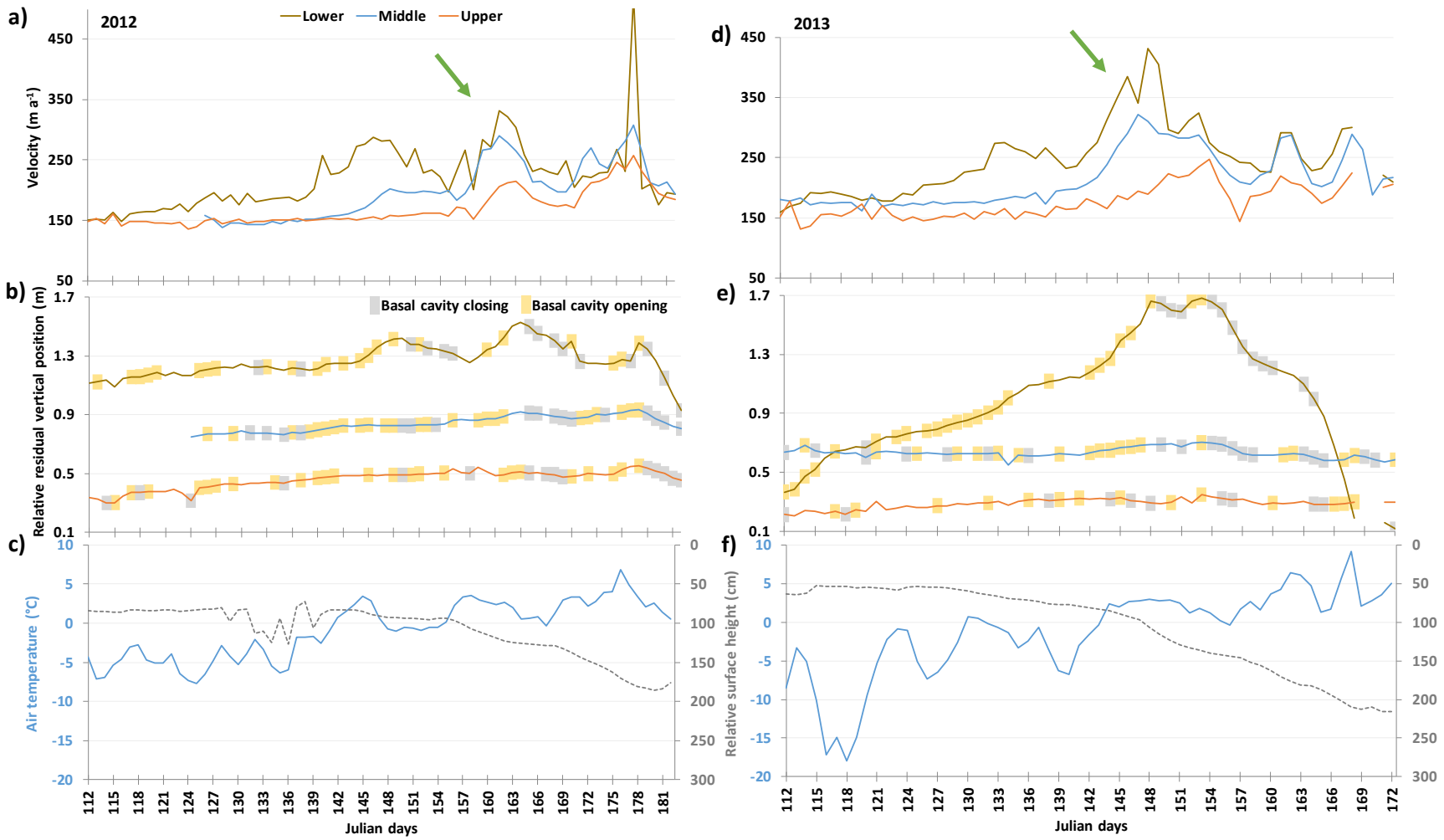

Figure 5.3 (a,d) Horizontal velocity; (b,e) Relative residual vertical position, (yellow shading = cavity opening; grey shading = cavity closing); (c,f) Air temperature and relative surface height at Kaskawulsh dGPS stations during the upglacier propagating events in spring 2012 and 2013. Relative surface height was measured at the Upper Station (2012) and at the South Arm Station (2013).

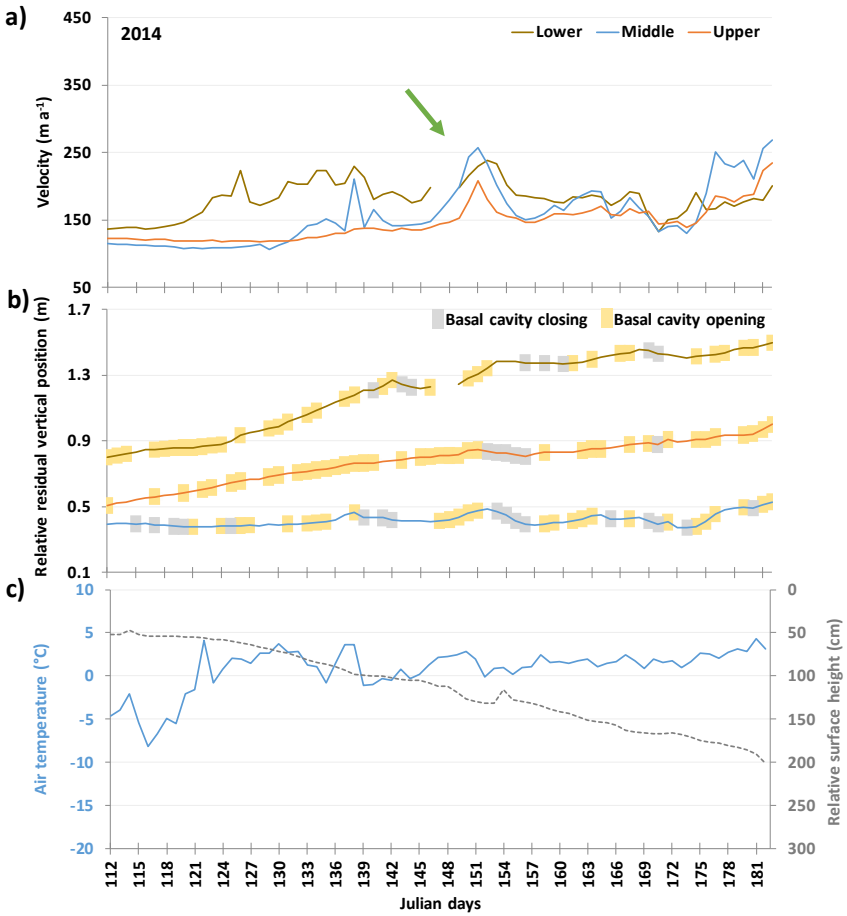

Figure 5.4 (a) Horizontal velocity; (b) Relative residual vertical position (yellow shading = cavity opening; grey shading = cavity closing); (c) Air temperature and relative surface height at Kaskawulsh dGPS stations during the upglacier propagating event in spring 2014. Relative surface height was measured at the Upper Station.

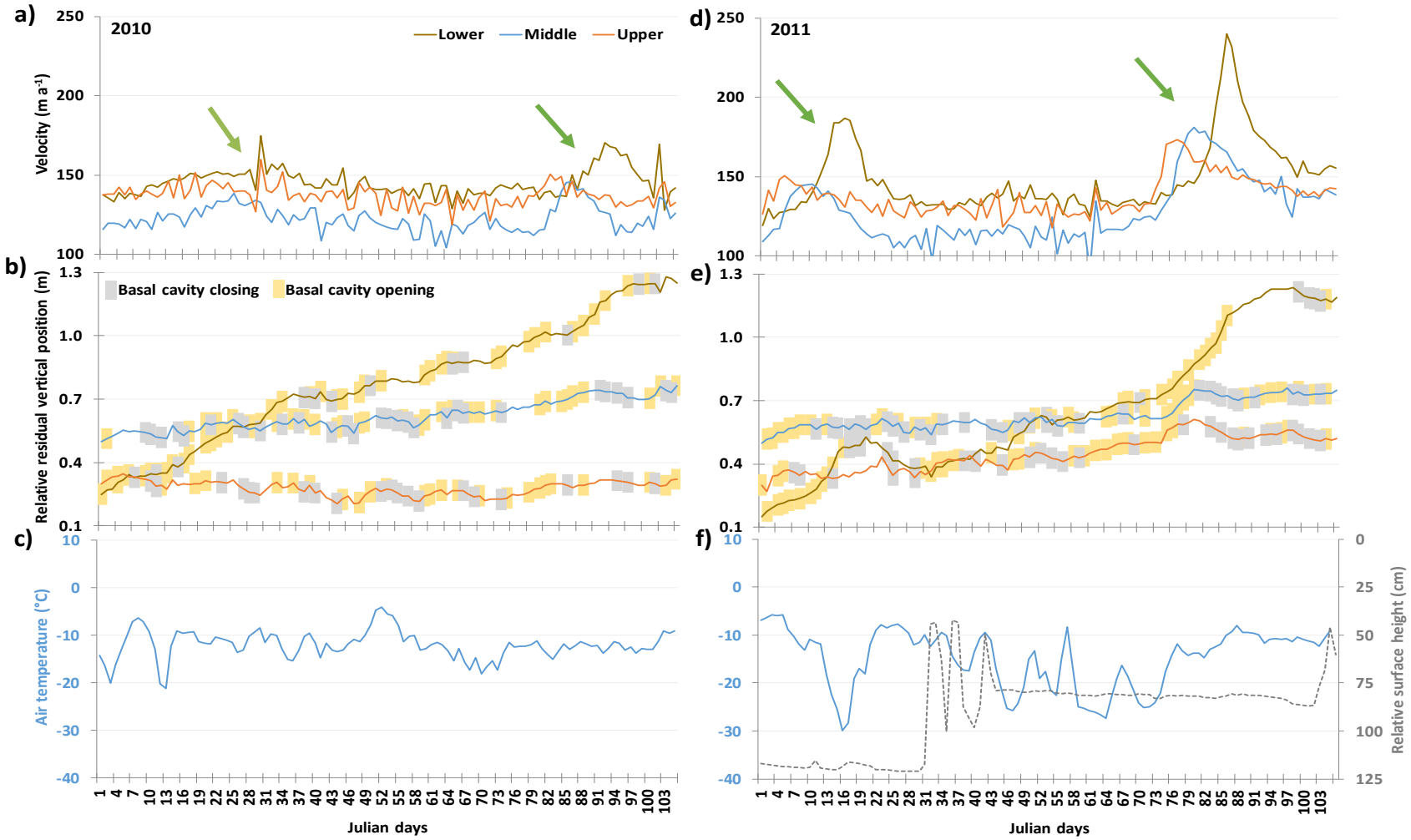

Figure 5.5 (a,d) Horizontal velocity; (b,e) Relative residual vertical position (yellow shading = cavity opening; grey shading = cavity closing); (c,f) Air temperature and relative surface height at Kaskawulsh dGPS stations during the downglacier propagating events in winter 2010 and 2011. Relative surface height was measured at the South Arm Station in 2011. No surface height was measured in 2010.

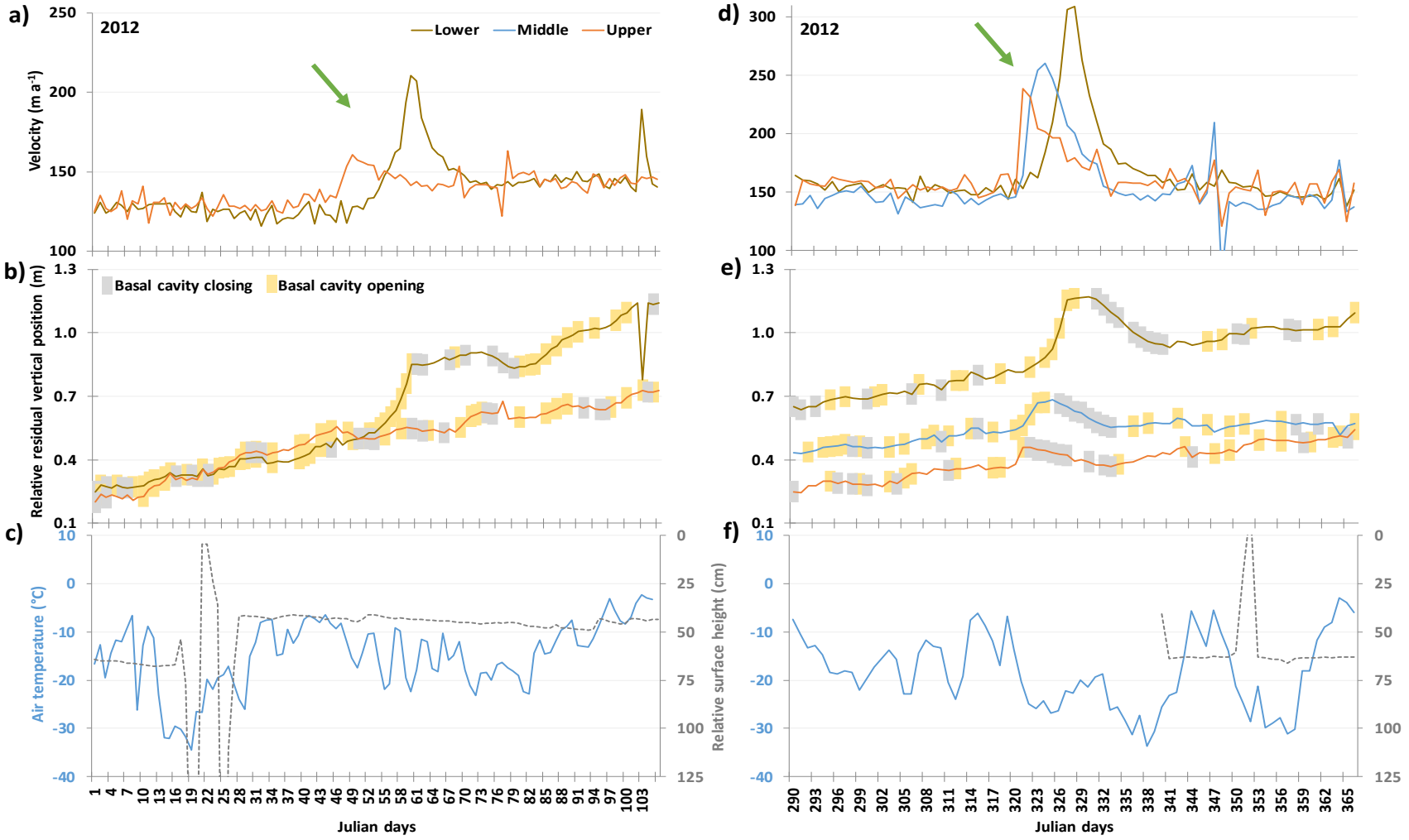

Figure 5.6 (a,d) Horizontal velocity; (b,e) Relative residual vertical position, (yellow shading = cavity opening; grey shading = cavity closing); (c,f) Air temperature and relative surface height at Kaskawulsh dGPS stations during the downglacier propagating events in winter 2012 and fall 2012. Relative surface height was measured at the Upper Station.

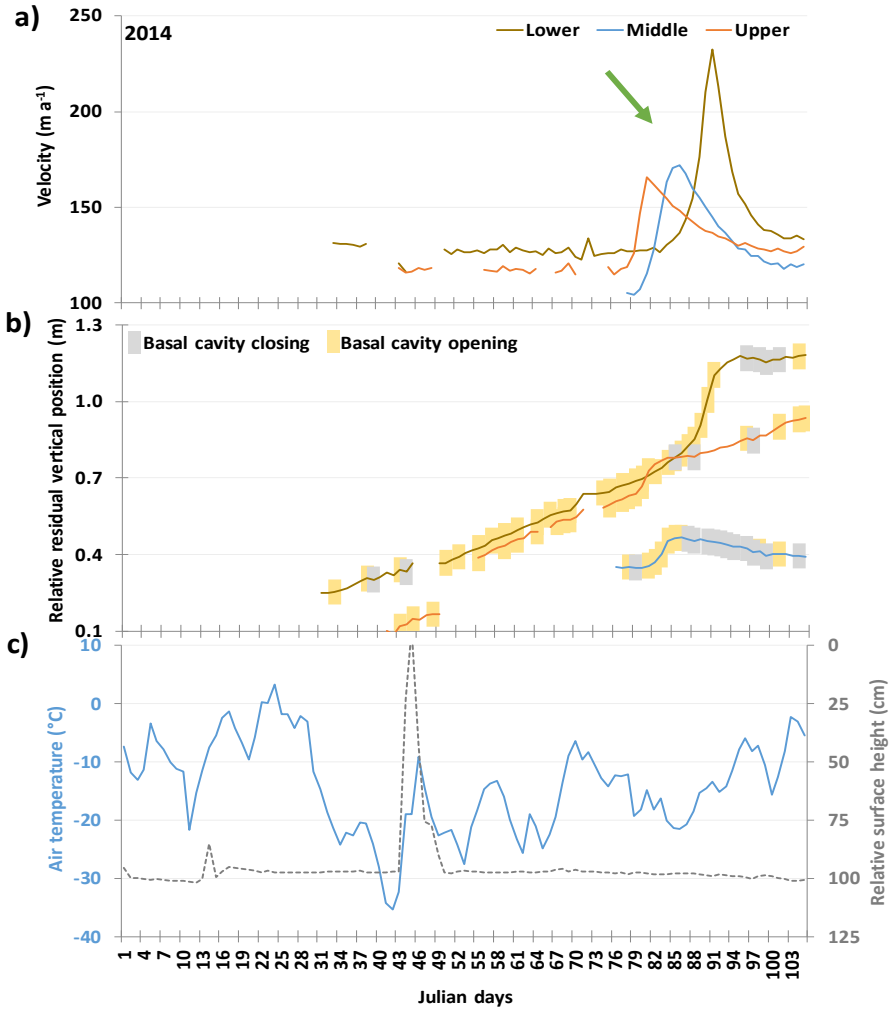

Figure 5.7 (a) Horizontal velocity; (b) Relative residual vertical position, (yellow shading = cavity opening; grey shading = cavity closing); (c) Air temperature and relative surface height at Kaskawulsh dGPS stations during the downglacier propagating event in winter 2014. Relative surface height was measured at the Lower Station.

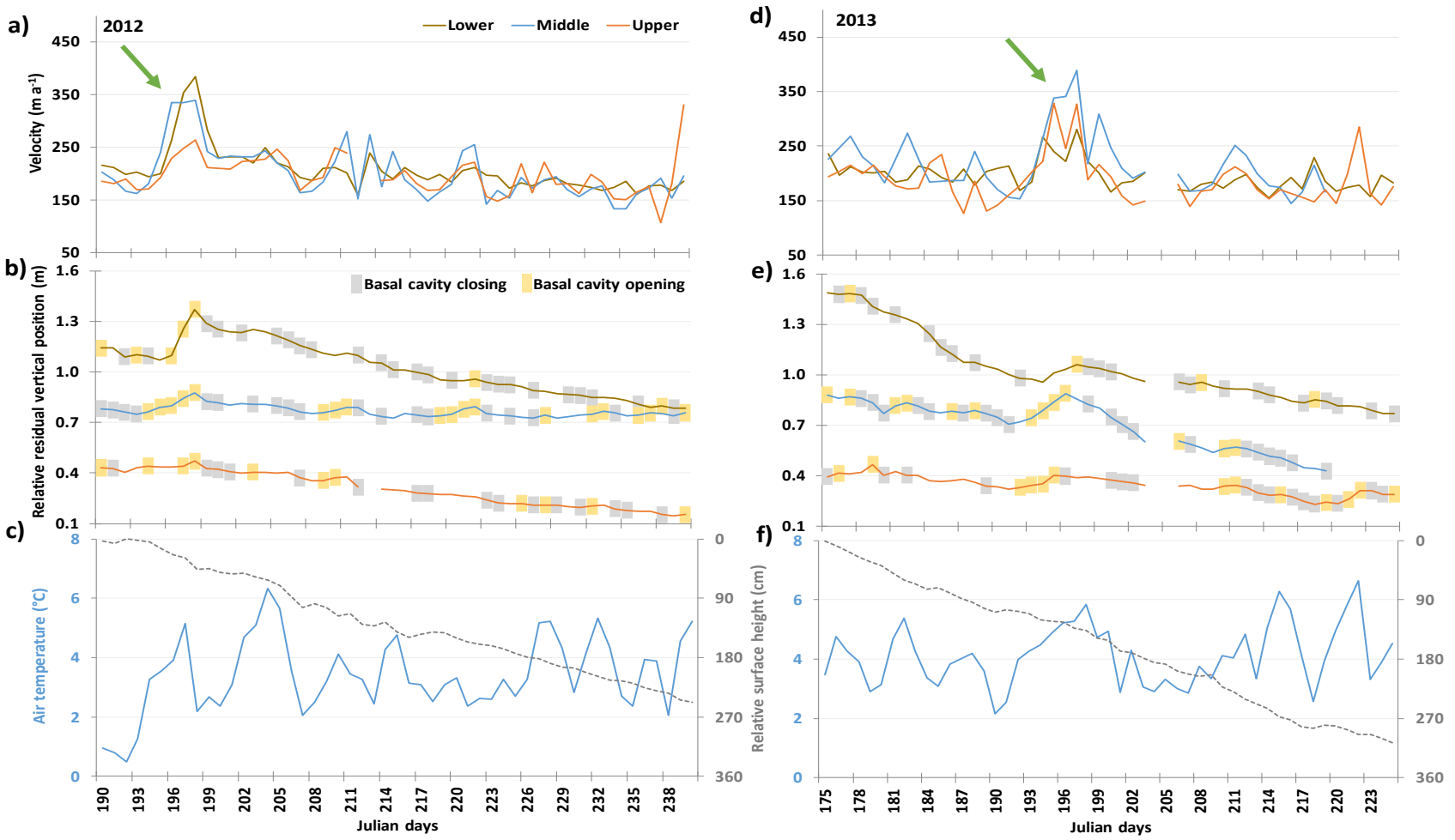

Figure 5.8 (a,d) Horizontal velocity; (b,e) Relative residual vertical position, (yellow shading = cavity opening; grey shading = cavity closing); (c,f) Air temperature and relative surface height at Kaskawulsh dGPS stations during simultaneous motion events in summer 2012 and 2013. Relative surface height was measured at the Upper Station.

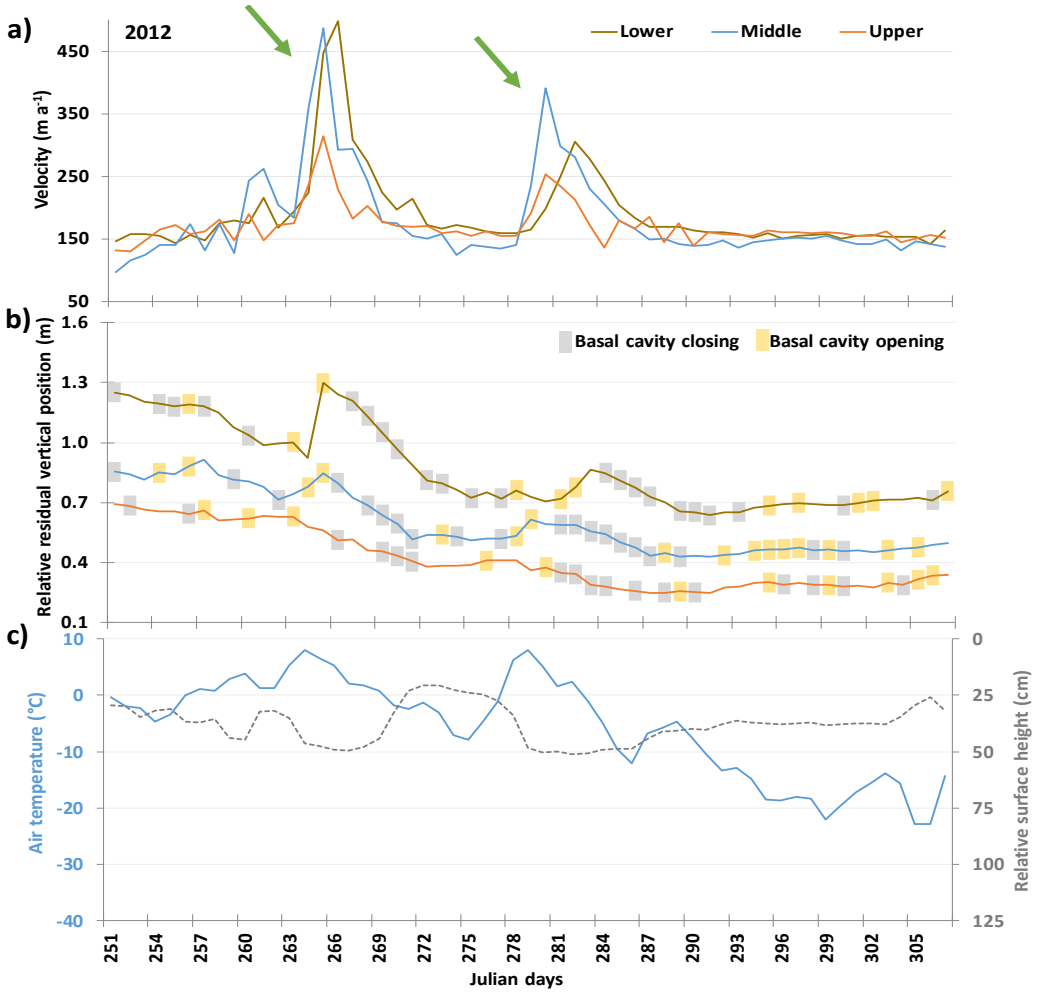

Figure 5.9 (a) Horizontal velocity; (b) Relative residual vertical position, (yellow shading = cavity opening; grey shading = cavity closing); (c) Air temperature and relative surface height at Kaskawulsh dGPS stations during simultaneous motion events in late summer/fall 2012. Relative surface height was measured at the Upper Station.

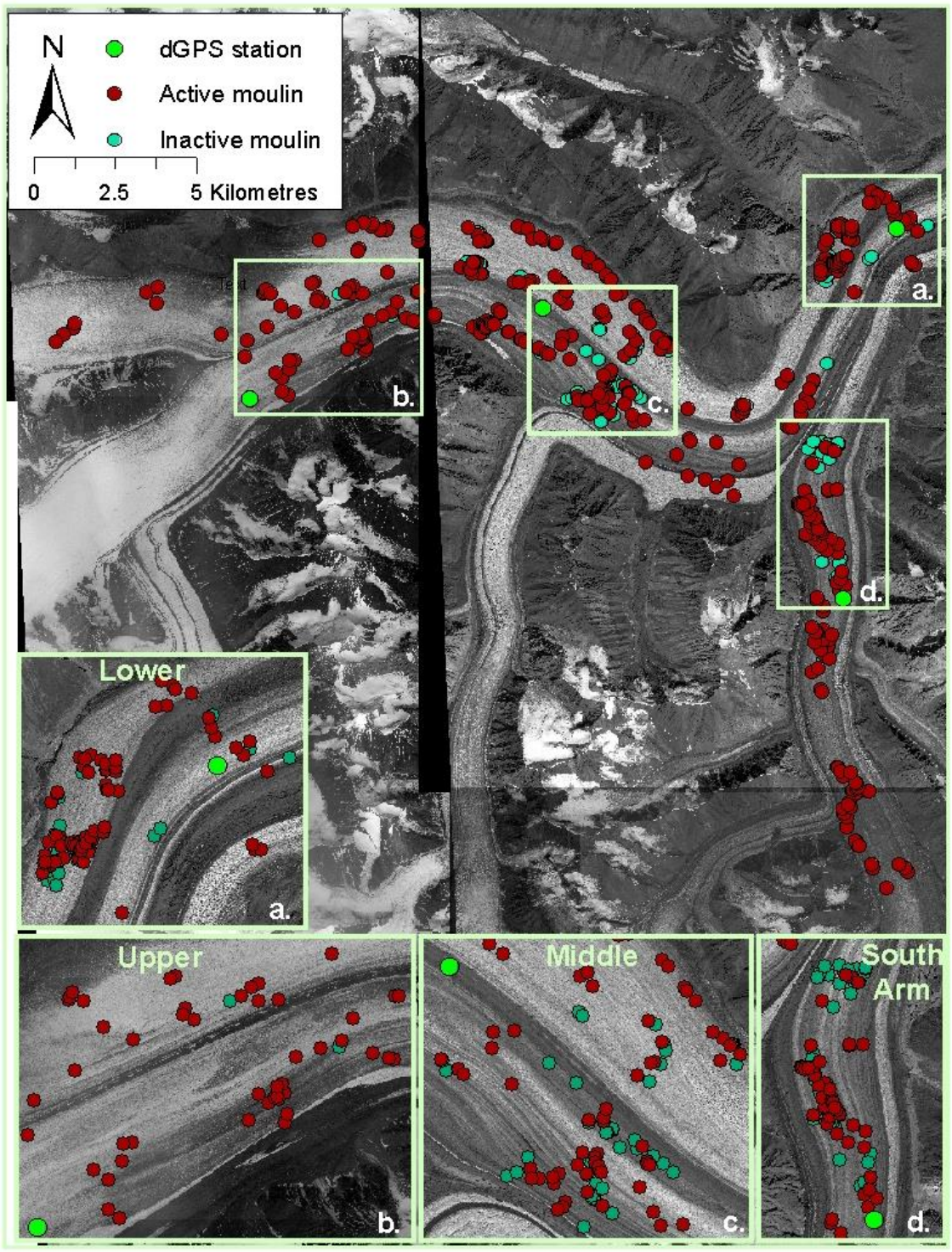

Figure 5.10 Location of active and inactive moulins on Kaskawulsh Glacier. Insets a-d show moulins that drain the surface water downglacier of dGPS stations. Moulins were identified from visual interpretation of high resolution imagery (GeoEye, 1 m ground resolution) from June and July 2009, show above.

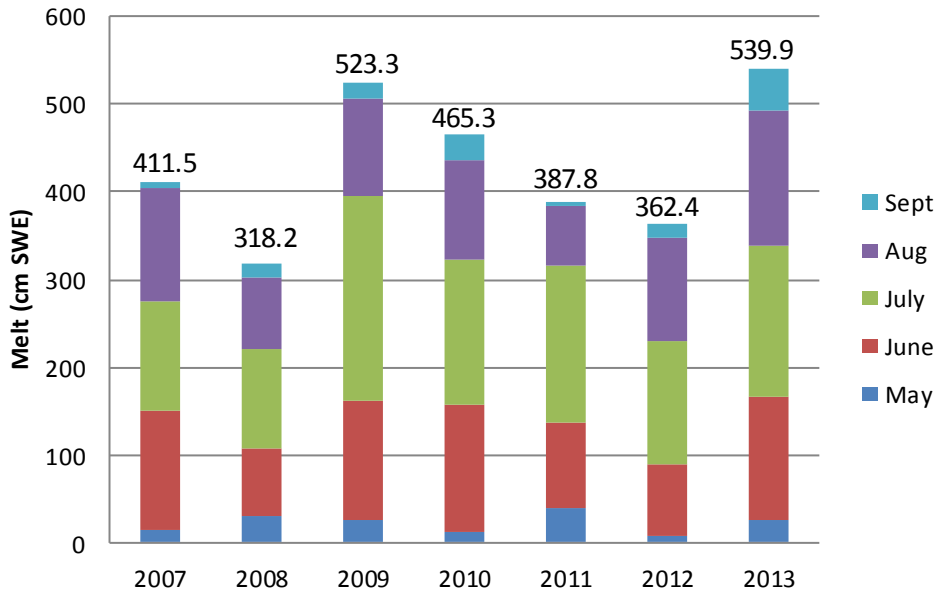

Figure 5.11 Monthly melt rates at the Upper Kaskawulsh dGPS station for 2007-2013. Annual melt values are presented at the top of each column.

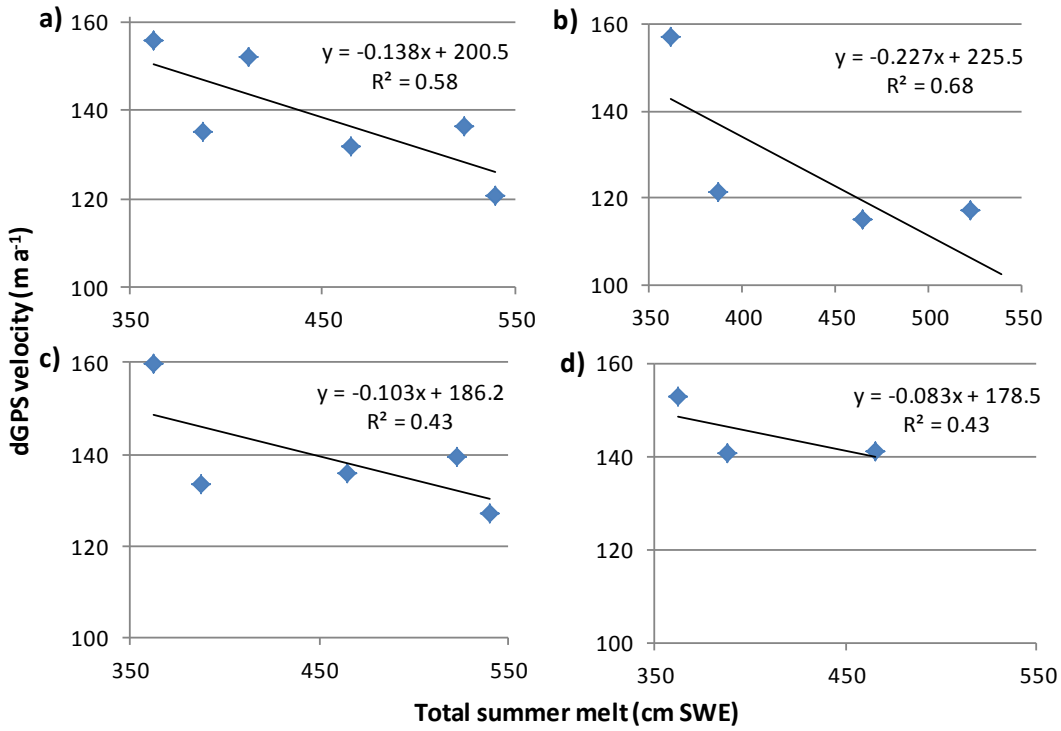

Figure 5.12 Total summer melt at the Upper Station compared with horizontal velocities the following fall-winter (JD 270-JD 90) at the Kaskawulsh dGPS stations: a) Upper, b) Middle, c) Lower, and d) South Arm.

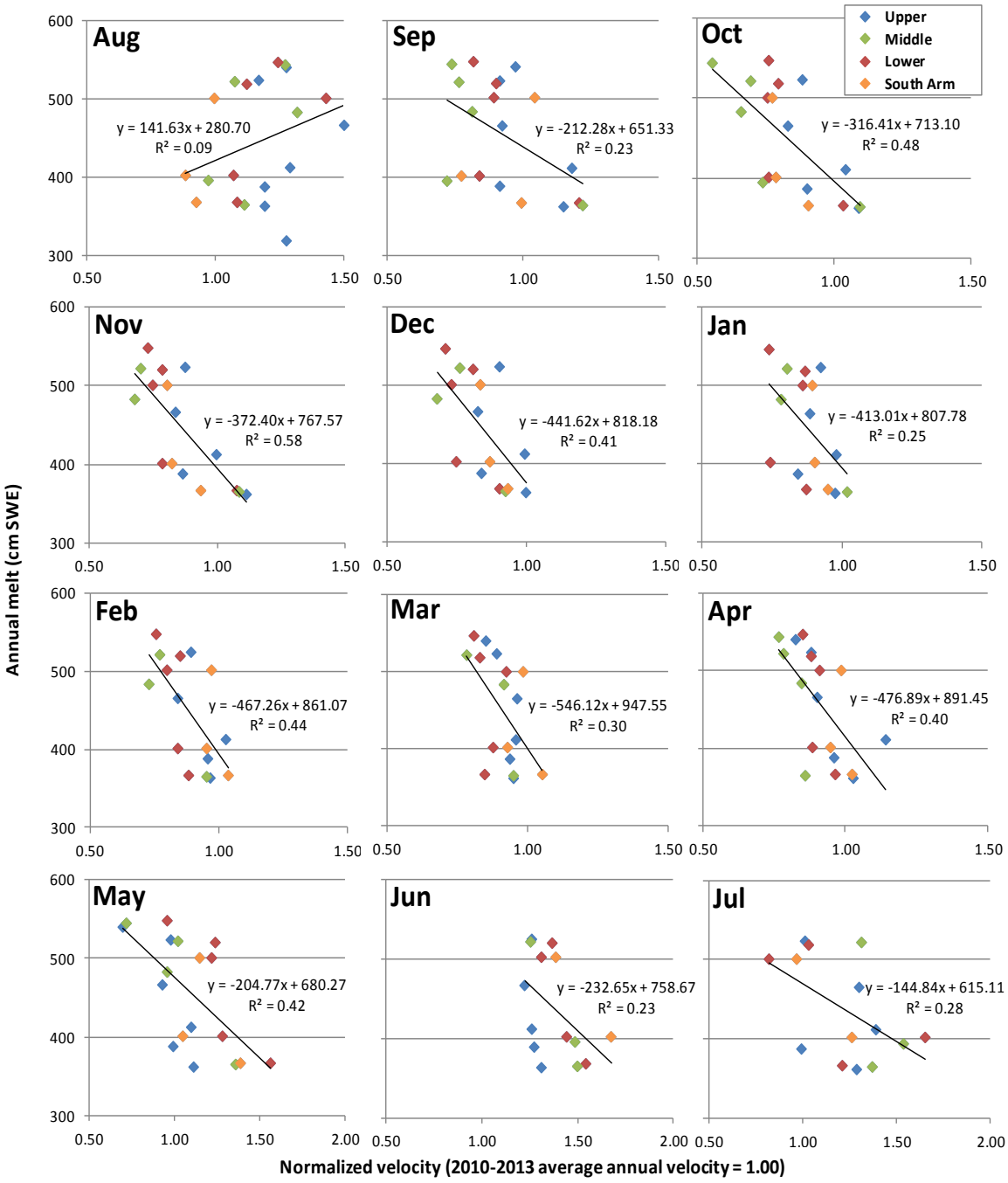

Figure 5.13 Monthly correlation of normalized velocity and annual melt from previous year at the Kaskawulsh dGPS stations. The linear regression equations and R^2 values of the monthly correlation coefficients for all stations combined are presented. Note the change in x axis scale for May-July.

Correlation between spring conditions and motion event characteristics (R^2)			
	Event start date	Event duration	Event Hz *v*
Previous summer melt	0.03	0.02	0.01
Overwinter velocity	0.06	0.01	0.00
Snowpack depth	**0.52**	0.04	**0.43**
PDDs prior to event	0.06	0.11	**0.36**
Event duration	**-**	-	**0.54**
	n *(p)*		
Previous summer melt	19 *(0.21)*	16 *(0.25)*	16 *(0.25)*
Overwinter velocity	14 *(0.28)*	14 *(0.28)*	14 *(0.28)*
Snowpack depth	14 *(0.28)*	14 *(0.28)*	16 *(0.25)*
PDDs prior to event	16 *(0.25)*	16 *(0.25)*	16 *(0.25)*
Event duration	**-**	-	16 *(0.25)*

Table 5.1 Correlation coefficients between spring conditions and spring motion event start date, duration and horizontal velocity. Correlations significant at the 95% level are shown in bold (blue shading = positive correlation; red shading = negative correlation). Sample size (n) and *p*-values for a 95% confidence level are presented in the lower part of the table.

Year	Previous summer melt (cm SWE)	Fall-Winter Velocity (m a^{-1})			
		Upper	Middle	Lower	South Arm
2007-08	411.5	152.1	-	-	-
2008-09	318.2	-	-	-	-
2009-10	523.3	136.5	117.3	139.3	-
2010-11	465.3	131.8	115.3	136.0	141.3
2011-12	387.8	135.0	121.7	133.3	140.6
2012-13	362.4	155.9	157.3	159.9	152.7
2013-14	539.9	120.6	97.6	127.0	-
2007-2014 Average	429.8	138.6	121.8	139.1	144.8

Table 5.2 Comparison between fall-winter horizontal velocity (JD 270-JD 90) at the Kaskawulsh dGPS stations and previous summer melt at the Upper station.

Monthly melt (cm SWE)	Velocity (*v*)						
	Aug *v*	Sep *v*	Oct *v*	Nov *v*	Dec *v*	Jan *v*	
May melt	0.05	**0.59**	**0.55**	**0.58**	**0.48**	**0.43**	
June melt	0.08	**0.24**	**0.31**	**0.56**	**0.31**	0.15	
July melt	0.02	0.18	0.15	**0.28**	0.16	0.14	
Aug melt	0.09	0.04	0.01	0.01	0.00	0.04	
Sep melt	-	0.05	**0.25**	0.17	**0.29**	0.12	
n *(p)*	20 *(0.20)*	19 *(0.21)*	18 *(0.22)*	16 *(0.25)*	16 *(0.25)*	16 *(0.25)*	
	Feb *v*	Mar *v*	Apr *v*	May *v*	Jun *v*	Jul *v*	Annual *v*
May melt	0.15	0.06	0.16	0.13	0.10	0.01	**0.67**
June melt	**0.29**	0.11	0.07	**0.28**	0.15	0.06	**0.21**
July melt	**0.26**	**0.38**	**0.32**	0.14	0.20	0.18	0.07
Aug melt	0.02	0.01	0.08	0.04	0.03	0.06	0.05
Sep melt	**0.38**	0.11	**0.35**	**0.33**	0.16	**0.29**	0.02
n *(p)*	16 *(0.25)*	17 *(0.23)*	18 *(0.22)*	18 *(0.22)*	14 *(0.28)*	14 *(0.28)*	19 *(0.21)*

Table 5.3 Correlation coefficients (R^2) between normalized monthly and annual horizontal velocities (*v*) and monthly melt. Correlations significant at the 95% level are shown in bold. Sample size (n) and *p*-values for a 95% confidence level are presented in the last row.

Chapter 6 : Conclusions

This study addresses horizontal and vertical velocity variations on the Kaskawulsh Glacier at interannual and intra-annual timescales, and the controls on them. The dGPS data enable an in-depth assessment of short-term velocity patterns, and provide insight into the structure and seasonal evolution of the subglacial drainage system of the glacier. The temperature and snow depth data enable derivation of melt rates on the glacier surface, and therefore, temporal variations in water input to the glacier bed. This study provides the longest known continuous velocity record available for any glacier (up to 7 years), and contributes to understanding how large valley glaciers in the Yukon and elsewhere are responding to the sustained negative mass balance trends observed in recent decades (Foy et al., 2011).

The most important finding is that the motion of glaciers appears to be self-regulating. That is, as melt rates increase, surface velocities decrease, and vice versa. This has major impacts for understanding the response of glaciers to climate change and, more specifically, predicting the long-term evolution of glacier motion to increased surface melt. To date, many of the studies that have looked at the effect of increased surface melt on glacier motion have assumed that winter velocities are stable and have therefore focused almost entirely on variations in melt season velocities. These studies have shown that short-term variations in meltwater input to a glacier bed can cause short-term increases in summer motion through increased basal sliding, suggesting that increased surface melt would lead to long-term glacier acceleration (e.g., Zwally et al., 2002; Shepherd et al., 2009; Shannon et al., 2013). However, this finding has been challenged

recently by hypotheses which argue that increased surface melt would lead to a long-term glacier deceleration, due to reduced ice thicknesses and driving stresses (Heid and Kääb, 2012) and/or a change in the efficiency of the subglacial drainage system (Schoof, 2010). At the Kaskawulsh Glacier, measurements of ice motion made throughout the year for this study make it clear that annual glacier motion is slower in years with higher melt. This is consistent with previous studies suggesting that dynamic sensitivity to interannual surface melt variations is limited due to the evolution of the subglacial drainage system (Schoof, 2010; Sundal et al, 2011; Sole et al., 2013; Burgess et al., 2013). It is therefore likely that glacier motion will show a net decrease under a warming climate, due to the increased efficiency of the subglacial drainage system (i.e., lower basal water pressures) above a critical rate of water input, as previously predicted theoretically by Schoof (2010).

This study has also found that future fall-winter velocity patterns could be accurately predicted from only a month or two of summer melt data, with May-June melt providing the best indication of fall-winter motion. The glacier motion data presented here also suggests that the common assumption that glaciers are 'stable' in the late fall and winter is incorrect (e.g., Werder et al., 2013); they can and do undergo marked variations in motion during these seasons. After summers with above average melt, fall and winter velocities are slower than in summers with low or average melt. In addition, minimum seasonal velocities are typically reached in the fall. However, in years when there is low summer melt minimum seasonal velocities occur the following winter, likely due to less development of the channelized subglacial drainage system the previous summer.

Downglacier propagating short-term motion events in the fall and winter, during which velocities increase by up to 180% in a matter of days, provide an indicator of the timing of the collapse of the channelized subglacial drainage system and the switch to distributed drainage. Similarly, short-term motion events in other seasons can be used as indicators of the evolution of the subglacial drainage system: upglacier propagating events (i.e., in spring) indicate the evolution of the system from distributed to channelized, while simultaneous events (i.e., in summer) suggest an over-pressurization of the existing channelized system.

Finally, this study demonstrates the importance of considering annual datasets (and not just summer) in studies of the response of glacier motion to future warming. The relationship between fall-winter velocities and melt the previous summer observed on the Kaskawulsh Glacier in this study and Gulf of Alaska glaciers by Burgess et al. (2012) has also been observed on the Greenland Ice Sheet (Sundal et al., 2011; Sole et al., 2013), suggesting that it is not unique to large temperate valley glaciers. Future work could focus on establishing the relationship between melt and fall-winter velocities on other glaciers for which an air temperature record is available. The dGPS network on the Kaskawulsh Glacier will continue to be run by the Laboratory for Cryospheric Research at the University of Ottawa, and in August 2014 the existing R7 dGPS receivers were replaced with new Trimble NetR9 units and moved back upglacier to near their 2010 installation locations. With this extended data record the possibilities for future research, and expanding our understanding of glacier dynamics under a changing climate, are numerous.

Chapter 7 : References

Andersen, M. L., Nettles, M., Elosegui, P., Larsen, T. B., Hamilton, G. S., and Stearns, L. A. (2011) Quantitative estimates of velocity sensitivity to surface melt variations at a large Greenland outlet glacier. Journal of Glaciology, 57 (204), 609-620, doi: 10.3189/ 002214311797409785.

Anderson, R.S., Anderson, S.P., MacGregor, K.R., Waddington, E.D., O'Neel, S., Riihimaki, C.A., and Loso, M.G. (2004) Strong feedbacks between hydrology and sliding of a small alpine glacier. Journal of Geophysical Research, 109, F03005, doi: 10.1029 /2004JF000120.

Anderton, P. (1973) Structural glaciology of a glacier confluence, Kaskawulsh Glacier, Yukon Territory, Canada. Institute of Polar Studies Report No. 26, Research Foundation and the Institute of Polar Studies, The Ohio State University, 109 pp.

Arendt, A. A., Luthcke, S. B., Larsen, C. F., Abdalati, W., Krabill, W. B., and Beedle, M. J. (2008) Validation of high-resolution GRACE mascon estimates of glacier mass changes in the St Elias Mountains, Alaska, USA, using aircraft laser altimetry. Journal of Glaciology, 54(188), 778-787, doi: 10.3189/002214308787780067.

Arendt, A. A., Walsh, J., and Harrison, W. (2009) Changes of Glaciers and Climate in Northwestern North America during the Late Twentieth Century. Journal of Climate, 22(15), 4117-4134, doi:10.1175/2009JCLI2784.1.

Arendt, A., Luthcke, S., Gardner, A., O'Neel, S., Hill, D., Moholdt, G., and Abdalati, W. (2013) Analysis of a GRACE global mascon solution for Gulf of Alaska glaciers. Journal of Glaciology, 59(217), 913-924, doi: 10.3189/2013JoG12J197.

Barrand, N. and Sharp, M. (2010) Sustained rapid shrinkage of Yukon glaciers since the 1957-1958 International Geophysical Year. Geophysical Research Letters, 37, 1-5, doi: 10.1029/2009GL042030.

Bartholomew, I., Nienow, P., Mair, D., Hubbard, A., King, M. A., and Sole, A. (2010) Seasonal evolution of subglacial drainage and acceleration in a Greenland outlet glacier. Nature Geoscience, 3(6), 408-411, doi: 10.1038/ngeo863.

Benn, D. and Evans, D. (2010) Glaciers and Glaciation (2nd Edition) 802pp. London: Hodder Education.

Berthier, E., Schiefer, E., Clarke, G.K.C., Menounos, B., and Rémy, F. (2010) Contribution of Alaskan glaciers to sea-level rise derived from satellite imagery. Nature Geoscience, 3(2), 92-95, doi: 10.1038/NGEO737.

Bingham, R. G., Nienow, P. W., and Sharp, M. J. (2003) Intra-annual and intra-seasonal flow dynamics of a High Arctic polythermal valley glacier. Annals of Glaciology, 37, 181–188.

Bingham, R. G., Hubbard, A. L., Nienow, P. W., and Sharp, M. J. (2008) An investigation into the mechanisms controlling seasonal speedup events at a High Arctic glacier. Journal of Geophysical Research, 113(F2), F02006, doi: 10.1029/2007JF000832.

Boulton, G.S. and Jones, A.S. (1979) Stability of temperate ice caps and ice sheets resting on beds of deformable sediment. Journal of Glaciology, 24, 29-43.

Brecher, H.H. (1966) Surface velocity measurements on the Kaskawulsh Glacier, Yukon Territory, Canada. Institute of Polar Studies Report No. 21, Research Foundation and the Institute of Polar Studies, The Ohio State University, 83 pp.

Burgess, E. W., Larsen, C. F., & Forster, R. R. (2013) Summer melt regulates winter glacier flow speeds throughout Alaska. Geophysical Research Letters, 40(23), 6160-6164. doi: 10.1002/2013GL058228.

Clarke, G. K. C. (1969) Geophysical measurements on the Kaskawulsh and Hubbard Glaciers. In V.C. Bushnell & R.H. Ragle (Eds.), Icefield ranges research project; scientific results (v. 1) (pp. 89-106). Montreal: Arctic Institute of North America.

Copland, L. et al. (2003). Links between short-term velocity variations and the subglacial hydrology of a predominantly cold polythermal glacier. Journal of Glaciology, 49(166), 337-348.

Copland, L., Pope, S., Bishop, M. P., Shroder, J. F., Clendon, P., Bush, A., Kamp, U., Seong, Y., and Owen, L.A. (2009) Glacier velocities across the central Karakoram. Annals of Glaciology, 50(52), 41-49, doi: 10.3189/172756409789624229.

Darling, S. (2012) Velocity Variations of the Kaskawulsh Glacier, Yukon Territory, 2009-2011. MSc. thesis, Department of Geography, University of Ottawa.

Den Ouden, M. A. G., Reijmer, C. H., Pohjola, V., van de Wal, R. S. W., Oerlemans, J., and Boot, W. (2010) Stand-alone single-frequency GPS ice velocity observations on Nordenskiöldbreen, Svalbard. The Cryosphere, 4(4), 593–604, doi: 10.5194/tc-4-593-2010.

Dunse, T., Schuler, T. V., Hagen, J. O., and Reijmer, C. H. (2012) Seasonal speed-up of two outlet glaciers of Austfonna, Svalbard, inferred from continuous GPS measurements. The Cryosphere, 6(2), 453–466, doi: 10.5194/tc-6-453-2012.

Dyurgerov, M.B. and Meier, M.F. (2005) Glaciers and the Changing Earth System: A 2004 Snapshot. Institute of Arctic and Alpine Research, Occasional Paper 58.

Fitzpatrick, A. A. W., Hubbard, A., Joughin, I., Quincey, D. J., Van As, D., Mikkelsen, A. P. B., Doyle, S. H., Hasholt, B, and Jones, G. A. (2013) Ice flow dynamics and surface meltwater flux at a land-terminating sector of the Greenland ice sheet. Journal of Glaciology, 59(216), 687–696, doi: 10.3189/2013JoG12J143.

Fountain, A. G. and Walder, J. S. 1998. Water flow through temperate glaciers. Reviews of Geophysics, 36, 299-328.

Foy, N., Copland, L., Zdanowicz, C., Demuth, M. and Hopkinson, C. (2011) Recent volume and area changes of Kaskawulsh Glacier, Yukon, Canada. Journal of Glaciology, 57(203), 1-11, doi: 10.3189/002214311796905596.

Heid, T. and Kääb, A. (2012) Repeat optical satellite images reveal widespread and long term decrease in land-terminating glacier speeds. The Cryosphere, 6(2), 467-478, doi: 10.5194/tc-6-467-2012.

Hock, R. (2005) Glacier melt: a review of processes and their modelling. Progress in Physical Geography, 29(3), 362-391, doi: 10.1191/0309133305pp453ra.

Hock, R. and Hooke, R. (1993) Evolution of the internal drainage system in the lower part of the ablation area of Storglaciaren, Sweden. Geological Society of America Bulletin, 105, 537-546.

Hooke, R., Calla, P., Holmlund, P., Nilsson, M., and A. Stroeven. (1989) A 3 year record of seasonal variations in surface velocity, Storglaciaren, Sweden. Journal of Glaciology, 35(120), 235-247.

Howat, I. M., Joughin, I., and Scambos, T. A. (2007) Rapid changes in ice discharge from Greenland outlet glaciers. Science, 315(5818), 1559-1561, doi: 10.1126/science.1138478.

Hubbard, B. P., Sharp, M. J., Willis, I. C., Nielsen, M. K., and Smart, C. C. (1995) Borehole water-level variations and the structure of the subglacial hydrological system of Haut Glacier d'Arolla, Valais, Switzerland. Journal of Glaciology, 41(139), 572-583.

Iken, A., Röthlisberger, H., Flotron, A., and Haeberli, W. (1983) The uplift of Unteraargletscher at the beginning of the melt season – a consequence of water storage at the bed? Journal of Glaciology, 29(101), 28-47.

Iken, A. and Truffer, M. (1997) The relationship between subglacial water pressure and velocity of Findelengletscher, Switzerland, during its advance and retreat. Journal of Glaciology, 13 (144), 328-338.

IPCCb. "Summary for Policymakers." In: Climate Change 2007: The Physical Science Basis. Contribution of Working Group I to the Fourth Assessment Report of the

Intergovernmental Panel on Climate Change [Solomon, S., D. Qin, M. Manning, Z. Chen, M. Marquis, K.B. Averyt, M.Tignor and H.L. Miller (eds.)]. Cambridge, United Kingdom and New York, NY, USA: Cambridge University Press, 2007.

Jacob, T., Wahr, J., Pfeffer, W. T., and Swenson, S. (2012) Recent contributions of glaciers and ice caps to sea level rise. Nature, 482, 514-518, doi: 10.1038/nature10847.

Joughin, I., Abdalati, W., and Fahnestock, M. (2004) Large fluctuations in speed on Greenland's Jakobshavn Isbrae glacier. Nature, 432, 608-610, doi: 10.1038/nature03130.

Kamb, B., Raymond, C.F., Harrison, W., Engelhardt, H., Echelmeyer, K., Humphrey, N., Brugman, M., and Pfeffer, T. (1985) Glacier surge mechanism: 1982-1983 surge of Variegated Glacier, Alaska. Science, 227(4686), 469-479.

Kamb, B. (1987) Glacier surge mechanism based on linked cavity configuration of the basal water conduit system. Journal of Geophysical Research Solid Earth, 92(B9), 9083-9100.

Kamb, B. and Engelhardt, H. (1987) Waves of accelerated motion in a glacier approchaing surge: The mini-surges of Variegated Glacier, Alaska, USA. Journal of Glaciology, 33(113), 27–46.

Larsen, C. F., Motyka, R. J., Arendt, A. A., Echelmeyer, K. A., and Geissler, P. E. (2007) Glacier changes in southeast Alaska and northwest British Columbia and contribution to sea level rise. Journal of Geophysical Research, 112(F1), F01007, doi: 10.1029/2006 JF000586.

Luthcke, S. B., Arendt, A. A., Rowlands, D. D., McCarthy, J. J., and Larsen, C. F. (2008). Recent glacier mass changes in the Gulf of Alaska region from GRACE mascon solutions, Journal of Glaciology, 54(188), 767-777.

Mair, D., Nienow, P., Willis, I., and Sharp, M. (2001) Spatial patterns of glacier motion during a high-velocity event: Haut Glacier d'Arolla, Switzerland, Journal of Glaciology, 47(156), 9-20.

Mair, D., Nienow, P., Sharp, M. J., Wohlleben, T., and Willis, I. (2002) Influence of subglacial drainage system evolution on glacier surface motion: Haut Glacier d'Arolla, Switzerland. Journal of Geophysical Research, 107(B8), 2175, doi: 10.1029/2001JB00 0514.

Mair, D., Willis, I., Fischer, U. H., Hubbard, B., Nienow, P., and Hubbard, A. (2003) Hydrological controls on patterns of surface, internal and basal motion during three "spring events": Haut Glacier d'Arolla, Switzerland. Journal of Glaciology, 49, 555-567.

Marcus, M.G. (1974) Investigations in Alpine Climatology: The St Elias Mountains, 1963-1971. In V.C. Bushnell and R.H. Ragle (Eds.) Icefield Ranges Research Project Scientific Results (v.4), 13-26, Montreal: Arctic Institute of North America.

Murray, T., Scharrer, K., James, T. D., Dye, S. R., Hanna, E., Booth, A. D., Selmes, N., Luckman, A., Hughes, A L. C., Cook, S., and Huybrechts, P. (2010) Ocean regulation hypothesis for glacier dynamics in southeast Greenland and implications for ice sheet mass changes. Journal of Geophysical Research, 115, F03026, doi: 10.1029/2009 JF001522.

Natural Resources Canada. (2014) Online Global GPS Processing Service (CSRS-PPP), online:http://www.nrcan.gc.ca/earth-sciences/geomatics/geodetic-reference-systems/ tools-applications/10925#ppp

Nienow, P., Sharp, M., and Willis, I. (1998) Seasonal changes in the morphology of the subglacial drainage system, Haut Glacier D'Arolla, Switzerland. Earth Surface Processes and Landforms, 23, 825-843.

Orgiazzi, D., Tavella, P., and Lahaye, F. (2005) Experimental Assessment of the Time Transfer Capability of Precise Point Positioning. Natural Resources Canada, online: http://www.geod.nrcan.gc.ca/publications/papers/abs36_e.php

Paterson, W. (1994) The Physics of Glaciers (3rd Edition) 481pp. Butterworth-Heinemann/Elsevier Science Ltd: Burlington, MA.

Podrasky, D., Truffer, M., Fahnestock, M., Amundson, J., Cassotto, R., and Joughin, I. (2012) Outlet glacier response to forcing over hourly to interannual timescales, Jakobshavn Isbræ, Greenland. Journal of Glaciology, 58(212), 1212–1226, doi: 10.3189/2012 JoG12J065.

Pritchard, H. D., Arthern, R. J., Vaughan, D. G., and Edwards, L. A. (2009) Extensive dynamic thinning on the margins of the Greenland and Antarctic ice sheets. Nature, 461(7266), 971-975, doi: 10.1038/nature08471.

Quincey, D. J., Copland, L., Mayer, C., Bishop, M., Lackman, and Belo, M. (2009) Ice Velocity and climate variations for Baltoro Glacier, Pakistan. Journal of Glaciology, 55(194), 1061-1671.

Rignot, E. and Kanagaratnam, P. (2006) Changes in the velocity structure of the Greenland Ice Sheet. Science, 311(5763), 986-990, doi: 10.1126/science.1121381.

Rignot, E., Velicogna, I., van den Broeke, M. R., Managhan, A., and Lenaerts, J. T. M. (2011) Acceleration of the contribution of the Greenland and Antarctic ice sheets to sea level rise. Geophysical Research Letters, 38(5), doi: 10.1029/2011GL046583.

Schoof, C. (2010) Ice-sheet acceleration driven by melt supply variability. Nature, 468, 803-806, doi: 10.1038/nature09618.

Shannon, S. R., Payne, A. J., Bartholomew, I. D., van den Broeke, M. R., Edwards, T. L., Fettweis, X., et al. (2013) Enhanced basal lubrication and the contribution of the Greenland ice sheet to future sea-level rise. Proceedings of the National Academy of Sciences of the United States of America, 110(35), 14156–61, doi: 10.1073/pnas.1212647110.

Shepherd, A., Hubbard, A., Nienow, P., King, M., McMillan, M., and Joughin, I. (2009) Greenland ice sheet motion coupled with daily melting in late summer. Geophysical Research Letters, 36(1), L01501, doi: 10.1029/2008GL035758.

Shepherd, A., Ivins, E. R., Geruo, A., Barletta, V. R., Bentley, M. J., Bettadpur, S., Briggs, K. H., et al. (2012) A reconciled estimate of ice-sheet mass balance. Science, 338(6111), 1183-1189, doi: 10.1126/science.1228102.

Sole, A., Nienow, P., Bartholomew, I., Mair, D., Cowton, T., Tedstone, A., and King, M. A. (2013) Winter motion mediates dynamic response of the Greenland Ice Sheet to warmer summers. Geophysical Research Letters, *40*(15), 3940–3944, doi: 10.1002/grl.50764.

Span, N. and Kuhn, M. (2003) Simulating annual glacier flow with a linear reservoir model. Journal of Geophysical Research, 108(D10), 4313, doi: 10.1029/2002JD002828.

Sundal, A. V., Shepherd, A., Nienow, P., Hanna, E., Palmer, S., and Huybrechts, P. (2011) Melt-induced speed-up of Greenland ice sheet offset by efficient subglacial drainage. Nature, 469(7331), 521-524, doi: 10.1038/nature09740.

Van de Wal, R.S.W., Boot, W., Van den Broeke, M. R., Smeets, C. J., Reijmer, C. H., Donker, J .J., and Oerlemans, J. (2008) Large and rapid melt induced velocity changes in the ablation zone of the Greenland Ice Sheet. Science, 321(5885), 111-113, doi: 10.1126/science.1158540.

Van Wychen, W., Copland, L., Gray, L., Burgess, D., Danielson, B., and Sharp, M. (2012). Spatial and temporal variation of ice motion and ice flux from Devon Ice Cap, Nunavut, Canada. Journal of Glaciology, 58(210), 657-664, doi: 10.3189/2012JoG11J164.

Vieli, A., Jania, J., Blatter, H., and Funk, M. (2004) Short-term velocity variations on Hansbreen, a tidewater glacier in Spitsbergen. Journal of Glaciology, 50(170), 389-398, doi: 10.3189/172756504781829963.

Vincent, C., Vallon, M., Reynaud, L., and Le Meur, E. (2000) Dynamic behaviour analysis of glacier de Saint Sorlin, France, from 40 years of observations. Journal of Glaciology, 1957-97, 46(154), 499-506, doi: 10.3189/172756500781833052.

Vincent, C., Soruco, A., Six, D., and Le Meur, E. (2009) Glacier thickening and decay analysis from 50 years of glaciological observations performed on Glacier d'Argentière Mont Blanc area, France. Annals of Glaciology, 50(50), 73-79, doi: org/10.3189/ 172756409787769500.

Waechter, A. (2013) Regional Assessment of Glacier Motion in Kluane National Park, Yukon Territory. MSc thesis, Department of Geography, University of Ottawa.

Waechter, A., Copland, L., and Herdes, E. In review. Distribution and variability of glacier velocities across the Icefield Ranges, St. Elias Mountains. Journal of Glaciology. Submitted August 7, 2014.

Weertman, J. (1983) Creep deformation. Annual Review of Earth and Planetary Science, 11, 215–240.

Werder, M. A., Hewitt, I. J., Schoof, C.G., and Flowers, G. E. (2013) Modeling channelized and distributed subglacial drainage in two dimensions, Journal of Geophysical Research Earth Surface, 118, 1-19, doi: 10.1002/jgrf.20146.

Willis, I. (1995) Intra-annual variations in glacier motion: a review. Progress in Physical Geography, 19(1), 61-106.

Wood, W. A. (1963) The Icefield Ranges Research Project. The Geographical Review, 53(2), 163-184.

Zhang, X. and Andersen, O. B. (2006) Surface ice flow velocity and tide retrieval of the Amery ice shelf using precise point positioning. Journal of Geodesy, 80(4), 171-176, doi: 10.1007/s00190-006-0062-8.

Zwally, H. J., Abdalati, W., Herring, T., Larson, K., Saba, J., and Steffen, K. (2002) Surface melt-induced acceleration of Greenland ice-sheet flow. Science, 297(5579), 218-222, doi: 10.1126/science.1072708.